Elif Tekin

DYNAMIC EXPRESSION OF THREE "RNA PROCESSING AND MODIFICATION" GENES OF *PHANEROCHAETE CHRYSOSPORIUM* UNDER Pb STRESS

ELİF TEKİN

SEPTEMBER 2011

METU 2011

DYNAMIC EXPRESSION OF THREE "RNA PROCESSING AND MODIFICATION" GENES OF *PHANEROCHAETE CHRYSOSPORIUM* UNDER Pb STRESS

A THESIS SUBMITTED TO
THE GRADUATE SCHOOL OF NATURAL AND APPLIED SCIENCES
OF
MIDDLE EAST TECHNICAL UNIVERSITY

BY

ELİF TEKİN

IN PARTIAL FULFILLMENT OF THE REQUIREMENTS
FOR
THE DEGREE OF MASTER OF SCIENCE
IN
BIOLOGY

SEPTEMBER 2011

Approval of the thesis:

DYNAMIC EXPRESSION OF THREE "RNA PROCESSING AND MODIFICATION" GENES OF *PHANEROCHAETE CHRYSOSPORIUM* UNDER Pb STRESS

submitted by **ELİF TEKİN** in partial fulfilment of the request for the degree of **Master of Science in Biology Department, Middle East Technical University** by,

Prof. Dr. Canan Özgen _____
Dean, Graduate School of **Natural and Applied Sciences**

Prof. Dr. Musa Doğan _____
Head of Department, **Biology**

Prof. Dr. Gülay Özcengiz _____
Supervisor, **Biology Dept., METU**

Examining Committee Members

Assoc. Prof. Dr. Mayda Gürsel _____
Biological Sciences Dept., METU

Prof. Dr. Gülay Özcengiz _____
Biological Sciences Dept., METU

Assoc. Prof. Dr. Bülent İçgen _____
Biological Sciences Dept., KU

Assist. Prof. Dr. Sreeparna Banerjee _____
Biological Sciences Dept., METU

Assist. Prof. Dr. Tülin Yanık _____
Biological Sciences Dept., METU

Date: 16.09.2011

I hereby declare that all information in this document has been obtained and presented in accordance with academic rules and ethical conduct. I also declare that, as required by these rules and conduct, I have fully cited and referenced all material and results that are not original to this work.

Name, Last name: Elif TEKİN

Signature :

ABSTRACT

DYNAMIC EXPRESSION OF THREE "RNA PROCESSING AND MODIFICATION" GENES OF *PHANEROCHAETE CHRYSOSPORIUM* UNDER Pb STRESS

Tekin, Elif

M. Sc., Department of Biology

Supervisor: Prof. Dr. Gülay Özcengiz

September 2011, 108 pages

RNA-binding proteins (RBP) shuttle between cellular compartments either constitutively or in response to stress and regulate localization, translation and turn over of mRNAs. In our laboratory, cytosolic proteome map of *Phanerochaete chrysosporium* was established and upon Pb exposure, the changes in cytosolic protein expressions were determined. The identified RBPs were a newly induced polyadenylate-binding protein (RRM superfamily) as well as two up-regulated proteins, namely splicing factor RNPS1 and ATP-dependent RNA helicase, all being very important candidates of post-transcriptional control in response to stress. This finding inspired us to conduct Real Time PCR studies in order to have a better understanding of the changes in the expression of corresponding genes at mRNA level in response to Pb exposure, thus the present study aims at examining the effect of lead exposure on the transcript levels of the genes coding for ATP-dependent RNA helicase, splicing factor RNPS1 and polyadenylate binding protein. As shown

via expression analysis based on Real Time PCR, the mRNA level of splicing factor RNPS1 showed 2.68, 2.62 and 4.86 fold increases in a dose-dependent manner when the cells were grown for 40 h in the presence of 25, 50 and 100 μM Pb, repectively. ATP-dependent RNA helicase mRNA level showed no significant increase in response to 25 μM Pb exposure while increased 2 and 1.84 fold in response to 50 and 100 μM Pb, respectively. Polyadenylate binding protein mRNA levels revealed no significant increase when exposed to 25, 50 and 100 μM Pb. As to the mRNA dynamics as a function of duration of lead exposure, the mRNA level of this protein showed 2.54-fold increase upon 1 h exposure to 100 μM Pb. Splicing factor RNPS1 mRNA level showed a significant increase of 19.22 fold at 2^{nd} h of 50 μM Pb exposure. Expression level of ATP-dependent RNA helicase was not affected by the time of exposure to Pb.

Keywords: *Phanerochaete chrysosporium*; Real Time PCR; expression analysis, mRNA dynamics.

ÖZ

Pb STRESİ ALTINDA *PHANEROCHAETE CHRYSOSPORIUM*'UN ÜÇ AYRI "RNA İŞLENMESİ VE MODİFİKASYON" GENLERİNİN DİNAMİK EKSPRESYONU

Tekin, Elif

Yüksek Lisans, Biyoloji Bölümü

Tez Yöneticisi: Prof. Dr. Gülay Özcengiz

Eylül 2011, 108 sayfa

RNA bağlanma proteinleri (RBP) devamlı ya da strese tepki olarak hücresel kompartmalar arasında gidip gelerek mRNA'nın lokalizasyonunu, translasyonunu ve yıkımını düzenlerler. Laboratuvarımızda *Phanerochaete chrysosporium*' un sitozolik proteom haritası çıkarılmış ve hücreler kurşun stresine maruz bırakıldığında sitozolik protein ifadelerindeki değişiklikler belirlenmiştir. Bu çalışmada tanımlanan RBP'ler ATP-bağımlı RNA helikaz ve splicing faktörü RNPS1 isimli seviyeleri Pb stresi ile artış gösteren iki proteinle birlikte sadece stres sonucunda ifade edildiği belirlenen polyadenilat bağlanma proteini (RRM süperfamilyası) olup her üç protein de stres yanıtında post-transkripsiyonel kontrolün çok önemli adaylarıdır. Bu bulgular bizleri ağır metal etkisi altında gen ifadelerindeki değişikliklerin mRNA düzeyinde daha iyi anlaşılması için Gerçek Zamanlı PZR çalışmalarına yöneltmiş olup şimdiki çalışma, kurşunun ATP-bağımlı RNA helikaz, splicing faktörü RNPS1 ve polyadenilat

bağlanma proteinlerini kodlayan genlerin mRNA seviyeleri üzerine etkisinin incelenmesini amaçlamaktadır. Gerçek Zamanlı PZR'ye dayalı ekspresyon analizi ile gösterildiği üzere, 25, 50 ve 100 µM kurşun varlığında 40 saat büyütülmüş hücrelerde splicing faktör RNPS1'nın mRNA seviyesi sırasıyla 2.68, 2.62 ve 4.86 kat artış göstermiştir. ATP-bağımlı RNA helikaz'ın mRNA seviyesi 50 ve 100 µM kurşuna yanıt olarak sırasıyla 2 ve 1.84 kat artarken, 25 µM kurşun varlığında belirgin bir artış görülmemiştir. Diğer yandan, polyadenilat bağlanma proteininin mRNA seviyesinde 25, 50 ve 100 µM kurşun etkisi altında belirgin bir artış gerçekleşmemiştir. mRNA dinamikleri, kurşuna maruz kalma süresinin bir fonksiyonu olarak incelendiğinde, hücreler 1 saat süresince 100 µM kurşuna maruz bırakıldığında bu proteine karşılık gelen mRNA seviyesi 2.54 kat, splicing faktör RNPS1'e karşılık gelen mRNA seviyesi ise 2 saat süresince 50 µM kurşuna maruz bırakıldığında 19.22 katlık önemli bir artış göstermiştir. ATP-bağımlı RNA helikaz enziminin mRNA seviyeleri, hücrelerin kurşuna maruz bırakılma süresinden etkilenmemiştir.

Anahtar kelimeler: *Phanerochaete chrysosporium*, Gerçek Zamanlı PZR, ifade analizi, mRNA dinamikleri

To My Family

ACKNOWLEDGEMENTS

I would like to start this acknowledgement by expressing my deepest gratitude and sincerest appreciation to my supervisor Prof. Dr. Gülay Özcengiz for her excellent guidance, continuous advice, invaluable help and understanding throughout this research. It was an honour for me to have a chance to work in her laboratory.

I would like to thank Doç. Dr. Bülent İçgen for his guidance, invaluable help and advices as well as invaluable time spent throughout this research.

I am grateful to Research Asistant Aslıhan Kurt for her kindness, guidance and advices.

I would like thank to my lab mates, Sezer Okay, Volkan Yıldırım, Orhan Özcan, Burcu Tefon, Eser Ünsaldı, Çiğdem Yılmaz, Aycan Apak, Alper Mutlu, İbrahim Sertdemir, İsmail Cem Yılmaz, Mustafa Demir, Mustafa Çiçek, Ayça Çırçır. Also, I would like to thank to my ex-lab mates İsmail Ögülür, especially, Güliz Vanlı and Aslı Aras Taşkın for their friendship, support and patience. I would like to thank to my friend Yaprak Dönmez for her friendship and invaluable help.

I would also like to acknowledge Ahmet Buğra İşlerel for his invaluable friendship, endless support, help and patience.

I would like to express my deepest appreciation to each member of my family starting from my mother Sevda Tekin and my father Mehmet Tekin, my sisters Ezel Tekin and Ezgi Tekin, my brother Emre Tekin for their endless love, support, patience and understanding.

TABLE OF CONTENTS

LIST OF TABLES

TABLES

LIST OF FIGURES

FIGURES

LIST OF ABBREVIATIONS

ATTC	American Type Culture Collection
bp	Base pair
DepC	Dietylpyrocarbonate
dH_2O	Distilled water
dNTP	Deoxy Nucleotide Triphosphate
EtBr	Ethidium Bromide
ORF	Open Reading Frame
qPCR	Quantitative Real-Time Polymerase Chain Reaction
rpm	Revolution per minute
RT	Reverse Transcription
SEM	Standard Error of the Means

CHAPTER 1

INTRODUCTION

1.1. *Phanerochaete chrysosporium*

The genus *Phanerochaete* is morphologically heterogeneous and based on the classic taxonomic methodologies, 46 species have been recognized (Burdsall, 1985; Koker *et al*., 2003). The *Phanerochaete* genus is characterized by having resupinate, flat, effused fruit bodies with smooth tuberculate to spinose hymenial surfaces. They have a monomitic hyphal system, which includes primarly simple septate generative hyphae and also clavate basidia with thin walled basidiospores (Koker *et al*., 2003). *Phanerochaete chrysosporium* is known as model of white rot fungi that are saprophytic on woody debris. The taxonomic classification of *P*. *chrysosporium* is given in Table 1.

Table 1.1. Taxonomic classification of *P. chrysosporium*

Kingdom	Fungi
Division	*Basidiomycota*
Class	*Hymenomycetes*
Subclass	*Homobasidiomycetes*
Order	*Aphyllophorales*
Family	*Corticiaceae*
Genus	*Phanerochaete*

P. chrysosporium is dispersed mainly in southern region of North America and due to its durability to 40 ^{o}C it can be also found in the forests of Europe and Iran; rarely found in South Africa (Burdsall, 1985; Lim, 2007).

Morphological features are important criteria for the classification and identification of fungi (Guarro *et al*., 1999). *P. chrysosporium* has an unusual life cycle (Figure 1.1.a); it produces an anamorphic state (asexual reproductive stage) which is obtained from the wood chips. The anamorphic state has the formation of conidium (Figure 1.1.b). Sometimes the anamorph is the only state for the fungus and named accordingly. Teleomorph state is a sexual reproductive stage having a spore bearing layer called cystidia (Figure 1.1 b). Teleomorph state of *P. chrysosporium* is also known therefore the anamorphic state become secondary (Burdsall, 1985).

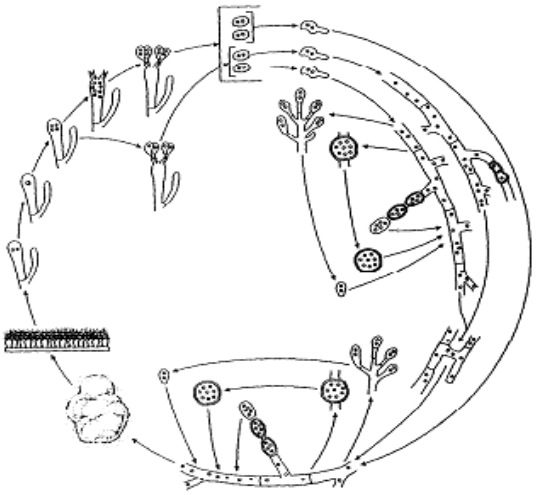

a

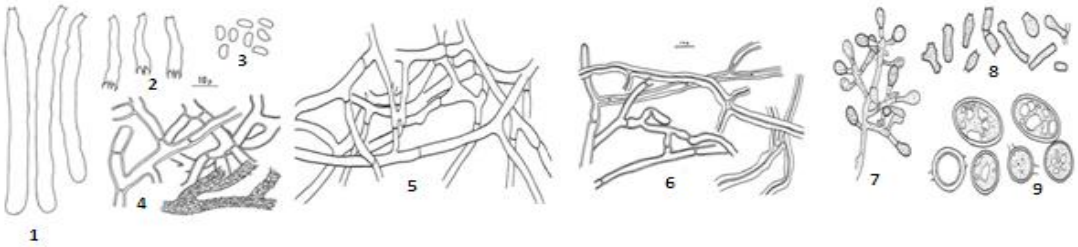

b

Figure 1.1. a. Life cycle of *P. chrysosporium* **b.** Microscopic characters of *Phanerochaete chrysosporium*; cystidia (1), basidia (2), basidiospores (3), subicular hyphae (4), aerialhyphae (5), submerged hyphae (6), aleuriospores and conidiophores (7), arthrospores (8), chlamydospores (9) (Burdsall, 1985).

The sequencing of *P. chrysosporium* revealed approximately 30 Mb genome which is composed of 10 chromosomes. *P. chrysosporium* is the first organism sequenced that represents the phylum *Basidiomycota*. It is significant since *P. chrysosporium* is phylogenetically distant from the other sequenced fungi like *Saccharomyces cerevisiae,, Schizosaccharomyces pombe, Neurospora crassa* which are belonging to the *Ascomycotina* (Martinez *et al*. 2004). The completed genome can be reached from the website http://w.jgi.doe.gov/whiterot.

1.2. The biotechnological significance of *Phanerochaete chrysosporium*

White rot basidomycetes are known for their capability of lignin degradation and especially lignocellulosics are the substrates of enormous biotechnological value due to their chemical properties (Howard, 2003). Lignin is composed of random phenylpropanoid units and has a structural heterogeneity, which makes it resistant to many forms of microbial degradation. Lignin is a constituent of wood biomass at an extend up to 30% and its degradation has an important role in carbon cycling (Zapanta, 1998; Abbas *et al*., 2005). *P. chrysosporium* has been extensively studied for microbial degradation of lignin (Srinivasan *et al*., 1995; Bogan and Lamar, 1996; Janse, 1997; Aifa *et al*., 1999; Kurihara, 2002; Ruggeri and Sassi, 2003; Reddy *et al*., 2010). Complete lignin degradation can only be achieved by white rot basidomycetes in nature and *P. chrysosporium* is a model strain since it leaves white cellulose nearly untouched besides complete lignin degradation as shown in Figure 2.a (Oliveira, 2010). Under lignilolytic conditions, *P. chrysosporium* secretes extracellular heme peroxidases, lignin and manganase peroxidases and secondary metabolites to catalyze oxidative cleavage and formation of aromatic fragments outside the fungal hyphae (Figure 2.b). The fragments formed are mineralized intracellularly (Zapanta, 1998; Kurihara, 2002; Shary, 2008).

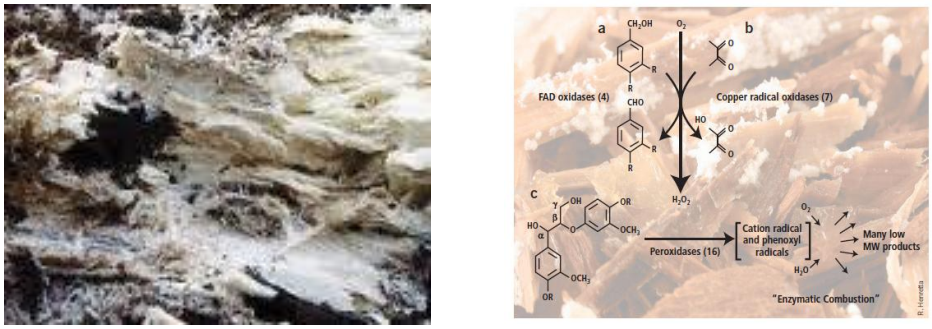

a **b**

Figure 1.2. a. *P. chrysosporium* on wood decay **b.** Major extracellular enzymes of lignin degrading fungi (Teeri, 2004).

Due to the complex extracellular ligninolytic enzyme system and high optimum temperature (40^{o}C), *P. chrysosporium* can be efficiently used in many industrial processes such as biopulping and pulp bleaching which leads to natural turnover of the organic materials (Breen and Singleton, 1999; Lim, 2007). In addition, *P. chrysosporium* has also shown to degrade variety of xenobiotics as well as organopollutants by the action of extracellular enzyme systems and free radicals (Steward *et al*., 1996; Lim *et al*., 2007).

P. chrysosporium can be applied to polluted environment for the purpose of bioremediation of different pollutants (Huang *et al*., 2006). Especially, heavy metals are one of the major environmental pollutants and admixtures of many heavy metals are carried by industrial wastewaters (Igwe *et al*. 2005). Traditional methods used for the removal of metals, such as ion exchange, chemical precipitation, membrane processes and solvent extraction are inefficient and expensive and therefore, *P. chrysosporium* has been extensively studied for its potential of being used in heavy metal bioremediation. It was shown as an effective biosorbent for heavy metals like Cd, Pb and Cu (Thakur, 2005; Yetiş *et al*., 2000; Çeribaşı and Yetiş, 2001; Say *et al*., 2001; Asamuda *et al*., 2005).

1.3. Reference proteome map of *Phanerochaete chrysosporium* and related studies

A reference proteome map for *P. chrysosporium* grown under normal physiological condition was established by using two dimensional gel electrophoresis (2-DE) and Matrix-Assisted Laser Desorption/Ionization Time-of-Flight Mass Spectrometry (MALDI-TOF MS) analysis by the team of Professor Ozcengiz at Middle East Technical University, Ankara. The reference proteome map is essential for the studies of heavy metal response of the organism that are undertaken in the same laboratory (Özcan *et al*., 2007). In their study, by using the genomic data from Joint

Genome Institute (JGI) database, a theoretical gel was calculated in order to decide for an optimal p*I* range that covers most of the proteins. A total of 920 spots were detected and separated by 2-DE. Of the 920, 720 spots were subjected to MALDI-TOF MS analysis. When the resulting MS data was processed by MASCOT software, from 720 spots only 517 could be identified. Furthermore, detailed analysis showed that 517 identified spots are the product of 314 distinct Open Reading Frames (ORFs). The distribution of ORFs over functional classes of cellular physiology is designated in Figure 1.3 (Özcan *et al*., 2007).

In another study (Wymelenberg *et al*. 2005), cultures were grown in cellulose containing medium and used for shotgun LC-MS/MS analysis. The results indicated that 182 unique peptide sequences which were obtained experimentally were correlated with 50 specific genes. Most of the identified proteins were members of functionally interconnected enzyme groups like cellulose attack enzymes, namely multiple endoglucanases and exocellobiohydrolases and hemicellulolytic system enzymes such as arabinofuranosidase acetyl xylan esterase and endoxylanases.

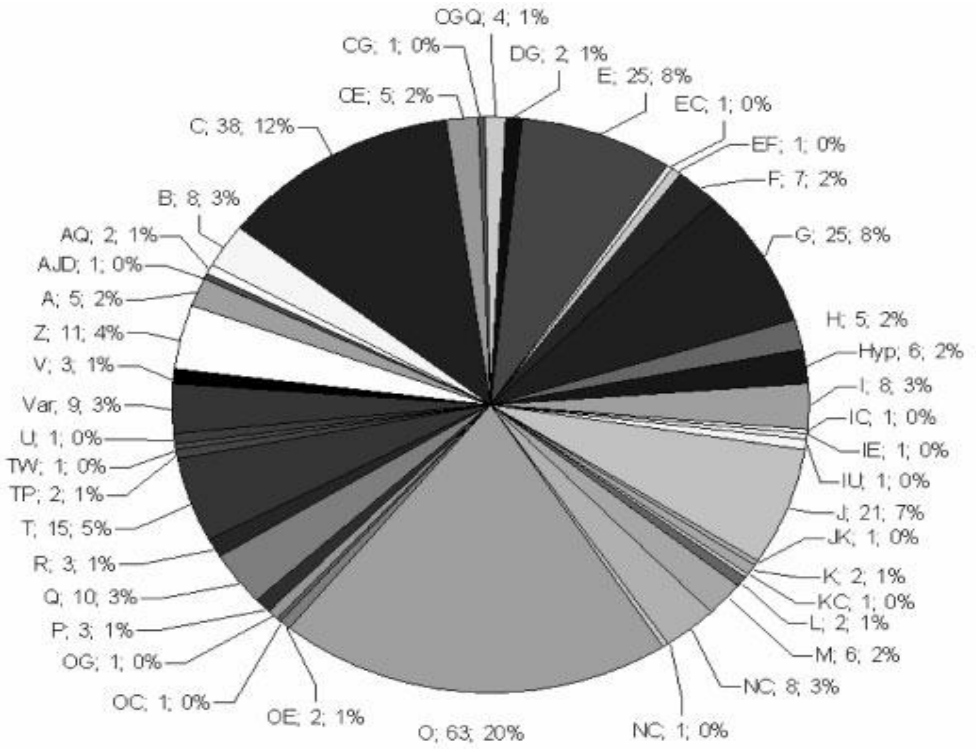

A: ARNA processing and modification
AJD: ARNA processing and modification, JTranslation, ribosomal structure and biogenesis, DCell cycle control, cell division, chromosome partitioning
AQ: ARNA processing and modification, QSecondary metabolites biosynthesis, transport and catabolism
B: BChromatin structure and dynamics
C: C Energy production and conversion
CE: C Energy production and conversion, EAmino acid transport and metabolism
CG: C Energy production and conversion, GCarbohydrate transport and metabolism
CGQ: C Energy production and conversion, GCarbohydrate transport and metabolism, QSecondary metabolites biosynthesis, transport and catabolism
DG: DCell cycle control, cell division, chromosome partitioning, GCarbohydrate transport and metabolism
E: EAmino acid transport and metabolism
EC: EAmino acid transport and metabolism, C Energy production and conversion
EF: EAmino acid transport and metabolism, FNucleotide transport and metabolism
F: FNucleotide transport and metabolism
G: GCarbohydrate transport and metabolism
H: HCoenzyme transport and metabolism
Hyp: HYPOTHETICAL
I: ILipid transport and metabolism
IC: ILipid transport and metabolism, C Energy production and conversion
IE: ILipid transport and metabolism, EAmino acid transport and metabolism
IU: ILipid transport and metabolism, UIntracellular trafficking, secretion, and vesicular transport*assigned
J: JTranslation, ribosomal structure and biogenesis
JK: JTranslation, ribosomal structure and biogenesis, Ktranscription
K: Ktranscription
KC: Ktranscription, C Energy production and conversion
L: LReplication, recombination and repair
M: MCell wall/membrane/envelope biogenesis
NC: Not Classified
N: Nucleotide repair
O: OPosttranslational modification, protein turnover, chaperones
OE: OPosttranslational modification, protein turnover, chaperones EAmino acid transport and metabolism
OC: OPosttranslational modification, protein turnover, chaperones, C Energy production and conversion
OG: OPosttranslational modification, protein turnover, chaperones, GCarbohydrate transport and metabolism
P: PInorganic ion transport and metabolism
Q: QSecondary metabolites biosynthesis, transport and catabolism
R: RGeneral function prediction only
T: TSignal transduction mechanism
TP: TSignal transduction mechanisms, PInorganic ion transport and metabolism
TW: TSignal transduction mechanisms, WExtracellular structures
U: UIntracellular trafficking, secretion, and vesicular transport
Var:VARIOUS
V: VDefense mechanisms
Z: ZCytoskeleton

Figure 1.3. The distribution of the 314 ORFs between various functional classes of cellular physiology (Özcan *et al*., 2007).

Later, by using similar approach, *P. chrysosporium* was grown under carbon and nitrogen limited conditions and secreted proteins were used for protemic studies. Based on the v2.1 gene models, 769 secreted proteins were predicted (Figure 1.4).

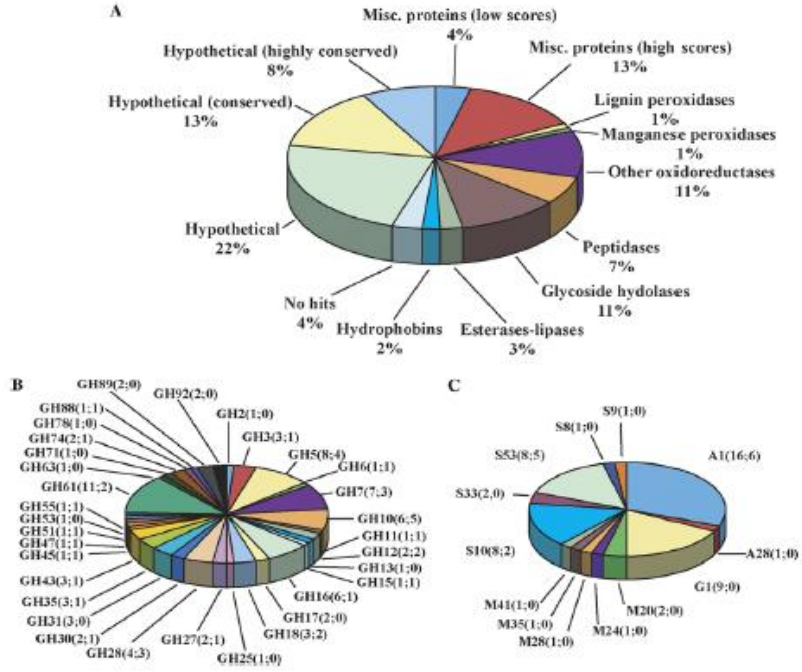

Figure 1.4. Distribution of *P. chrysosporium* secretome gene models (A). The total 794 models (B) Eighty-seven models assigned to specific glycoside hydrolase families (C) Fifty-two peptidases were classified by MEROPS server (Wymelenberg, *et al*., 2006).

407 models in a total of 769 proteins, showed similarity to known proteins like glycoside hydrolases, esterases, oxidoreductases, peptidases and lipases. Remaining ones were designated to specific groups like hydrophobins, lignin peroxidase and manganese peroxidases. Also 134 models could not be assigned to any groups but significant similarity was found. In addition, peptidases and glycosyl hydrolases were allocated to specific families or clans (Wymelenberg, *et al*. 2006).

Secretome analysis of the *P. chrysosporium* cultures grown on red oak wood chips was made by separating the extracellular proteins on 2-DE gels followed by MALDI-TOF MS or by LC-MS/MS sequencing. This study detected the enzymes that act on the three major components of wood: cellulose, hemicellulose and lignin. 40 different proteins spots were detected on 2-D gels and from the 25 proteins analyzed, only two were identified by MALDI/TOF; laminarinase and cellobiose dehydrogenase. However, the Capillary Liquid Chromatography–Nanoelectrospray Ionization–Tandem MS (CapLC-ESI MS/MS) method was able to identify 16 protein spots (Abbas *et al*., 2005).

Very recently, proteome analysis of *P. chrysosporium* in response to lead (Pb) was performed by using 2DE in combination with MALDI-TOF-MS. For this purpose, cells were cultivated with three different concentrations of Pb (25, 50 and 100 μM) for 40 h. As a result, 14 upregulated and 21 downregulated proteins were identified in response to different concentrations of Pb. In parallel, upon induction by 50 μM Pb after 40 h incubation for 1, 2, 4 and 8 h resulted in the identification of 23 upregulated and 67 downregulated proteins. It was shown for the first time that elements of apoptosis, post-transcriptional control, DNA repair as well as heterotrimeric G protein signaling were upregulated in a basidomycete under metal stress (Yıldırım *et al*., 2011).

1.4. RNA processing and modification

The regulation of gene expression is a fundamental process which occurs at multiple levels. In order to perform biological functions properly, cells use internal and external information to coordinate multiple regulatory mechanisms of gene expression. Even though transcriptional control is the most fundamental and important step for the regulation of gene expression, post-transcriptional regulation is

also very important since it includes processing, export, localization, turnover and translation of mRNAs (Mata *et al*., 2005)

1.4.1. Post-transcriptional modification in eukaryotes

In some cases, where the changes in cytoplasmic mRNA levels occur without alterations in the rate of gene transcription, post-transcriptional control can be considered (Latchman, 2005). Post-transcriptional regulation can take place at any steps between gene transcription and translation of the corresponding mRNA in the cytoplasm. Such kind of regulation is based on specific RNA–protein interactions that can lead to degradation of the target mRNA or can prevent access of the ribosome to the translation start codon (Day and Tuite, 1998). mRNA stability, splicing, elongation, transport as well as other processes like RNA editing are included in the post transcriptional regulation (Sachs, 1998).

1.4.1.1. Regulation of RNA splicing

In higher eukaryotes, regulation of alternative splicing of mRNA precursors is a versatile mechanism in order to regulate gene expression and it constitutes for a large part of the proteomic complexity (Smith and Valcárcel, 2000). Alternative splicing is a process including a differential use of splice sites to create protein diversity. There are four basic modules namely; alternative 5′ or 3′ splice-site choice, intron retention and cassette-exon inclusion or skipping (Nilsen and Graveley, 2010). These modulations are gained through multiple interactions of regulatory signals in RNA and the complexes having members like the heterogeneous nuclear ribonucleoproteins (hnRNP) and serine–arginine (SR) protein families that recognize such signals (Smith and Valcárcel, 2000). As a result, distinct proteins can be generated from the same mRNA via alternative splicing by increasing the coding

capacity of genes. In addition, gene expression can be turned on and off via alternative splicing which can introduce premature stop codons (Smith and Valcárcel, 2000).

Strikingly, alternative splicing is also important for adaptations to a variety of stress conditions. For example, under cold stress, splicing factor SR1 showed different splicing variants from those identified under other growth conditions (Lida *et al*. 2004).

1.4.1.2. RNA editing

Similar to alternative splicing, two different proteins can be produced from the same RNA by RNA editing via the sequence change in mRNA (Latchman, 2005). RNA editing includes the change in the selected nucleotide sequences in RNA that was originally encoded in the genome. There are diverse types of RNA editing (Figure 1.5) such as insertion or deletion editing as well as substitution or modification editing (Siomi and Dreyfusst, 1997). RNA editing can repair or correct the information encoded by the genome as well as diversifies this information and provides a potential for greater complexity (Bass, 2002).

One type of RNA editing involves deamination of cytidine (C) and formation of uridine (U), and the other, deamination of adenosine (A) form into inosine (I). RNA editing by adenosine deamination is catalyzed by adenosine deaminases that act on RNA. Inosine is translated as a guanosine (G) and this leads to change the primary sequence information in RNA (Bass, 2002).

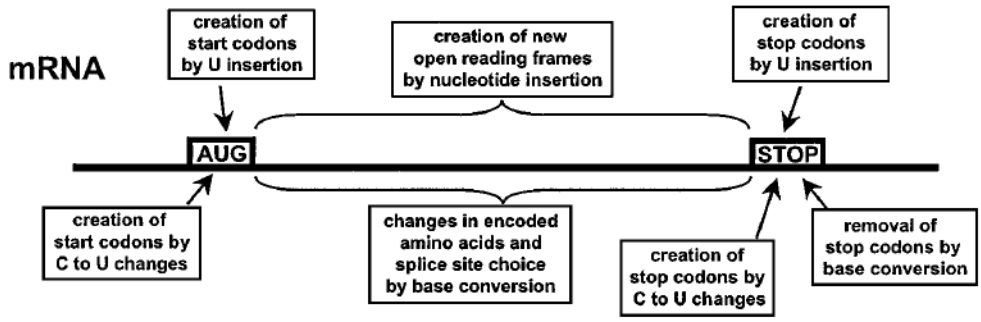

Figure 1.5. Summary of RNA editing (Gott and Emeson, 2000).

On the other hand, by the U insertion and C to U conversions new start and stop codons can be created. By the conversion by U-to-C changes, stop codons can be removed. In addition, internal changes involve creation of open reading frames (ORFs), and also frameshifts between alternative ORFs, amino acid substitutions due to C-to-U, U-to-C and adenosine to inosine changes; and alterations in splice sites by A-to-I conversion and within introns. Even silent codon changes are observed, generally editing creates codons for highly conserved or functionally essential amino acids. In RNA editing, alterations within the untranslated regions (UTRs) are seen rarely and by this way, stability, translatability, and processing of mRNA are also affected (Gott and Emeson, 2000).

1.4.1.3. Regulation of RNA transport

After splicing of mRNA in nucleus, spliced mRNA must be transported to the cytoplasm for translation process. In nucleus, different RNA species are produced and exported through the nuclear pore complexes via mobile export receptors. Different from other RNAs in terms of length and sequence, mRNA export is unique since it is in association with transcription and splicing and includes specific export receptors and strategies. Moreover, many RNA binding and modifying proteins are

recruited to the transcripts as well as export adaptors serving as physical bridge between the mRNA molecule and its export receptor. It was also shown that by using different model organisms, mRNA export pathway is conserved from yeast to humans. The mRNA export receptor is targeted to different transcripts by export adaptors that are typically mRNA-binding proteins. Also, mRNA exporter can physically interact with the Phe-Gly (FG) rich repeats of nucleoporins, in order to overcome the permeability barrier of the nuclear pore complex formed by the FG-nucleoporin meshwork. In addition, SR (Serine/Arginine-rich) proteins are essential for splicing function as adaptors and regulators of multiple steps of mRNA metabolism including mRNA export (Latchman, 2005; Köhler and Hurt, 2007).

1.4.1.4. Regulation of RNA stability

The regulation of RNA stability is very important since the translation rate and the amount of protein produced is determined by mRNA stability. Therefore, changing RNA stability in response to some regulatory signals is an effective way of gene regulation (Latchman, 2005). For instance, the *Aspergillus nidulans areA* gene which is a positive transcription factor has a central regulatory role in nitrogen assimilation. Under nitrogen limited conditions, its expression increases and half-life of *areA* RNA, which is normally 7 min, is increased to 40 min by the deletion of sequences in the UTR region in order to stabilize the RNA (Sachs, 1998). Besides, the mRNA of the milk protein, casein, having a 1 h half life under normal conditions undergoes similar type of regulation. When there is the hormone prolactin, its half-life increases to over 40 h and the casein mRNA accumulates and protein production increases (Latchman, 2005).

In order to understand the mechanism of RNA stability, the mRNA sequence and properties should be considered (Latchman, 2005). First of all, majority of eukaryotic mRNAs carry a 5’ 7-methylguanosine cap structure and a 3’ poly (A) tail of up to

200 adenosine residues in length in order to be protected from degradation by 5→'3' or 3'→5'exonucleases. In eukaryotes, mRNA stability is linked to the level of mRNA polyadenylation which can be influenced by cytoplasmic poly (A)-binding proteins (Sachs, 1998). Therefore, poly(A)-binding protein (PABP) in association with poly(A) tail of mRNA, and the specific internal sequence elements found in 3′ and 5′ UTRs have an effect on the stability of mRNA. For example, the mRNAs of *S. cerevisiae* contains such sequences in 5′ UTR and in the 3′ UTR as well as coding region of different mRNAs (Day and Tuite, 1998).

The localization of the sequences involved in the regulated degradation of specific mRNA species generally occurs in the 3′ UTR and the importance of this region in determining differences in stability observed between different RNA species is in agreement. These sequences, which are recognized by various RNA binding proteins (RBPs), can determine the decay rates of the mRNA (Mata *et al*., 2005). Also such sequences can either promote endonucleotic cleavage or poly(A) tail loss followed by exonucleotic attack as shown in the Figure 1.6. (Latchman, 2005).

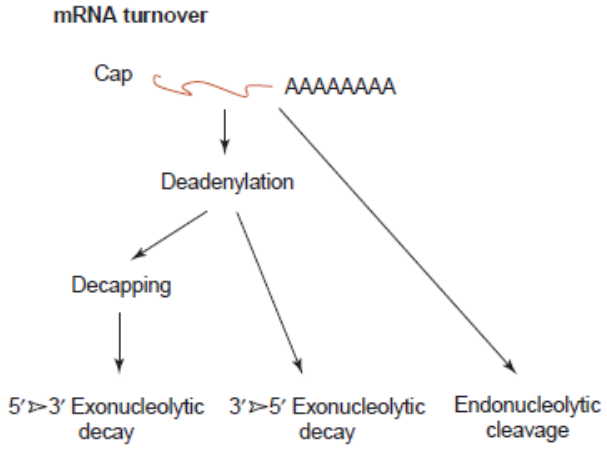

Figure 1.6. mRNA turnover mechanisms (Mata *et al*., 2005).

Besides transcription rates, mRNA decay rates are also precisely controlled. Since decay rates can determine how quickly the adaptation responses to new conditions are established. In detail, mRNA decay rate regulation is a response to variety of different external and internal stimuli such as specific hormones, cell cycle progression and cell differentiation signals, external stimuli like viral infection and iron (Wang *et al*., 2002). In addition, there is a correlation between high mRNA decay rates and the presence of AU-rich elements in the 3′ UTRs of transcripts. In addition, cooperative binding of multiple RBPs to different sites can control the mRNA-decay regulons. Global studies of degradation mutants have identified factors that regulate the stability of dozens or hundreds of mRNAs (Mata *et al*., 2005). The transcripts which encode core metabolic proteins have long half-lives, while those encoding transcription factors or members of the ribosome-biogenesis machinery are markedly unstable. As short transcript half-lives enable both more rapid and more dramatic changes in mRNA levels in response to different conditions, this might be an advantage for transcripts encoding regulatory proteins. Interestingly, orthologous genes found in yeast and humans share similar mRNA-turnover patterns which imply that the regulation of mRNA stability is a conserved, widespread and highly regulated mechanism for the control of gene expression. In the study of Fan and his colleagues (2002), upon subjected to stress-inducing agents, 50% of the affected transcripts showed altered abundance due to changes in mRNA stability rather than changes in transcription. Garcia-Martinez and colleagues (2004) assessed the effect of a carbon-source shift on transcription and mRNA stability in yeast. Developmental and environmental stimuli were also shown to cause fluctuations on the half-life of many mRNAs (Day and Tuite, 1998). To conclude, transcript turnover is an important target of regulation in response to perturbations and RBPs have important roles in this regulation (Mata *et al*., 2005).

1.4.1.5. Regulation via noncoding small RNAs

The discovery of small noncoding RNAs (20–30 nucleotides in length) was among the most important advances in eukaryotic gene regulation. They are involved in regulations that are critical for genome function, including chromatin structure, chromosome segregation, transcription, RNA processing, RNA stability, and translation. Generally, they have inhibitory effects on gene expression; therefore, the corresponding regulations are categorized into RNA silencing mechanisms (Carthew and Sontheimer, 2009). microRNAs (miRNAs) and short interfering RNAs (siRNAs) are the two classes of small noncoding RNAs that have important roles in the regulation of gene expression in plants and animals (Sunkar and Zhu, 2004; Carthew and Sontheimer, 2009). Single-stranded forms of both miRNAs and siRNAs were found to be associated with effector assemblies known as RNA-induced silencing complexes (RISCs) and these forms were primarily related with post-transcriptional regulation. miRNAs are derived from the intergenic regions of organism's own genome and transcribes as long pre-miRNAs. These pre-miRNAs can be composed of 30 to 700 nucleotides with stem-loop structures, which then processed to form mature miRNAs. The miRNA acts as an adaptor for miRISC to specifically recognize and regulate particular mRNAs. This regulation is generally resulted in the translational repression or cleavage of target mRNAs. On the other hand, siRNAs are exogenous origin such as virus, transposon or transgene. Long complementary double stranded precursor was excised into siRNAs (Tomari and Zamore, 2005). The siRNA guide strand directs RISC to perfectly complementary RNA targets, which are then degraded. In case of mismatches at or near the center of the siRNA/target duplex, endonucleolytic cleavage is suppressed and similar to miRNA regulation, targets can be silenced at a post-transcriptional level (Carthew and Sontheimer, 2009). The miRNA and siRNA formation and regulation was summarized in Figure 1.7.

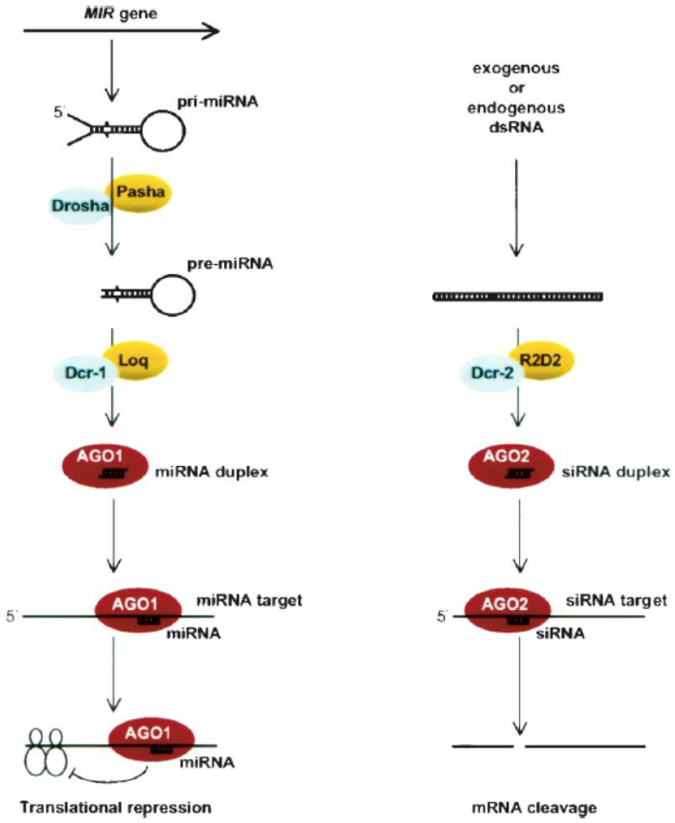

Figure 1.7. miRNA and siRNA regulation mechanisms.

Recently discovered plant miRNAs and endogenous siRNAs have emerged as important players for adaptation to various stress conditions (Sunkar *et al*., 2006). For instance, miR395 and miR399 were shown to be induced by sulfate and phosphate deprivation, respectively. This induction is important for the downregulation of certain genes under nutrient deficiency stress (Jones-Rhoades and Bartel, 2004; Fujii et al., 2005; Chiou et al., 2006). Two Cu/Zn superoxide dismutases (cytosolic CSD1 and chloroplastic CSD2) that can detoxify superoxide radicals were found to be regulated by miR398-directed mRNA cleavage in response to oxidative stress. The downregulation of miR398 expression under oxidative stresses were important for post-transcriptional CSD1 and CSD2 mRNA accumulation and oxidative stress tolerance (Sunkar *et al*., 2006).

1.5. Correlation of mRNA level with protein level

Proteins are the driving force of biological processes but the methods used for studying protein expression levels are costly, labor intensive and a limited range when compared to mRNA expression methods (Fu *et al*., 2007). The 2-DE and shotgun MS, which have a bias towards highly expressed proteins, are mostly used techniques for the quantification of protein expression levels (Fu *et al*., 2007). Generally, mRNA is translated into protein so that some sort of correlation between mRNA and protein is expected or assumed, however, the degree of validity of this assumption is not established (Greenbaum *et al*., 2003; Guo *et al*., 2008). Therefore, mRNA expression levels are generally used to estimate functional differences that occur at the protein level (Fu *et al*., 2007; Guo *et al*., 2008). Another view is that there may be no significant correlation between mRNA and protein levels which, in itself, is an informative conclusion (Greenbaum *et al*., 2003). Most of the observed differences in mRNA expression are shown to have no functional consequences since they are not reflected at the protein level (Fu *et al*., 2007). The correlation coefficient, which is generally used for indication of relationship between mRNA and protein levels, shows a statistical dependence between two variables and it has a value between -1 and 1. Perfect linear correlation is implied by the positive value 1. The value of -1 corresponds to negative correlation (Lawrence and Kuei, 1992). Finally, zero corresponds to no relation between variables. Generally, the correlation between mRNA and protein expression is described as moderately or weakly positive having a correlation value ranging from 0.2 to 0.6. This is due to post-transcriptional regulation, different mRNA and protein turnover rates, mRNA and protein stability, translation and transcription efficiency; intracellular location and molecular association of the protein products of expressed genes as described previously (Gygi *et al*., 1999; Fu *et al*., 2007; Abreu *et al*., 2009). Translation and protein degradation processes are highly regulated both at a global and at a gene-specific level (Abreu *et al*., 2009). In the case of no correlation between mRNA and protein data, both results

are regarded as independent sources of information and can be used to predict protein interactions (Greenbaum*et al*., 2003).

The quantification of mRNA and protein levels is necessary in order to get a complete understanding of the function of the cell (Gygi *et al*., 1999; Greenbaum *et al*., 2003). In other words, biological system is not understood from mRNA transcript level analysis alone, the accurate measurement of protein expression levels and their respective activities are also necessary (Gygi *et al*., 1999).

On the other hand, the mRNA-protein expression correlation in yeast or human tissues is identified only in limited studies and this correlation is relatively inconsistent (Guo *et al*., 2008). In the study performed by Anderson and Seilhamer (1997), one of the earliest analyses of correlation, 19 proteins of the human liver were under focus. The results showed positive correlation of 0.48 (Greenbaum *et al*., 2003). Another study done by Gygi *et al*. (1999) showed that either the similar mRNA levels for some genes could be end up with different protein levels up to 20-fold or proteins with steady state levels observed with variant mRNA levels up to 30-fold.

1.6. The proteins under study

The expression of three RBPs which are polyadenylate-binding protein (RRM superfamily), splicing factor RNPS1 (RNA-binding protein with serine-rich domain) and ATP-dependent RNA helicase was analyzed in the present study. In eukaryotic cells, RBPs are the important participants in gene expression by taking roles in the post-transcriptional regulation (Saliciani *et al*., 2000). RBPs shuttle between cellular compartments either constitutively or in response to stress in order to regulate localization, translation, or turnover of mRNAs (Shyu and Wilkinson, 2000). As the RNA is transcribed, the processes like RNA splicing, transport, localization, capping,

editing, and polyadenylation, translation, mRNA stability are mediated by the help of protein factors or ribonucleoproteins that have the ability to recognize the pre-mRNA and assemble the appropriate pre-mRNA processing complexes (Saliciani *et al*., 2000; Kielkopf *et al*., 2004; Lunde *et al*. 2007). Some structural or biochemical studies also revealed that several RNA-binding proteins can bind to other proteins in addition to RNA or instead of RNA (Chen *et al*., 2005). These proteins have a dynamic association with the target RNA that defines its lifetime, processing, translation rate, cellular localization (Lunde *et al*. 2007). Many of these processes guided by different RBPs having limited number of conserved modular structures and multiple repeats of different arrangements of few basic domains that provides diverse functionality (Kielkopf *et al*., 2004; Lunde *et al*. 2007). Such kind of structure modularity and repeats provide versatility as well as higher specificity and affinity when compared to the structures that have individual domains. The interaction surfaces are constructed by means of multiple modules that form multiple specific weak interactions, which makes easier to regulate by disassembling (Lunde *et al*. 2007). The key feature of many RBPs is the presence of one or more RNA-recognition motifs (RRMs). One of the most abundant eukaryotic RNA-binding motifs is the RRM domain, (also known as Ribonucleoprotein (RNP)) (Saliciani *et al*., 2000; Kielkopf *et al*., 2004). The RRM domain (Figure 1.8) which is a 90-amino-acid protein domain forms a four-stranded anti-parallel β-sheet with two helices packed against it, giving the domain the split αβ (βαββαβ) topology and it binds single stranded RNA (Saliciani *et al*., 2000; Lunde *et al*., 2007).

There are approximately 20 known structures of RRM–RNA complexes in which RNA recognition usually occurs on the surface of the β-sheet and binding is mediated mostly by an Arg or Lys residue (a salt bridge to the phosphodiester backbone) and two aromatic residues (stacking interactions with the nucleobases). These three amino acids found in the two highly conserved motifs namely; RNP motif-1 (RNP1) and RNP2 which are located in the two central β-strands (Lunde *et al*., 2007).

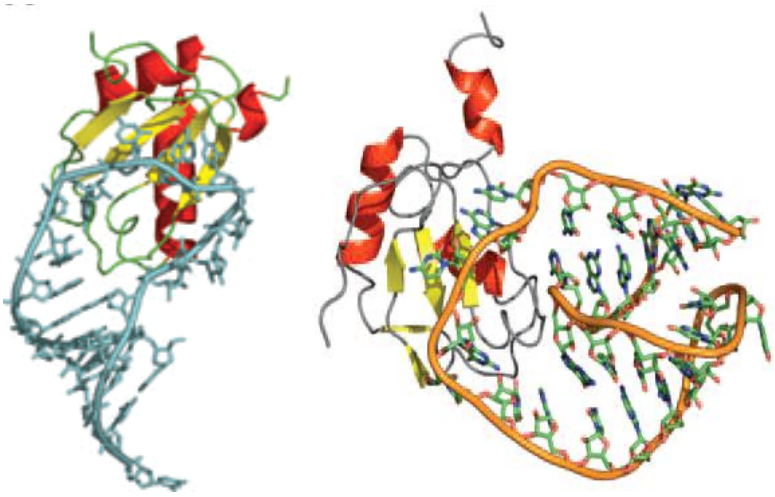

Figure 1.8. RRM domain (Lunde *et al*. 2007; Chen *et al*., 2005).

RRM has a primary function in post-transcriptional gene-expression processes and it supplies an RNA binding platform and directs RNA processing factors to specific RNAs in the cell (Chen *et al*., 2005; Lunde *et al*., 2007). Besides mRNA binding, RRM domains also have a role in diverse protein–protein interactions (Table 1.2). Yang and Carrier (2001) reported that RBPs translocate to the cytoplasm in response to stress. They showed that when induced by UV radiation, a18 hnRNP targets stress-activated transcripts and stimulates translation. In addition, RNA-binding modules have an ability to regulate the biological activity of enzymes that act on RNAs (Lunde *et al*., 2007). Surprisingly, some of these proteins bind not only to RNA but also to other proteins, even involved in RNA recognition (Chen *et al*., 2005; Lunde *et al*., 2007).

Table 1.2. Properties of RRM domain

Domain	Topology	Recognition Surface	Protein-RNA interactions	Representatative
RRM	αβ	β-sheet	Occur via ~4 nucleotides of ssRNA	U1A N-terminal RRM18

1.6.1. Polyadenylate binding protein

Polyadenylate binding protein (PABP) is an evolutionary conserved protein that can bind to the poly(A) tails of eukaryotic mRNAs by the help of RNA-recognition motifs which are globular domains common to eukaryotic RNA-binding protein (Gray *et al*., 2000). Single-celled eukaryotes have a single polyadenylate binding protein while humans have five and *Arabidopis* has eight, but polyadenylate binding protein appear to be absent from prokaryotes. Polyadenylate binding proteins are the major class of regulatory factors that are involved in various processes. Polyadenylate binding proteins having no catalytic activity, take place in gene expression mediation by involving in poly(A) tail synthesis and length, mRNA maturation and export as well as translation initiation and termination, recycling of ribosome, and stability of the mRNA (Mangus *et al*., 2003).

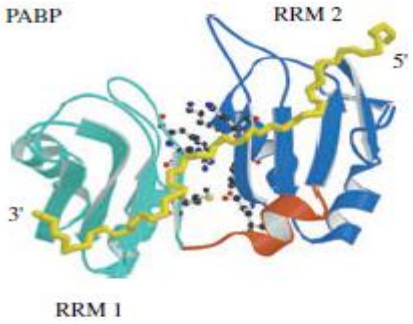

Figure 1.9. Polyadenylate binding protein in complex with RNA (Maris *et al*., 2005).

As shown in Figure 1.9, the inter-domain interactions are mediated by many salt bridges and van der Waals contacts between α_2 and β_4 of RRM1 and β_2 and α_1 of RRM2 and hydrogen bonds and stacking interactions with conserved residues within the RNP motifs (Gray *et al*., 2000; Mangus *et al*., 2003). The polyadenylate binding proteins binding to poly (A) needs a minimal binding site of 12 adenosines, also multiple polyadenylate binding proteins molecules can bind to the same poly(A) tract. In addition, polyadenylate binding proteins provide a scaffold for the binding of variety of factors and as well as are antagonist to the binding of factors that enable the terminal steps of mRNA degradation (Mangus *et al*., 2003). Binding of Polyadenylate binding protein to poly (A) tail promotes 5' to 3' interactions that result in stimulation of translation initiation. Also formation of 'closed loop' was shown to promote the recruitment of 40S ribosomal subunits and depends on interactions between initiation factor eIF4G and polyadenylate binding proteins, and also concurrent interactions between eIF4G and the cap-binding protein eIF4E (Mangus *et al*., 2003).

Cytoplasmic poly (A)-binding protein plays a crucial role in regulating translation as well as stability of eukaryotic mRNA (Bag and Bhattacharjee, 2010). It is believed that PABP1 protects mRNAs from degradation by binding to their poly(A) tract (Ma *et al*., 2009). For instance, the study done by Sagliocco *et al*., 2006 showed that the

AU-rich element-binding polypeptide AUF1 may control mRNA stability by binding to PABP1. In another study done with HeLa cells, the expression level of PABP1 was upregulated by the increase in translation effiency during the recovery period after heat shock. The terminal oligopyrimidine cis-element of PABP1 mRNA was responsible for the upregulation (Ma *et al*., 2009). In addition, human polyadenylate binding protein, cytosolic 1 (Pabpc1) was shown to have anti-apoptic activities under osmotic stress. It is stated that the overexpression of this protein could protect the cells against oxidative stress (Nagano-Ito *et al*., 2009). Even in different cancer forms polyadenylate binding protein had an increased expression levels (Bag and Bhattacharjee, 2010).

1.6.2. ATP-dependent RNA helicase

DEAD-box proteins constitute the largest family of superfamily 2 (SF2) helicases and have a helicase core composed of two RecA-like domains and a common set of sequence motifs (Jarmoskaite and Russell, 2010). DEAD-box proteins function in diverse set of processes such as transcription, pre-mRNA splicing, assembly and function of ribosome and spliceosome, gene expression control mechanisms, resolution of inhibitory mRNA secondary structures and nuclear export of mRNA, folding of self splicing RNA introns, translation initiation and RNA degradation (Linder, 2006; Jarmoskaite and Russell , 2010). In addition, DEAD-box proteins are very crucial for various RNA-mediated processes by coupling cycles of ATP binding and hydrolysis to changes in affinity for single-stranded RNA. Efficient separation of the strands of short RNA duplexes in a process that involves little or no translocation is performed by DEAD-box proteins. By this activity, RNA folding steps and rearrangements are promoted and remodeling of RNA–protein complexes is accelerated. The ability to bind and hydrolyze ATP in a cycle is stimulated by binding to single-stranded or double-stranded RNA (ssRNA or dsRNA) and this leads to changes in ssRNA affinity, allowing DEAD-box proteins to bind and release

RNA in a regulated manner in order to promote RNA structural rearrangements and folding events as well as separation of the strands of helices (Jarmoskaite and Russell, 2010).

It was shown that ATP-dependent RNA helicase is involved in adaptive response to oxidative stress in *Clostridium perfringens* (Briolat and Reysset, 2002) and with a few or medium delay in adaptive response of *Aspergillus fumigates* under heat shock conditions (Albrecht *et al*, 2010). Moreover, this enzyme is involved in different type of stress responses such as salt response in barley (Nakamura *et al*, 2004), pathogen infection and oxidative stress response of transgenic *Arabidopsis* and salt stress response in the halophyte *Apocynum venetum* (Liu *et al*, 2008). A cold-induced RNA helicase unwind cold-stabilized secondary structure in the 5' UTR of RNA in cyanobacteria suggesting that DEAD box proteins are important in different environmental stress adaptations (Nakamura *et al*, 2004).

1.6.3. Splicing Factor RNPS1

Pre-mRNA splicing process includes spliceosome and the small nuclear ribonucleoprotein particles (snRNPs) as well as a large number of non-snRNP protein factors (Sakashita *et al*., 2004). Also, RNPS1 is known as a protein component of the splicing dependent messenger ribonucleoprotein (mRNP) complex, or exon-exon junction complex (EJC), and is also involved in post-splicing processes (Trembley *et al*., 2005). For instance, human RNPS1 is a pre-mRNA splicing activator that has also a role in the post splicing process. The human RNPS1 is a typical RNA-binding protein having a single canonical RRM domain with a characteristic serine-rich domain (S domain) in the N-terminal region while an arginine/serine/proline-rich domain (RS/P domain) is found in C-terminal region. Ribonucleoprotein 1 (RNP1) is the most conserved RRM signature having conserved eight residue motif [RK]-G-[FY]-[GA]-[FY]-[ILV]-X-[FY] (where X is any amino

acid) (Adam *et al*., 1986; Sachs *et al*., 1986 ; Kielkopf *et al*., 2004). In addition, it was also shown by in vitro studies that purified RNPS1 with a limited amount of SF2/ASF synergistically stimulates both constitutive and alternative splicing (Sakashita *et al*., 2004).

RNPS1 was also identified in the complex termed the apoptosis- and splicing-associated protein (ASAP) implying a link between RNA processing and apoptosis. In addition to other functions like splicing activation of constitutive pre-mRNAs, RNPS1 has a potential role in post-splicing processes and regulation of alternatively splicing which is often regulated in response to tissue-specific, physiologic, or developmental signals (Sakashita *et al*., 2004; Trembley *et al*., 2005).

1.6.4. Findings from a recent proteomics study

In the study reported by Yıldırım *et al*., 2011, polyadenylate binding protein, ATP-dependent RNA helicase and splicing factor RNPS1 were identified as up regulated RBPs in response to Pb stress. Polyadenylate binding protein was found in multiple spots in the 2DE gels and one of such spots was observed as a newly induced protein in response to dose-dependent Pb stress (Figure 1.10). Although ATP-dependent RNA helicase did not show any significant change in response to 25 μM Pb, it was found to increase 7.89-fold and 1.86-fold when compared to the control upon exposure to 50 and 100 μM Pb, respectively, in a dose-dependent manner.

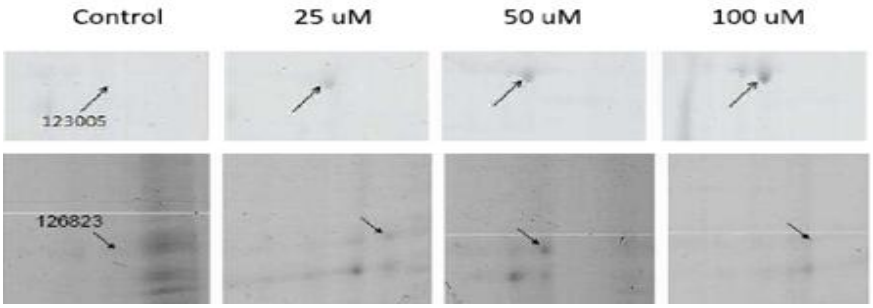

Figure 1.10. Up regulation of polyadenylate binding protein (123005) and ATP-dependent RNA helicase (126823) in response to different doses of Pb exposure (Yıldırım *et al*., 2011).

Splicing factor RNPS1 was upregulated in response to 50 µM Pb in an exposure time-dependent pattern (Figure 1.11). Nearly 3-fold increase in the expression of this protein was identified upon 1h, 2 h and 8 h. Interestingly, the expression of the protein leveled off at 4^{th} h of exposure.

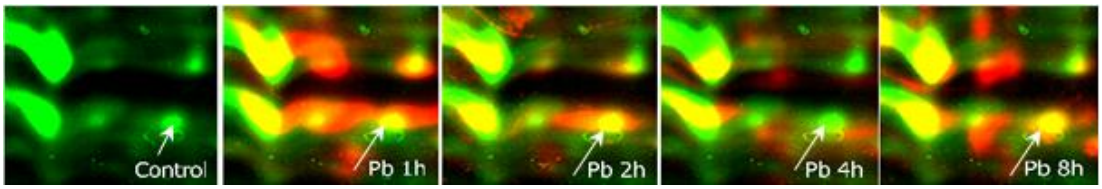

Figure 1.11. Up regulation of splicing factor RNPS1 in response to time-dependent 50 µM Pb exposure as a function of duration of exposure (Yıldırım *et al*., 2011).

Taken together, up-regulation of above-mentioned proteins in *P. chrysosporium* in response to Pb stress strongly suggests that these proteins might act in concert to mediate post-tanscriptional regulations in a direction to overcome Pb toxicity.

1.7. Real Time PCR

The Real Time PCR is a fluorescence based reverse transcription polymerase chain reaction in which data collection is at the time of progress. It combines amplification and detection in a single step (Bustin *et al*., 2005; Wong and Medrano, 2005). It is a powerful, sensitive, economic, reliable, rapid, high throughput technique for the detection of mRNA and gene expression analysis. It has broad application areas such as diagnostics, clinical studies, pathogen detection, forensics, food technology, cancer quantification and functional genomics (Yuan *et al*., 2008).

Most commonly used methods for gene expression analysis are Northern blotting, *in situ* hybridization, cDNA arrays, RNAse protection assays and the reverse transcription polymerase chain reaction (RT-PCR). Real Time PCR has apparent advantages over other quantification techniques by having a larger dynamic range, assay homogeneity, sensitivity, no need for post-amplification manipulation and being a quantitative as well as a qualitative assay (Bustin *et al*., 2005; Yuan *et al*., 2008). Although Northern blotting is an important technique for mRNA analysis and it provides determination of both the size and amount of a specific mRNA as well as alternative splicing, it has relatively low sensitivity (Bustin, 2000). Moreover, high amount of high quality purified RNA is needed and the use of toxic chemicals like formaldehyde/formamide is another disadvantage of Northern blot analysis (Hofstätter *et al*., 2010). In order to compare Northern blot and Real Time PCR (Taqman) techniques with respect to mRNA quantification levels, different subclones of a recombinant EpoFc (erythropoietin-huIgG1Fc fusion protein) producing cell line were analyzed. It was indicated that quantitative PCR (qPCR) results, when compared to the data obtained from two independent Northern blot experiments, gave up to 2-3 times higher expression values, as shown in Figure 1.12. In addition, both methods can be set in direct correlation ($R2 = 0.93$) and the discrepancy was due to the usage of DNA plasmid standard which can lead to methodical errors (Lattenmayer *et al*., 2007; Hofstätter *et al*., 2010).

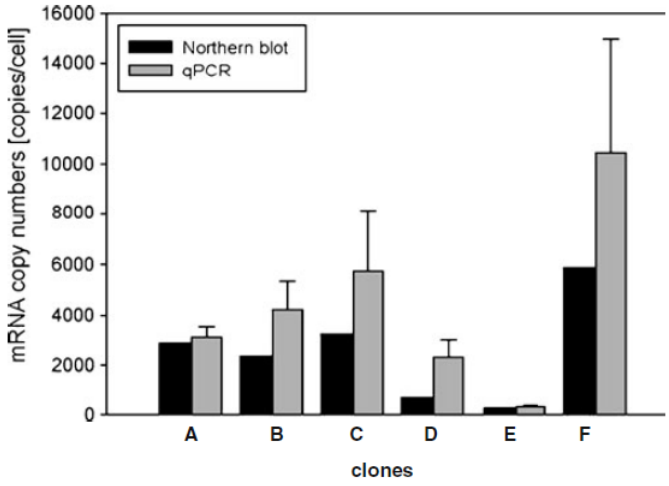

Figure 1.12. The transcript levels of different clones analyzed by Real Time PCR and Northern blot (Lattenmayer *et al*., 2007; Hofstätter *et al*., 2010).

RNase protection assay which is used for mapping transcript initiation and termination sites, intron/exon boundaries and for discriminating between related mRNAs of similar size, is ten times more sensitive technique than Northern blotting due to RNA losses during a blotting step. However, for mRNA quantification, RNase protection assay is less straightforward (Wang and Brown, 1999). Real Time PCR technique has 10,000- to 100,000 times higher sensitivity as compared to RNase protection assays and more importantly even a single copy of a specific transcript can be detected (Wong and Medrano, 2005). Moreover, Real Time PCR can reliably detect gene expression differences as small as 23% and have lower coefficients of variation (cv; SYBR® Green at 14.2%; TaqMan® at 24%) than end point assays such as band densitometry (44.9%) and probe hybridization (45.1%). Also by Real Time PCR, mRNAs with almost identical sequences can be discriminated. Much less RNA template requirement and its high throughputness are very important advantages over other quantification methods (Wong and Medrano, 2005).

Besides its advantages, Real Time PCR has some disadvantages such as necessity of expensive equipment and reagents. Also, careful experimental design and efficient normalization is very crucial and must be optimized due to extremely high sensitivity of the technique, otherwise, there is a high risk of false results (Wong and Medrano, 2005; Hofstätter *et al*., 2010). In addition, Real Time PCR has other problems coming from RT and PCR such as nonspecific product amplifications, primer-dimer formations, amplification efficiency problems and hetero-duplex formation (Pfaffl, 2004).

1.7.1. Principle of Real Time PCR

Real Time PCR is based on the fact that starting amount of template is directly proportional to the quantity of PCR products in exponential phase under ideal conditions (Ginzinger, 2002; Yuan *et al*., 2006; Dussault and Pouliot; 2006). During the exponential phase, at each cycle of amplification, the increase of a fluorescent reporter molecule is detected since it increases as the product accumulates (Dussault and Pouliot; 2006).

Real Time PCR is composed of mainly four major phases; the initial phase, so called linear ground phase composed of 10-15 cycles in which the fluorescence emission at each cycle is below the background fluorescence and baseline fluorescence is determined (Pfaffl, 2004; Wong and Medrano; 2005). Then, the next is exponential phase at which exponential amplification can be detected and fluorescence is above the background. During the exponential phase, PCR product will ideally double during each cycle if efficiency is perfect, i.e. 100%. It is possible to make the PCR amplification efficiency close to 100% in the exponential phases if the PCR conditions, primer characteristics, template purity, and amplicon lengths are optimal (Yuan *et al*., 2006). Third phase has linear amplification efficiency with a steep increase in the fluorescence (Pfaffl, 2004). The final phase is plateau phase defined

as the attenuation in the rate of exponential product accumulation due to limited reaction components and product degradation. Plateau phase covers the later cycles at which the fluorescence is not used for quantification (Pfaffl, 2004; Wong and Medrano; 2005). Real Time PCR is characterized by the PCR cycle at which the target amplification is first detected and fluorescence intensity is greater than the background fluorescence. The cycle at which this occurs is known as cycle threshold (Ct) in ABI Prism® literature (Applied Biosystems, Foster City, CA, USA) or crossing point (CP) in LightCycler® literature (Roche Applied Science, Indianapolis, IN, USA) (Wong and Medrano; 2005). The Ct values are directly proportional to the initial template amount and are used for calculation of experimental results (Ginzinger, 2002). In other words, as the initial target amount is greater, the increase in fluorescent signal is faster and appear as a lower Ct value (Wong and Medrano; 2005). The efficacy of kinetic RT-PCR is also measured by its specificity, low background fluorescence, steep fluorescence increase, high amplification efficiency, and high level plateau (Pfaffl, 2004).

1.7.2. Chemistry of Real Time PCR

There are two methods generally used for the quantitative detection of the amplicons, employing gene-specific fluorescent probes and specific double strand (ds) DNA binding agents, respectively which are based on fluorescence resonance energy transfer (FRET). SYBR Green I (Figure 1.13. A) is a fluorescent intercalating dsDNA binding dye which is not sequence specific (Pfaffl, 2004). ABI's TaqMan (Figure 1.13.B) is an example of probe based system which exploits the 5'-3' exonuclease activity of *Taq* polymerase for quantification. Another one is Probe hydrolysis (Figure 1.13.C) system that separates fluorophore and quencher which results in an increased fluorescence signal called "Förster type energy transfer" (Pfaffl, 2004). Molecular beacons (Figure 1.13.D), which consist of a sequence-specific region (loop region) flanked by two inverted repeats, are the simplest hairpin

probe. Scorpions (Figure 1.13.E) combine the detection probe with the upstream PCR primer and consist of a fluorophore on the 5′ end, followed by a complementary stem-loop structure, quencher dye, DNA polymerase blocker and final PCR primer on the 3′ end. In addition, there are some other chemistries; Sunrise™ primers (Figure 1.13.F) created by Oncor (Gaithersburg, MD, USA), LUX™ (Figure 1.13.G) fluorogenic primers (Invitrogen, Carlsbad, CA, USA) (Wong and Medrano, 2005).

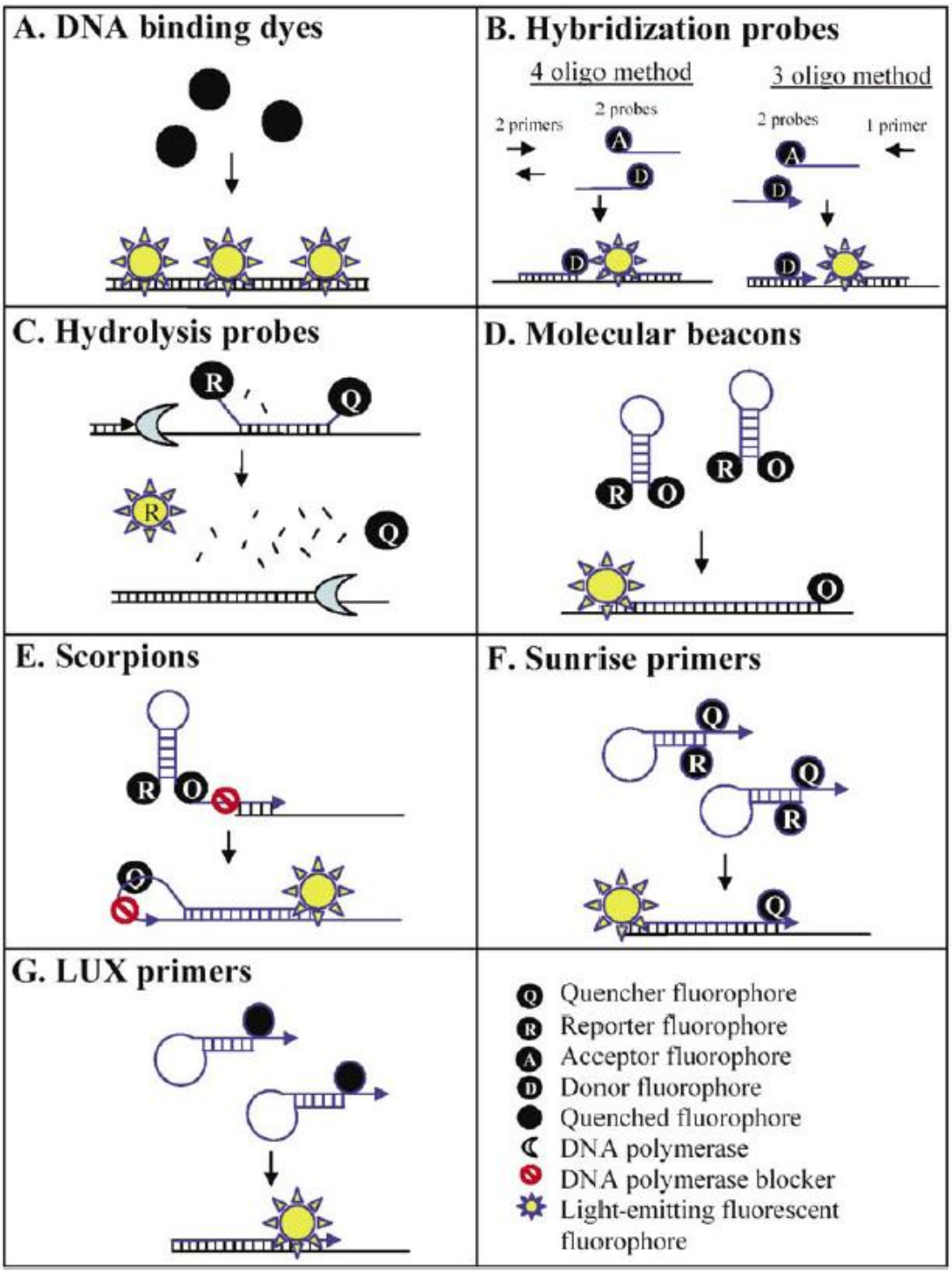

Figure 1.13. Real Time PCR quantification strategies (Wong and Medrano, 2005).

1.7.3. Quantification strategies in Real Time PCR

Real Time PCR products can be quantitated by two approaches namely; absolute and relative quantification methods (Chini *et al*, 2007; Dussault and Pouliot, 2006). The choice of quantification method mainly depends on the target sequence, mRNA amount and the degree of accuracy required. In absolute quantification based on the calibration curve, PCR signal is related to the input copy number whereas, relative quantification provides the relative change in the mRNA levels with respect to a reference sample (Pfaffl, 2004; Chini *et al*, 2007).

1.7.3.1. Absolute quantification

Absolute quantification can be the method of choice in situations where determination of the absolute transcript copy number is necessary (Livak and Schmittgen, 2001). In absolute quantification, the absolute mRNA copy number is determined in comparison to appropriate external calibration or standard curves (Pfaffl *et al*., 2002). The standard curve that is used for quantification is generally derived from plasmid DNA or other forms of DNA (Dussault and Pouliot, 2006). The standards having known concentrations are used for generating a calibration curve by serial dilution.

Real Time PCR can be performed via two different methods namely; one step and two step reaction. One step Real Time PCR uses RNA as template and both cDNA synthesis and Real Time PCR are performed in a single tube. On the other hand, two step Real Time PCR method, cDNA synthesis and Real Time PCR are separated. Experimental variation is minimized by one step reaction, but it uses RNA as a template prone to degradation problem. Two step reaction is quite reproducible and eliminates primer dimers, but quite vulnerable to contamination (Wong and Medrano 2005).

For the construction of standards for two-step Real Time PCR, the target sequence can be synthesized by cloning into a plasmid or purified by conventional PCR or synthesized directly. DNA standards have a large range of quantification, highly sensitive, stable and reproducible as compared to RNA standards (Pfaffl, 2004; Wong and Medrano; 2005). The dynamic range of calibration curve can be nine orders of magnitude from $< 10^1$ to $> 10^{10}$ start molecules, depending on the applied standard (Pfaffl, 2004). In addition, there is a linear relationship between Ct and initial amount of total RNA or cDNA in the standard curve which allows quantification of knowns based on their Ct values (Wong and Medrano; 2005). Moreover, PCR efficiency should be the same for the standards and the samples of interest (Dussault and Pouliot, 2006). It is easier to use data of different days or laboratories in order to compare the expression by using absolute quantification. Since the calibration curve is not changing and has a reliable basis (Pfaffl *et al*., 2002).

1.7.3.2. Relative quantification

Nowadays, the use of relative expression is increasing and target gene is standardized by a non-regulated reference gene to compensate the differences in the RT-PCR input quality and quantity (Pfaffl *et al*., 2002; Cikos *et al*., 2007). However, the selection of appropriate control genes that have an equal expression across all samples can be a challenge (Dussault and Pouliot, 2006). Relative quantification is adequate in order to investigate physiological changes in gene expression levels (Pfaffl, 2004). The amount of target mRNA in samples relative to each other can be quantified by relative quantification (Cikos *et al*., 2007). In order to quantify the relative changes in gene expression by using real-time PCR, certain assumptions or equations based on Real Time PCR efficiency and the crossing point deviation of an unknown sample versus a control are required (Livak and Schmittgen, 2001; Pfaffl *et al*., 2002; Chang *et al*., 2009).

In some models, it is assumed that the amplification efficiency of the reaction is ideal and the PCR product doubles at each cycle during the exponential phase of the reaction. However, due to the decrease in the PCR components and polymerase activity, and as well as PCR product competition, amplification efficiency changes from a relatively stable state in the early exponential phase and then gradually declining to zero. Therefore, amplification efficiency is important for the reliable relative quantification (Wong and Medrano 2005).

For the data analysis in Real Time PCR, stable and accurate mathematical model for relative quantification is crucial (Chang *et al*., 2009). There are numerous models available, but two different relative mRNA quantification models are frequently used, namely the delta delta Ct (ΔΔCt) and the efficiency-corrected Ct model (Fleige *et al*., 2006; Chang *et al*., 2009). Both of these models have their advantages and disadvantages in terms of simplification and efficiency correction (Fleige *et al*., 2006). $2^{-\Delta\Delta Ct}$ method is one of the most commonly used methods, it is valid when the target and the reference gene have the same amplification efficiency. The quantification includes normalization by a reference gene and gives relative ratio to control (Livak and Schmittgen, 2001).The formula used for such quantification is as follows:

$R=2^{-(\Delta\Delta Ct)}$ where;

$(\Delta\Delta Ct) = (\Delta Ct \text{ target} - \Delta Ct \text{ reference})_{\text{treated samples}} - (\Delta Ct \text{ target} - \Delta Ct \text{ reference})_{\text{untreated control}}$

On the other hand, efficiency corrected Ct model gives relative quantification of a target gene in comparison to a reference gene by including amplification efficiencies of target and reference gene (Pfaffl, 2002). Also, amplification efficiency is calculated by using data collected from a standard curve as based on the following formula (Wong and Medrano; 2005).

$$\text{Exponential amplification} = 10^{(-1/\text{slope})}$$

$$\text{Efficiency} = [10^{(-1/\text{slope})}]^{-1}$$

The equation used for relative quantification in the efficiency corrected Ct model which is described by Pfaffll (2002) is shown below;

$$\text{ratio} = \frac{(E_{\text{target}})^{\Delta CP}{}_{\text{target}}\ (\text{control} - \text{sample})}{(E_{\text{reference}})^{\Delta CP}{}_{\text{reference}}\ (\text{control} - \text{sample})}$$

Several software tools have been developed to accomplish relative quantification results. For example, the relative expression software tool (REST©) provides an automated data analysis based on the same principle described by Pfaffl (2002). In addition, REST calculate the significance of the results based on the Pairwise Fixed Reallocation Randomization Test© and indicates whether the reference gene is suitable for normalization or not (Pfaffl, 2002; Wong and Medrano; 2005).

When compared to absolute quantification, relative quantification is easier to perform since a calibration curve is not required. In addition, in relative quantification, standards having known concentrations are not necessary and the reference can be any transcript which has a known sequence. The units used for the expression of relative quantities are irrelevant and the relative quantities can be compared across multiple real-time RT-PCR experiments (Pfaffl, 2004).

1.8. Aim of the present study

The cytosolic proteome map of *P. chrysosporium*, a biotechnologically important fungus, was constructed earlier (Özcan *et al*., 2007) and the dynamic changes in cytosolic protein expressions upon exposure to lead (Pb) were studied by our group (Yıldırım *et al*, 2011). Polyadenylate binding protein, ATP-dependent RNA helicase and splicing factor RNPS1 were shown to be among the upregulated proteins in response to Pb stress. In that study, it was thought that these proteins might be induced to act together in order to regulate gene expression analysis via post-transcriptional processes for adaptation to Pb toxicity for which Q-RT PCR could provide a better understanding. Based on this, the aim of the present study is to find out the effect of Pb stress on the expression of the genes coding for ATP-dependent RNA helicase, splicing factor RNPS1 and polyadenylate binding proteins.

CHAPTER 2

MATERIALS AND METHODS

2.1. Microorganism and its maintenance

The *Phanerochaete chrysosporium* (ATTC 24725) used in this study was kindly provided by Professor Filiz B. Dilek (Environmental Engineering Department, METU). For the sporulation process, the organism was inoculated to Sabaroud Dextrose agar slants (Appendix A) and incubated for 4 days at 35 ^{o}C. The organism was maintained on agar slants at 4 ^{o}C and transferred monthly.

2.2. Culture conditions and preparation of biomass

P. chrysosporium spore suspension were prepared by scrapping the spores from Sabaroud Dextrose agar slant surfaces with sterilized distilled water and homogenized gently by using a teflon homogenizer (Yetiş *et al*. 2000). The spore suspension containing 2.5 x 10^6 spores /ml at an absorbance of 0.5 at 650 nm was inoculated into 250 ml Erlenmayer flasks each containing 150 ml of the growth medium (Appendix A) which was described by Prouty (1990). The cultures were grown at 35 ^{o}C (200 rpm) for 40 h. The growth was terminated while the cultures were still in the exponential growth and the diameter of bead-like mycelia was 2.5 to 4 mm (Özcan, 2003).

2.3. Heavy metal exposure

In order to determine Pb (II)-induced changes as a function of Pb (II) concentration, the cultures containing 25, 50 and 100 μM $Pb(NO_3)_2$ were incubated in parallel for 40 h. The cells were then removed by filtration, washed twice with distilled water and stored at –80 ^oC for RNA isolation. To see the effect of duration of temporal exposure to lead, $Pb(NO_3)_2$ solution was added at 25, 50 or 100 μM final concentration to a 40-h old culture which was further cultivated for 1, 2, 4 and 8 h, respectively before harvesting. The time intervals were selected based on the growth curve constructed earlier (Parlakgöz, 1997 and Yetiş *et al*., 2000) and doubling time (5.2 h) of the organism (Michel *et al*., 1991). A negative control culture without lead exposure and two biological replicates of each set were also included in the same set of experiment for each of the above-mentioned variables.

2.4. Total RNA isolation

2.4.1. Manual total RNA isolation

For the isolation of total RNAs, after crushing the cells with liquid nitrogen, phenol-chloroform-isoamyl alcohol extraction was performed as described by Kempken *et al*. (1996). Shortly after breaking harvested mycelium in liquid nitrogen, an equal amount of boiling extraction buffer (Appendix B) was added and mixed, then centrifuged at 4000 rpm for 15 min. The pellet was decanted, the supernatant was extracted twice with phenol-chloroform-isoamyl alcohol (25:24:1) and centrifuged at 10000 g for 20 min. After an additional extraction with chloroform- isoamyl alcohol (24:1), the supernatant was incubated with LiCl to a final concentration of 2 M at -20 ^oC for 2 h. Then, remaining pellet was washed with 96.7 % ethanol and dissolved in 50 μl DEPC distilled water. The RNAs isolated by using this procedure represented

total RNAs since LiCl selectively precipitates RNA. The isolated RNA samples were kept at -80 ^{o}C for long period storage.

In addition, another manual RNA isolation method was also performed as in Mukthar *et al*. (1998). Similarly, cells were crushed with liquid nitrogen and were mixed with solution D (Appendix B). At the same time, 0.05 ml of 2 M sodium acetate (pH 4), 0.5 ml of water saturated phenol, and 0.2 ml of chloroform-iso-amyl alcohol mixture (49:1) were added and mixed by inversion after the addition of each reagent. The mixture was shaked vigorously for 10 sec. and incubated for 15 min. on ice. Then, the suspension was centrifuged for 10,000 g for 20 min. at 4 °C. Afterwards, the aqueous phase was taken and mixed with 1 ml of isopropanol. In order to precipitate RNA, the mixture was incubated at -20 °C for 2.5 h and then centrifuged 10,000 g for 20 min. The obtained pellet containing RNA was dissolved in solution D and further incubated with isopropanol at -20 °C for 1 h and centrifuge for 10 min at 10,000 g. The RNA pellet was suspended in 1 ml of 75 % ethanol followed by centrifugation for 10 min. at 10,000 g. Finally, RNA pellet was vacuum dried and dissolved in 50 µL depC water.

2.4.2. Total RNA isolation with RNeasy mini kit

Qiagen RNeasy Mini Kit (Appendix C) was used for total RNA isolation according to the manufacturer's instructions. After crushing the cells with liquid nitrogen, 600µl RLT Buffer was added to the powder and mixed by vortex. Next, 300 µl of aquaphenol (water saturated) (Appendix C) and 300 µl of chloroform-isoamyl alcohol mix was added and the solution was mixed by inversion. This step was followed by the transfer of mixture to the gel lock tubes and centrifugation at top speed for 5 min The supernatant was taken to a new tube and mixed with 150 µl RLT Buffer plus 400 µl of pure ethanol (Appendix C). The mixture was then transferred to an RNeasy Column in a 2 mL collection tube and centrifuged at 10.000 rpm for 15 sec The flow-through was discarded and 350 µl of RW1 Buffer was added to the

RNeasy Column. After centrifugation at 10.00 rpm for 15 sec, 10 µl Dnase was mixed with 70 µl of RDD buffer then added to the column and incubated at 30 °C for 30 min. This step was repeated and the mixture was centrifuged at 10.000 rpm for 15 sec. after the addition of 350 µl RW1 and flow through was discarded again. Next, 500 µl of RPE Buffer was added to the column and it was centrifuged at 10.000 rpm for 15 sec. After the addition of 500 µl RPE Buffer to the column, it was centrifuged for 2 min and flow through was poured off. The RNeasy column was taken into a new Eppendorf and at first 30 µl of Rnase free water added and incubated for 2 minute followed by centrifugation at 10.000 rpm for 1 min. Then additional 20 µl of Rnase free water was added to the column and incubated for 2 min followed by centrifugation at 10.000 rpm for 2 min and in total 50 µl RNA was eluted.

2.4.3. Dnase treatment

For the removal of remaining DNAs, 5 µl of DNase buffer (Appendix C) and 2 µl of DNase (Appendix C) were added to 50 µl of eluted RNA sample. It was followed by the incubation at 37 ^{o}C for 30 min. Afterwards, 1 µl of DNase was added again and it was further incubated at 37 ^{o}C for 15 min. For the inactivation, 10 µl of DNase inactivation reagent was added and centrifuged at top speed for 2 min. Finally the supernatant which contains RNA sample was taken to a new Eppendorf tube which was stored at – 80 ^{o}C.

2.4.4. Quantitation of RNA

To determine the concentration and purity of total RNA samples, Thermo Nanodrop2000 (Thermo Scientific, Wilmington, DE, USA) was used according to the manufacturer instructions. 1.5 µl of 1/10 diluted total RNA sample was used to

determine RNA concentration in ng/µl. The purity of the samples was determined by their A_{260}/A_{280} ratio which should be equal to 2.0±0.1.

2.5. Isolation of genomic DNA

Genomic DNA isolation was performed as described by Lim *et al* (2007). After crushing the cells with liquid nitrogen, lysis buffer (Appendix B) having an equal amount with the crushed sample and 60 µl Proteinase K (20mg/ml) and 20 µl RNase A (10 mg/ml) was added. Afterwards, the mixture was incubated at 37 ^{o}C for 1 h and centrifuged at 4000 g for 15 min. The supernatant part was taken and extracted twice with phenol-chloroform-isoamyl alcohol (25:24:1) and centrifuged at 10.000 rpm for 15 min. Additional extraction was performed by using chloroform and followed by centrifugation at 10.000 rpm for 15 min. Then, the purified DNA was precipitated with 0.7 vol. of isopropanol and centrifuged at 5.000 rpm for 20 min. The pellet was washed with 70% ethanol, dried at 37 °C, and then resuspended in 300 µl of TE Buffer (Appendix B).

2.6. cDNA synthesis and RT-PCR

First strand cDNA synthesis was performed using 1 µg of total RNA with Roche Transcriptor First Strand cDNA Synthesis Kit (Appendix C) in recommended conditions. The reaction mixture was prepared by adding total RNA, 1 µl of primer (Anchored oligo$(dT)_{18}$) and PCR-grade water up to 13 µl. Then, denaturation of the template-primer mixture was achieved by incubating the mixture for 10 min at 65 ^{o}C. After addition of Transcriptor Reverse Transcriptase Reaction Buffer (4 µl), Protector Rnase Inhibitor (0,5 µl), deoxynucleotide mix (2 µl, 10mM each) and Transcriptor Reverse Transcriptase (0,5 µl), total of 20 µl mixture was incubated at 55 ^{o}C for 30 min for the synthesis. Finally, the reaction was terminated by incubating

for 5 min at 85 ^{o}C which leads to inactivation of Transcriptor Reverse Transcriptase. The cDNA was kept at -20 ^{o}C for long period storage.

For the splicing factor RNPS1 (8607), cDNA synthesis was performed as described above with a minor difference; instead of oligo (dT), a specific primer (reverse primer) was used.

The synthesized cDNA was used as the template for RT-PCR. Optimized RT-PCR mixture was as follows; 3 µl $MgCl_2$ (25 mM), 5 µl PCR Buffer-$MgCl_2$ + KCl (10X), 1 µl dNTP mix (10 mM each), 2 µl cDNA template, 2 µl each primer (10µM), 1 µl Taq polymerase (5u/µl) and 34 µl dH_2O. After initial denaturation at 94 ^{o}C for 10 min, Taq polymerase was added. Optimized RT-PCR conditions were as follows; denaturation at 94 ^{o}C for 2 min, annealing 60 ^{o}C for 1 min, extension at 72 ^{o}C for 20 sec and final extension at 72 ^{o}C for 10 min. RT-PCR cycles were set as 29 cycles for all genes.

2.7. Primer design

The nucleotide sequences and locations of the primers used in this study is given in the Table 2.1. Primers were designed according to the sequences obtained from the DOE Joint Genome Institute's *P. chrysosporium* genomic database. The primers were synthesized at Iontek Co.

Table 2.1. Sequences and locations of oligonucleotide primers

Primer	Oligonucleotide Sequence	Amplicon Size (bp)	Location Start-Stop
8607 F	CTCTCGACGGCGCACACCTC	144	191-210
8607 R	TGAGCTTGTAACCCCGCGCA		334-315
123005 F	AAGAACCTTGACCCCGAAGT	110	700-719
123005 R	CCCTTGCTCTTACCCTCCTC		809-790
126823 F	CCACAACATCCAGCAGATTG	146	930-949
126823 R	ACTTCGTGATATCATCCGCC		1075-1056
4000667 F	GCGCCAAACACGGAGGGTCA	111	649-668
4000667 R	GAGGGTTCCCGTGGTGTCGC		759-740

2.8. Agarose gel electrophoresis and ethidium bromide staining

Agarose gel electrophoresis was performed by using a horizontal electrophoresis apparatus. Depending on the sample properties, 1-1.5 % agarose gel was prepared with TAE buffer (Appendix C) and loading dye (6X) was added to the samples. Afterwards, 90 Volts were applied for 45-60 min. For staining, agarose gel was incubated in ethidium bromide solution (0.4 ng/ml) for 5-10 min. The bands were visualized and photographed by UV transilluminator (UVP) and Vilber Lourmat Gel Imaging System respectively. In order to determine the molecular weights of the bands O'GeneRuler 100 bp DNA Ladder Plus (Appendix C) was used.

2.9. Real Time PCR (Q-PCR)

Real Time PCR was performed in glass capillary tubes with Roche LightCycler® 1.5 Instrument (Basel, Switzerland). Lightcycler FastStart DNA Master Sybergreen I Kit was used for Real Time PCR reaction according to instructions. Each reaction mixture contained 2 µl of cDNA as a template, 0.3 µM of each primer, 2 mM $MgCl_2$ and 1X SyberGreen I. Optimized amplification condition for the genes under study was represented in the Table 2.1. Three independent Real Time PCR runs were performed and each run included two biological replicates and two technical replicates for each sample. NTC (no template control) having dH_2O instead of cDNA was also included to detect the background signal and unwanted primer dimer formation.

Melting curve analysis was also performed as shown in the Table 2.2 and melting peaks were formed by plotting –d/dT Fluorescence (530) vs temperature (^oC) in order to ensure that a single product was amplified.

Table 2.2. Real Time PCR conditions

Analysis Mode		**Temperature, Time**	**Cycle**
Initial Denaturation		95 ^{o}C, 10 min.	1 cycle
Amplification	Denaturation	95 ^{o}C, 10 sec.	
	Annealing	60 ^{o}C, 10 sec.	45 cycles
	Extension	72 ^{o}C, 10 sec.	
Melting Analysis		65 ^{o}C-95 ^{o}C, 15 sec. 0.1 ^{o}C/sec.	1 cycle
Cooling		40 ^{o}C, 30 sec.	1 cycle

Sample maximization method was used for the Real Time PCR experiments since it is the most appropriate choice when the expression levels of a particular gene having different samples are investigated. The most important point is that there is no run-to-run technical variation between samples. According to the sample maximization method, each hour for target and reference gene are amplified in the same run as suggested by Hellemans *et al*., 2007; and Dervaux *et al*., 2010.

2.9.1. Evaluation of Real Time PCR data

The relative quantification which is valid for the investigation of the physiological changes in gene expression was used for the quantification of Real Time PCR data.

In order to get the relative quantity of target mRNA, the fluorescent data from Real Time PCR must be evaluated according to data analysis methods (Cikos *et al*., 2007). The relative quantification was based on the relative expression of a target gene normalized by a reference gene, which is mainly a non-regulated gene or housekeeping gene. Besides, the relative expression ratio is calculated only from the Real Time PCR efficiencies and the crossing point deviation of an unknown sample versus a control (Pfaffl, 2001; Livak and Schmittgen, 2001). In this study, the mathematical model below (Pfaffl, 2002) which includes an efficiency correction was used for the quantification and crossing points (Cp) were determined by the 'Second Derivative Maximum Method' of LightCycler software 4.01 (Roche Diagnostics) (Pfaffl *et al*., 2002).

$$\text{ratio} = \frac{(E_{\text{target}})^{\Delta CP}{}_{\text{target}}\ (\text{control} - \text{sample})}{(E_{\text{reference}})^{\Delta CP}{}_{\text{reference}}\ (\text{control} - \text{sample})}$$

2.9.2. Statistical analysis of Real Time PCR data

Real Time PCR data was collected from three independent runs and each run included two biological replicates and two technical replicates for each sample. One way ANOVA test was carried out by using Graphpad Prism (Graphpad Software. San Diego,CA) to determine whether the differences in the gene expressions are statistically significant ($p < 0.05$). The significance levels were represented as * ($p<0.05$), ** ($p<0.01$) and *** ($p<0.001$). In addition, individual pair differences were determined by TukeyHSDpost-hoc test.

CHAPTER 3

RESULTS AND DISCUSSION

3.1. Total RNA isolation and reverse transcription PCR

3.1.1. Manual total RNA isolation

Two different methods described by Kempken and Kück, (1996) and Mukhtar *et al*., (1998) were used for the isolation of total RNA from *P. chrysosporium*. Although both methods are based on phenol, chloroform, isoamylalcohol extraction the former uses boric acid while the latter uses guanidium thiocyanate in lysis buffer.

Total RNA samples prepared by these procedures were analyzed with Thermo Nanodrop2000 (Thermo Scientific, Wilmington, DE, USA) and 1/10 diluted samples had 221.94 and 431.54 ng/µl with $A_{260/280}$ ratios of 2.22 and 2.18. After electrophoresis of the isolated RNA by using both methods (Figure 3.1) the method described by Kempken and Kück, (1996) was chosen for the isolation of total RNA from *P. chrysosporium.* Although it gave less amount of RNA, we had higher quality of RNA bands.

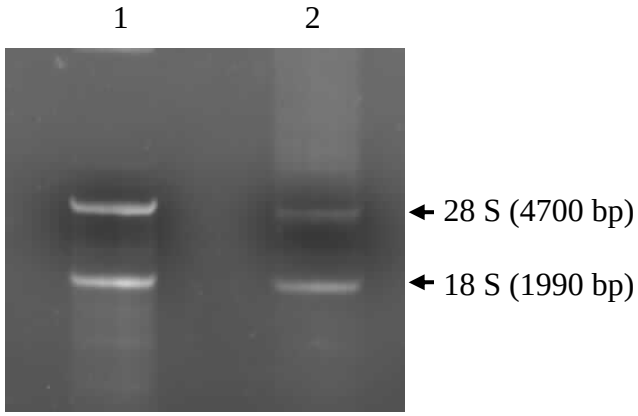

Figure 3.1. Total RNA isolated with two different methods described by Kempken and Kück, 1996 (1st lane) and Mukhtar *et al*., 1998 (2nd lane), respectively.

Figure 3.2 and 3.3 show total RNAs isolated from different cultures that will be compared for RBP gene expression levels. Nanodrop quantification of RNA from the respective cultures are tabulated in Table 3.1 and Table 3.2.

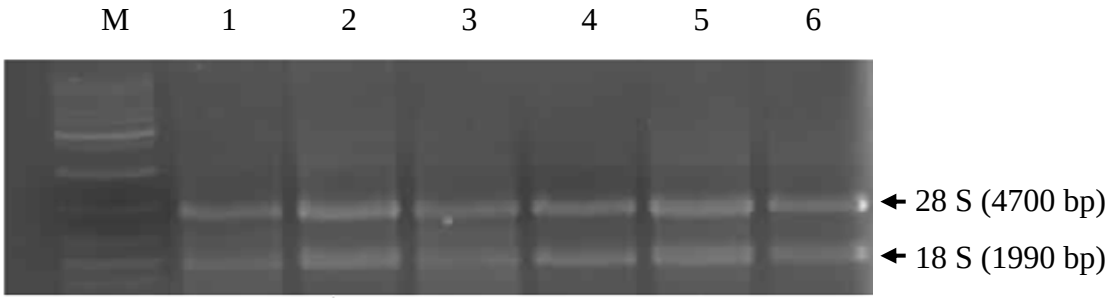

Figure 3.2. Total RNAs isolated manually from cultures exposed 25 and 50 µM Pb. Lane 1: O'GeneRuler 100 bp DNA ladder plus, 2 and 5: Control samples, 2 and 5: 25 µM Pb exposure, 3 and 6: 50 µM Pb exposure.

Table 3.1. Quantification of RNA isolated from the cultures exposed to different doses of Pb.

RNA Samples	260	260/280	ng / µl
1- Control	7.24	2.21	289.53
2- 25 µM Pb	5.68	2.28	227.23
3- 50 µM Pb	6.67	2.26	266.73
4- Control	14.06	2.11	562.41
5- 25 µM Pb	8.97	2.31	358.78
6- 50 µM Pb	11.75	2.16	470.15

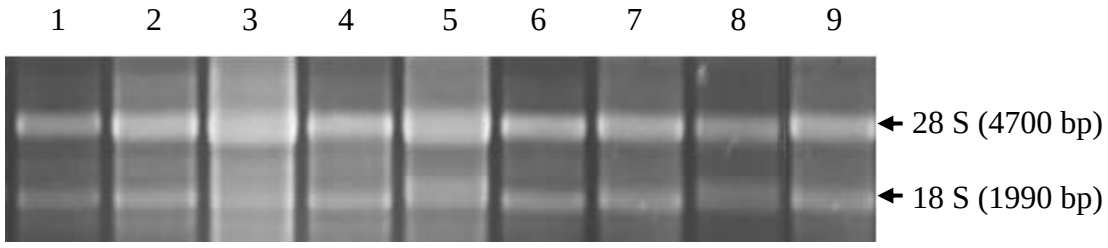

Figure 3.3. Total RNAs isolated manually from cultures exposed to Pb (50 µM) for different time periods. Lane 1: Control 0 hr, Lanes 2, 4, 6, 8: Control and Lanes 3, 5, 7, 9: 50 µM Pb exposure for 1 h, 2 h, 4 h and 8h, respectively.

Table 3.2. Quantification of RNA isolated the cultures exposed to 50 µM Pb for different time periods.

RNA Samples	260nm	260/280	ng/ µl
1- Control 0 h	5,54	2,34	221,70
2- Control 1h	4,20	2,29	167,97
3- Pb exposure 1h	6,53	2,25	263,46
4 -Control 2h	1,96	2,33	78,59
5 -Pb exposure 2h	4,87	2,26	194,78
6 -Control 4h	2,93	2,34	117,00
7 -Pb exposure 4h	10,40	2,15	416,17
8- Control 8h	4,07	2,27	162,83
9-Pb exposure 8h	9,89	2,15	395,67

3.1.2. Reverse transcription PCR (RT-PCR) for manually isolated RNA

RNA samples mentioned in section 3.1.1. were used as the templates for reverse transcription reaction and further amplified with the conventional thermal cycler. The RT-PCR conditions were optimized as follows; initial denaturation at 94 ^{o}C for 10 min (Taq polymerase was added); denaturation at 94 ^{o}C for 2 min, annealing 60 ^{o}C for 1 min, extension at 72 ^{o}C for 20 sec and final extension at 72 ^{o}C for 10 min. RT-PCR cycles were set as 29 cycles for all genes. Expected product sizes are 146 bp, 144 bp, 111 bp, 110 bp for the genes with respective protein identification numbers of 126823, 8607, 4000667 and 123005, respectively. RT-PCR experiments were performed for polyadenylate binding protein and ATP-dependent RNA helicase

together with the reference gene hexokinase (data not shown). However, Real Time PCR experiments gave inconsistent results. This was thought to be due to the low quality of the RNA samples obtained by using the manual method. Therefore, a decision was made to use RNeasy mini kit in order to obtain high quality RNA.

3.1.3. Total RNA isolation with RNeasy mini kit

The modified isolation protocol of RNeasy mini kit (Quiagen) was used for total RNA isolation in order to get consistent Real Time PCR data. For both dose-and time-dependent Pb exposure experiments, three concentrations of Pb (25, 50 and 100 μM) were included in order to perform a more comprehensive analysis. The RNA samples were run on agarose gel electrophoresis as shown in Figure 3.4. and 3.5. These samples were further used for cDNA synthesis.

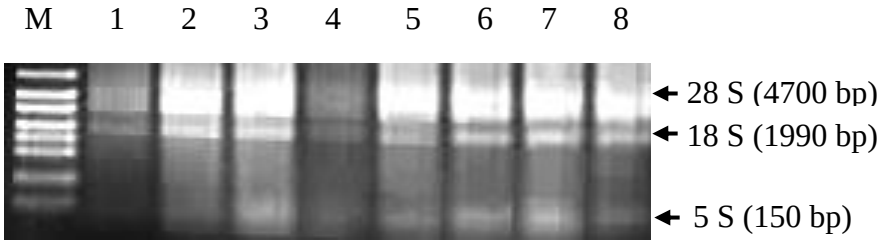

Figure 3.4. Total RNAs isolated with RNeasy mini kit from cultures exposed to different doses of Pb. Lane M: RNA ladder. Lane 1 and 4: Control. Lane 2 and 5: 25 μM Pb exposure. Lane 3 and 6: 50 μM Pb exposure. Lane 4 and 8: 100 μM Pb exposure.

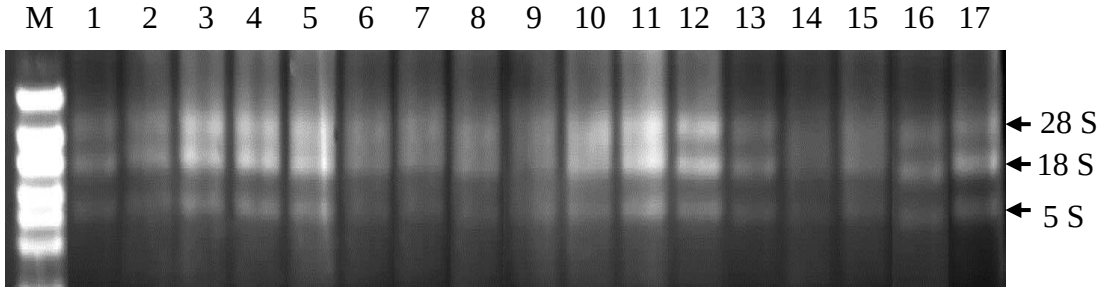

Figure 3.5. Total RNAs isolated with RNeasy mini kit from cultures exposed to 25, 50 and 100 μM Pb for different time periods. Lane M: Marker. Lane 1: Control 0 h. Lane 2, 6, 10, 14: Control and Lanes 3, 7, 11, 15: 25 μM Pb exposure, Lanes 4, 8, 12, 16: 50 μM Pb exposure, Lanes: 5, 9, 13, 17: 100 μM Pb exposure of 1 h, 2 h, 4 h, 8 h, respectively.

Isolated RNA samples were used for cDNA synthesis in order to use for both RT-PCR and Real Time PCR studies.

3.1.4. Reverse transcription PCR (RT-PCR) for RNA isolated using RNeasy mini kit

3.1.4.1. RT-PCR results for dose-dependent Pb exposure

The RT-PCR experiments of the dose-dependent Pb exposure revealed that there was not a change in the expression of the reference gene hexokinase upon Pb exposure (Figure 3.6a). On the other hand, the expression level of ATP-dependent RNA helicase was increased upon exposure to 50 and 100 μM Pb but no visible change was observed upon 25 μM Pb exposure as compared to control with no Pb exposure (Figure 3.6b).

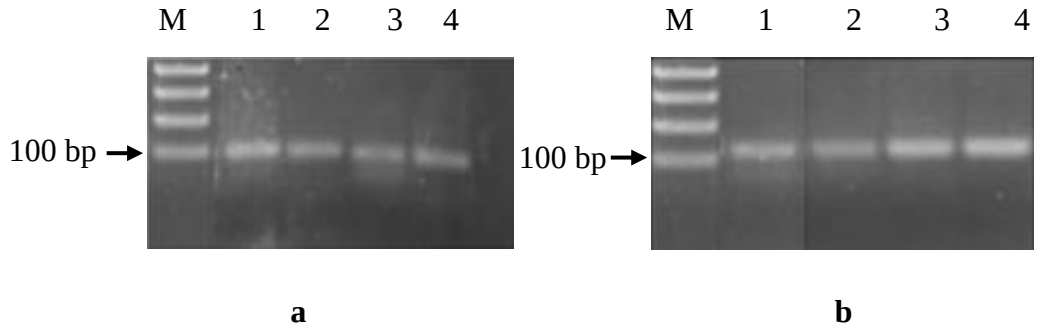

Figure 3.6. RT-PCR analyses of the expression of the genes encoding hexokinase (a) and ATP-dependent RNA helicase (b) in response to Pb (25, 50 and 100 μM) exposure. Lane M: 100 bp DNA ladder. Lane 1: Control without Pb exposure. Lane 2: 25 μM Pb exposure. Lane 3: 50 μM Pb exposure. Lane 4 : 100 μM Pb exposure.

Expression levels of polyadenylate binding protein and hexokinase were also compared upon 25, 50 and 100 μM Pb exposure (Figure 3.7a,b). According to the agarose gel visualization, no change in the expression levels of polyadenylate binding protein and hexokinase were observed at different Pb concentrations.

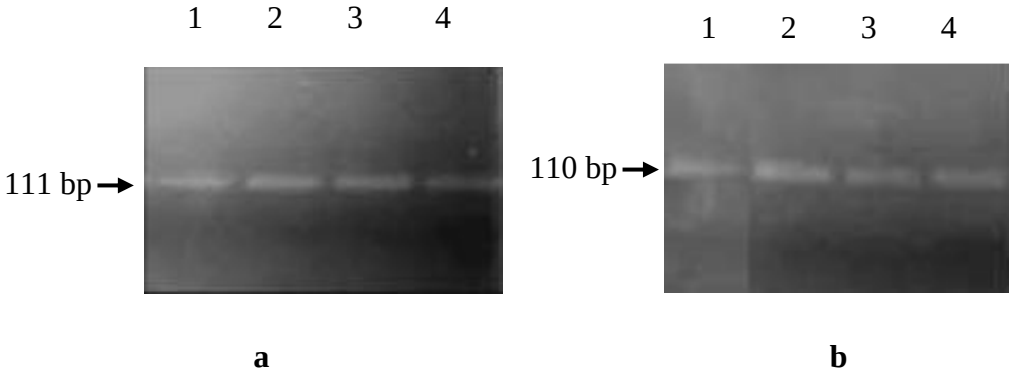

Figure 3.7. RT-PCR analyses of the expression of the genes encoding hexokinase (a) and polyadenylate binding protein (b) in response to Pb (25, 50 and 100 μM) exposure. Lane M: 100 bp DNA ladder. Lane 1: Control without Pb exposure. Lane 2: 25 μM Pb exposure. Lane 3: 50 μM Pb exposure. Lane 4: 100 μM Pb exposure.

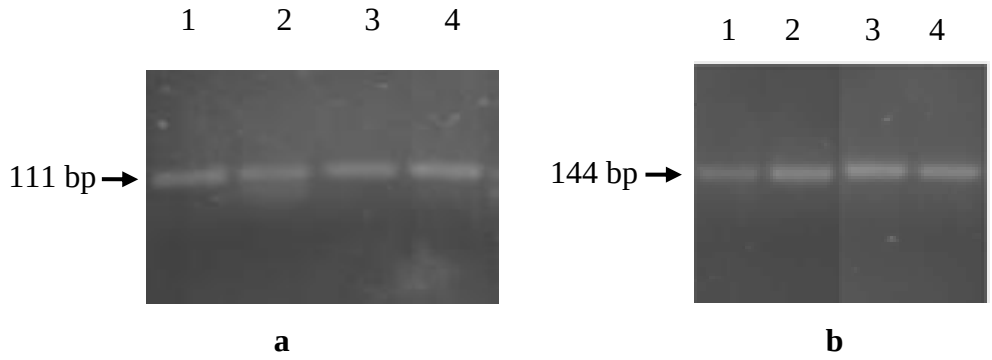

Figure 3.8. RT-PCR analyses of the expression of the genes encoding hexokinase (a) and splicing factor RNPS1 (b) in response to dose-dependent Pb (25, 50 and 100 μM) exposure. Lane M: 100 bp DNA ladder. Lane 1: Control without Pb exposure. Lane 2: 25 μM Pb exposure. Lane 3: 50 μM Pb exposure. Lane 4: 100 μM Pb exposure.

According to the RT-PCR results, the expression of hexokinase gene was not altered in response to Pb exposures (Figure 3.8a) whereas transcription levels of splicing factor RNPS1 were increased when the cells were exposed to 25, 50 and 100 μM Pb (Figure 3.8b).

3.1.4.2. RT-PCR results for time-dependent Pb exposure

RT-PCR experiments were performed to analyze the expression of the genes coding for splicing factor RNPS1, hexokinase, ATP-dependent RNA helicase and polyadenylate binding protein exposed to 25 μM, 50 μM, 100 μM Pb for 1 h, 2 h, 4 h and 8 h. An increament was observed for the expression levels of polyadenylate binding protein in the presence of 100 μM Pb for 1h (Figure 3.9c) and splicing factor RNPS1 in the presence of 50 μM Pb for 2h (Figure 3.10b). Neverthless, no change was observed in the transcription levels for the rest of experimental setups (Figure 3.9-3.12).

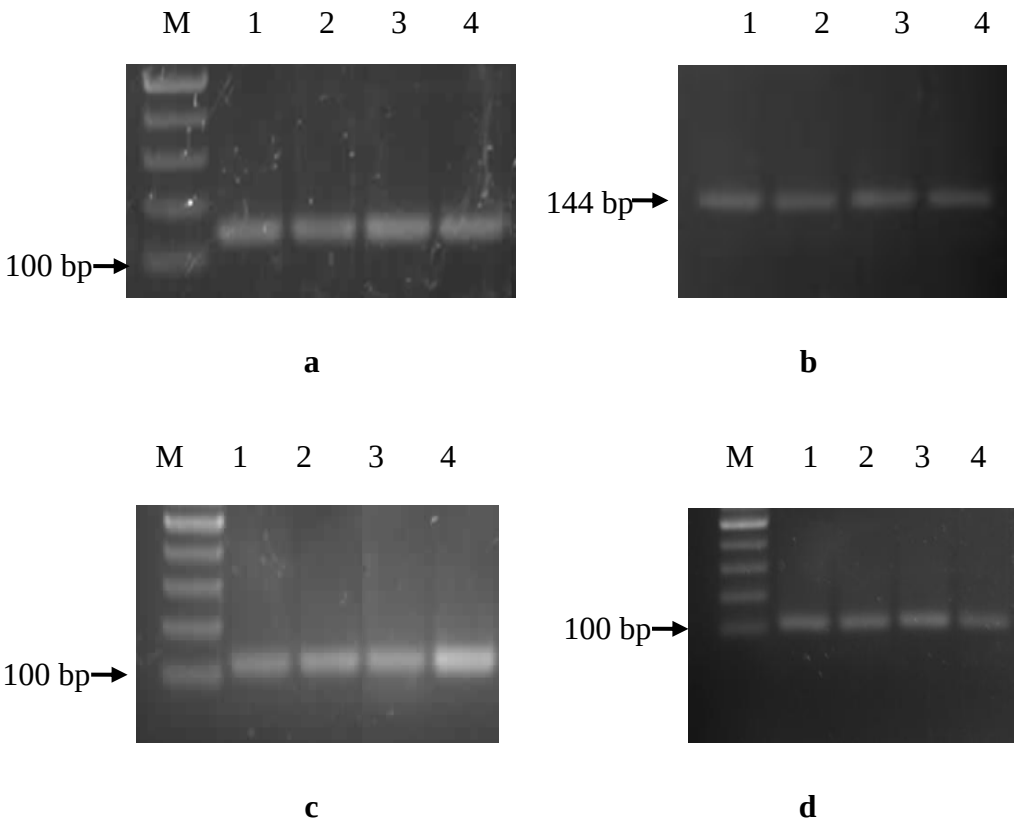

Figure 3.9. RT-PCR analyses of the expression of the genes encoding ATP-dependent RNA helicase (a), splicing factor RNPS1 (b), polyadenylate binding protein (c) and hexokinase (d) in response to 1 h exposure to 25, 50 and 100 μM Pb after 40th h of cultivation. Lane M: 100 bp DNA ladder. Lane 1: Control. Lane 2: 25 μM Pb exposure. Lane 3: 50 μM Pb exposure. Lane 4: 100 μM Pb exposure.

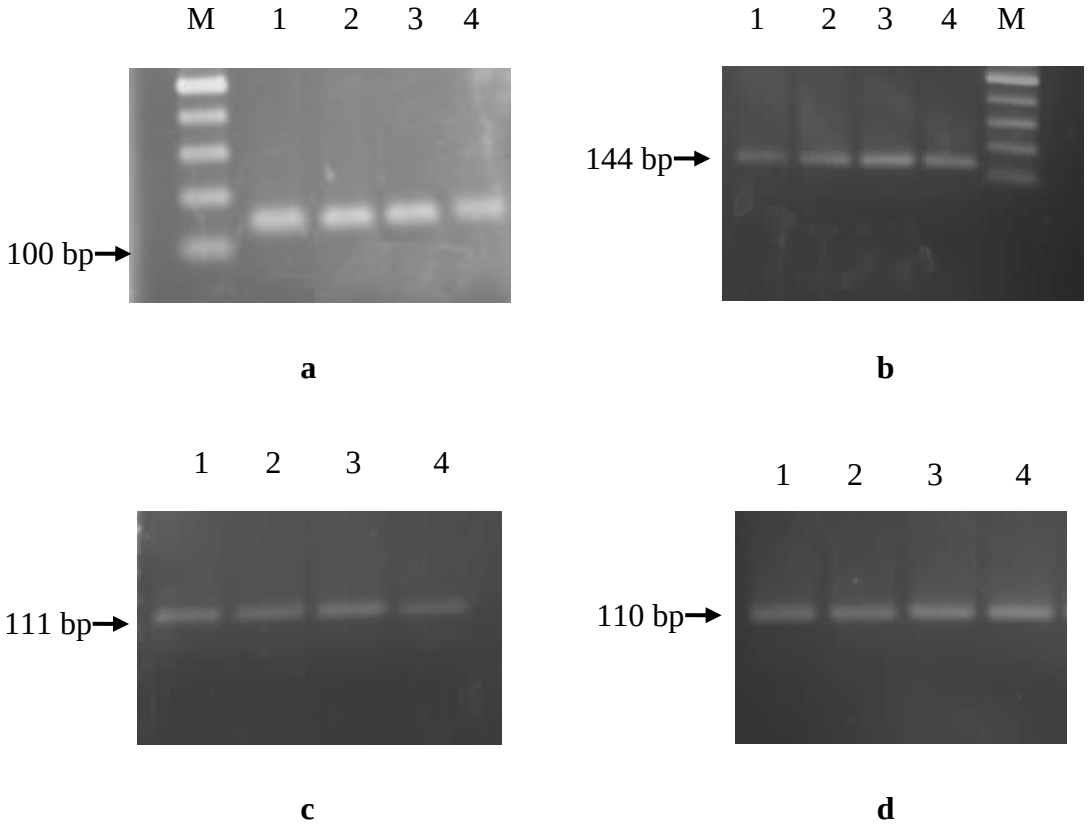

Figure 3.10. RT-PCR analyses of the expression of the genes encoding ATP-dependent RNA helicase (a), splicing factor RNPS1 (b), polyadenlate binding protein (c) and hexokinase (d) in response to 2 h exposure to 25, 50 and 100 μM Pb after 40th h of cultivation. Lane M: 100 bp DNA ladder. Lane 1: Control. Lane 2: 25 μM Pb exposure. Lanes 3: 50 μM Pb exposure. Lane 4: 100 μM Pb exposure.

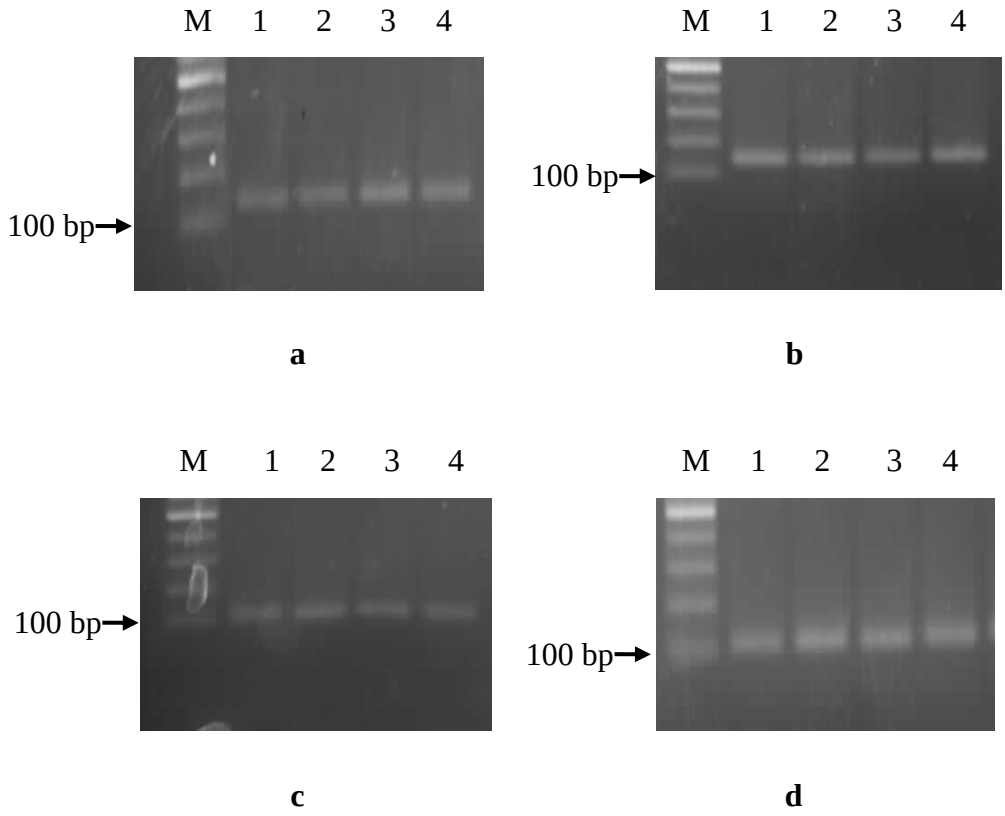

Figure 3.11. RT-PCR analyses of the expression of the genes encoding ATP-dependent RNA helicase (a), splicing factor RNPS1 (b), polyadenylate binding protein (c) and hexokinase (d) in response to 4 h exposure to 25, 50 and 100 μM Pb after 40th h of cultivation. Lane M: 100 bp DNA ladder. Lanes 1: Control. Lane 2: 25 μM Pb exposure. Lanes 3: 50 μM Pb exposure. Lane 4: 100 μM Pb exposure.

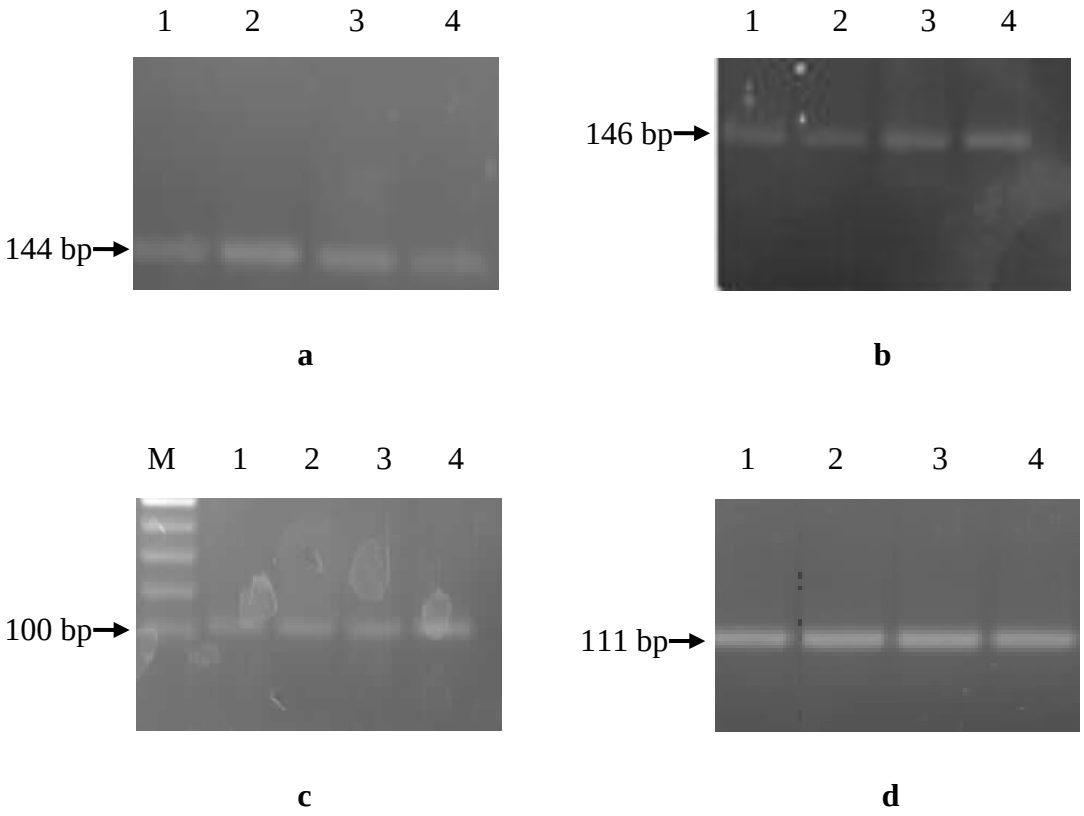

Figure 3.12. RT-PCR analyses of the expression of the genes encoding for ATP-dependent RNA helicase (a), splicing factor RNPS1 (b), polyadenylate binding protein (c) and hexokinase (d) in response to 8 h exposure to 25, 50 and 100 µM Pb after 40th h of cultivation. Lane M: 100 bp DNA ladder. Lanes 1: Control. Lane 2: 25 µM Pb exposure. Lane 3: 50 µM Pb exposure. Lane 4: 100 µM Pb exposure.

RT-PCR detects the gene expression by measuring the the end products and the wide variability of results are the characteristic of conventional RT-PCR assays. Therefore, the reproducibility and reliability of RT-PCR is under question. On the contrary, Real Time PCR detection is mainly based on the initial amount of starting material and assessment of transcript amount occurs during the amplification step (Gatton *et al*., 2006). Therefore, further expression analyses of the target genes were performed by Real Time PCR.

3.2. Optimization of Real Time PCR conditions

Real Time PCR conditions were optimized in order to eliminate the significant test-to-test variations. For this, different concentrations of primers and $MgCl_2$, and annealing temperatures were tested for polyadenylate binding protein, splicing factor RNPS1, ATP-dependent RNA helicase and hexokinase. These parameters were outlined in Table 3.3.

Table 3.3. Optimization parameters for Real Time PCR.

Tested parameters	**Values**	**Units**
Primer Concentration	0.3 - 0.5 - 0.7 - 1.0	μM
$MgCl_2$ Concentration	2 - 3 - 4 - 5	mM
Annealing Temperature	55 - 56 - 57 - 58 - 59 - 60	°C

Depending on our results (data not shown), the primer concentration of 0.3 μM, the $MgCl_2$ concentration of 2 mM and the annealing temperature of 60°C were chosen as the optimum Q-PCR conditions for best amplifications. Due to the high GC content of the organism, primers were prone to form dimers in the absence of cDNA as shown in Figure 3.13.

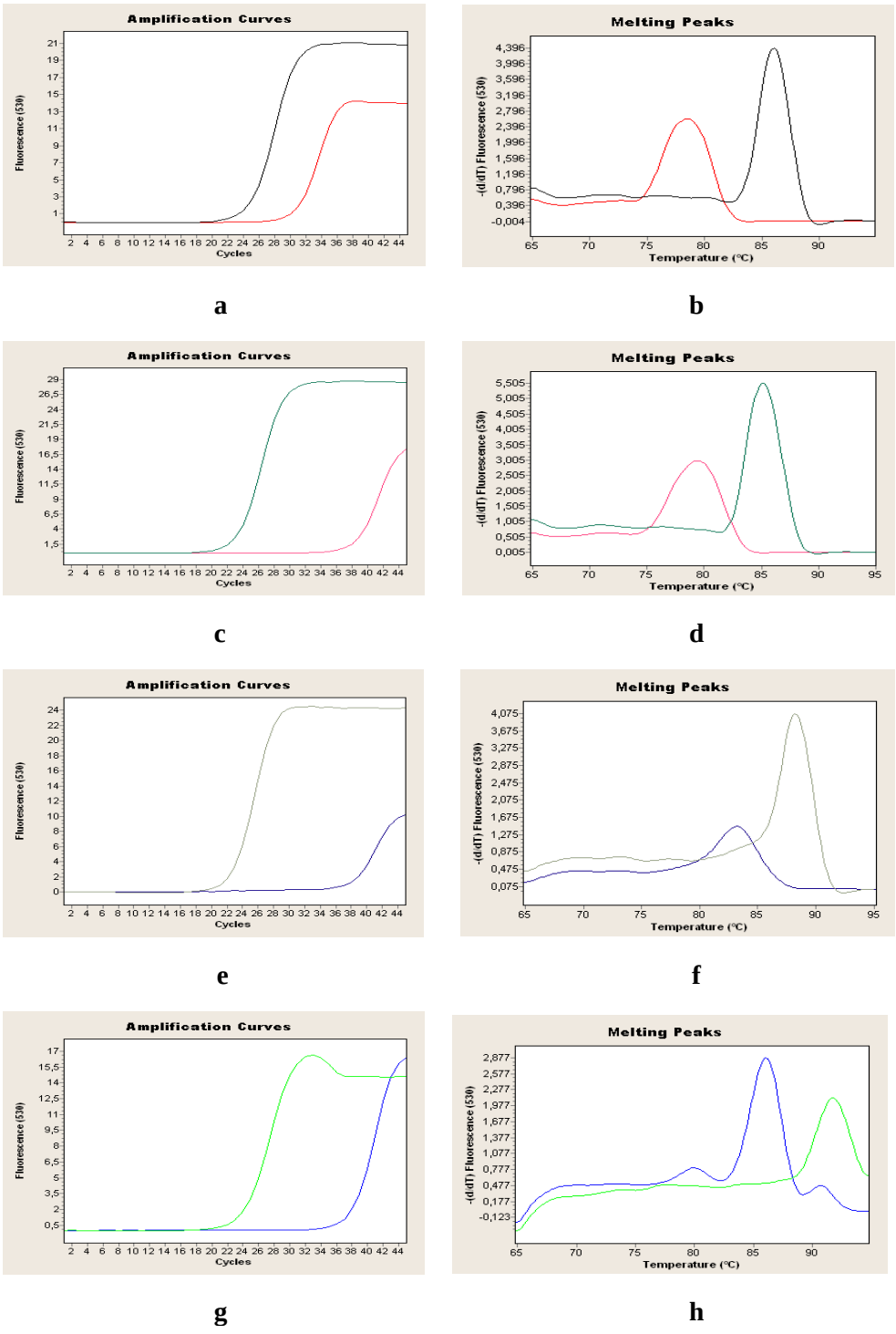

Figure 3.13. Optimized amplification plots and melting peaks for NTC (no template control) and the target of polyadenylate binding protein (a, b), ATP-dependent RNA helicase (c, d), hexokinase (e, f) and splicing factor RNPS1 (g, h).

The analysis of the results was made by using LightCycler software and the Cp and Tm values corresponding to the amplification plots (Figure 3.13) were given in Table 3.4. As seen from the values, the conditions which resulted in the lowest CP value and the highest fluorescent signal was therefore optimum condition (Edwards *et al*., 2008).

Table 3.4. Ct and Tm values of the optimized amplification plots and melting peaks.

	Ct		**Tm**	
	NTC	**Sample**	**NTC**	**Sample**
Polyadenylate binding protein	29.5	23.75	78.65	85.86
ATP-dependent RNA helicase	37.10	22.12	79.59	86.17
Splicing factor RNPS1	36.62	23.12	86.12	92.31
Hexokinase	36.84	21.45	83.55	88.45

3.2.1. Standard curve formation and efficiency calculation

Efficiency corrected mathematical model described by Pfaffl (2001) was used for the relative quantification of Real Time PCR results. In this model, the PCR efficiencies of the target and reference gene are included. Since there is a significant decrease in the PCR components and polymerase activity, and as well as PCR product competition, amplification efficiency changes gradually declining to zero (Wong and Medrano 2005; Platts *et al*., 2008). No matter how much is the starting concentration of the sample, even small differences in the amplification efficiency can be resulted

in noticeable differences in Ct values (Platts *et al*., 2008). Therefore, amplification efficiency is an important parameter for the reliable relative quantification.

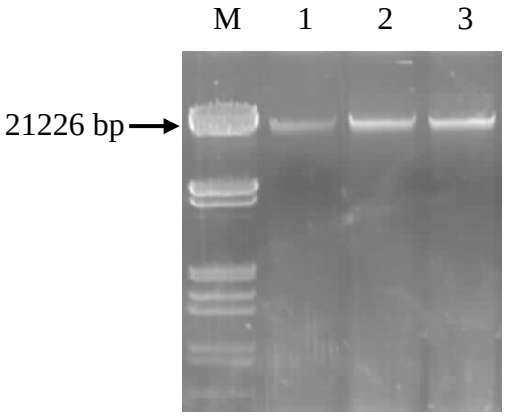

Figure 3.14. Genomic DNA isolated from *P. chrysosporium.* Lane M: Lambda DNA/EcoRI+HindIII marker, Lane 1: 385 ng/µL, Lane 2: 770 ng/µL, Lane 3: 1155 ng/µL DNA.

Serially diluted genomic DNA (Figure 3.14) was used as a template to calculate the efficiency of each primer set as suggested by Lopez-Garcia *et al*., 2010. Genomic DNA sample was amplified by using the optimized conditions. Only for splicing factor RNPS1, serially diluted cDNA amplified with specific primer was used since no amplification was obtained with genomic DNA. The slope of the curve was used to calculate the corresponding efficiencies according to the formula $E = 10^{[-1/slope]}$ given by Pfaffll (2002). The standard curve was established for each primer set as shown in Figure 3.15.

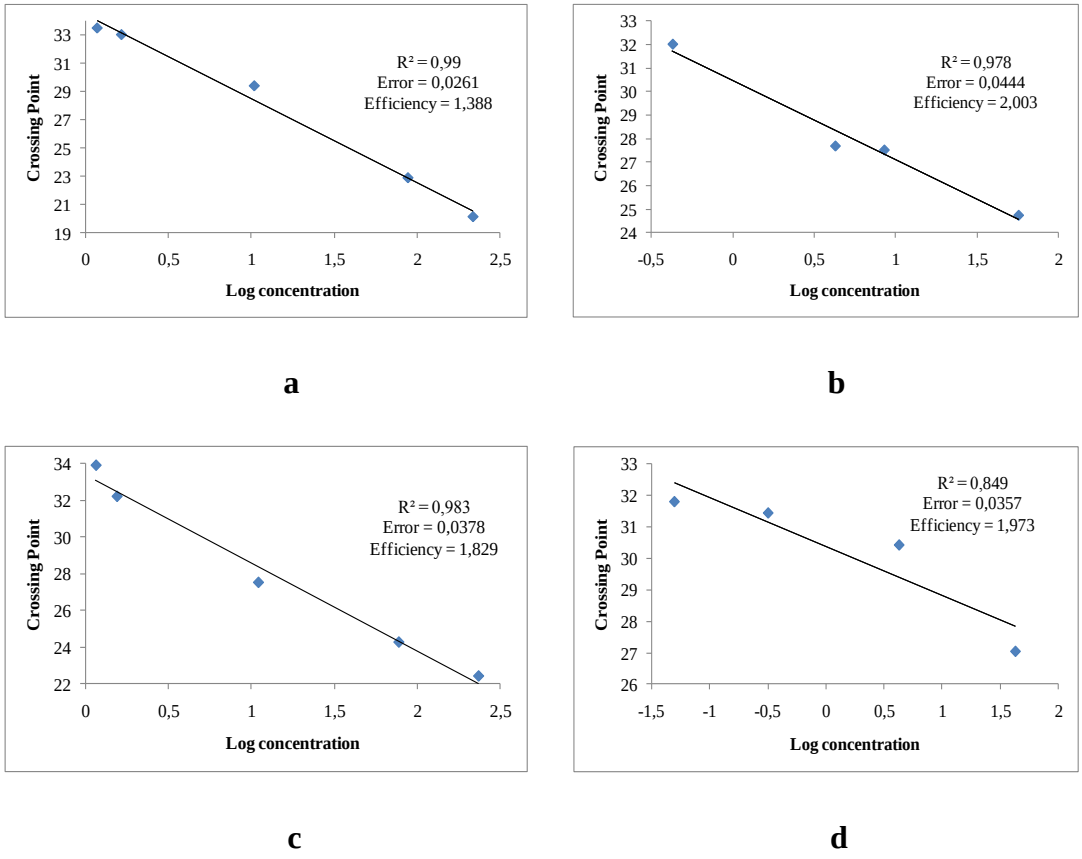

Figure 3.15. Standard curve of the genes coding for splicing factor RNPS1 (a), hexokinase (b), ATP-dependent RNA helicase (c), polyadenylate binding protein (d).

Several factors including amplicon length, contaminants, primer properties play important roles in amplification reaction and resulted in the delay on the efficiency of the reaction. As shown in Figure 3.15, the amplification efficiencies obtained were within the acceptable range of 1.60 to 2.10. (Meijerink *et al*., 2001; Pfaffl, 2004).

3.2.2. Expression analysis via Real Time PCR

The dynamics of the expression of the genes coding for polyadenylate binding protein, ATP-dependent RNA helicase and splicing factor RNPS1 in response to the dose and duration of Pb exposure, qRT-PCR experiments were performed. The differences in the amount and quality of mRNA samples can be compensated to minimize the experimental variabilities in Real Time PCR by using a reference gene. The reference gene expression should be stable and not affected by experimental conditions (Aerts *et al*., 2004). Although, glyceraldeyde-3-phosphate dehydrogenase (GAPDH) gene was widely used as a reference gene for normalization, hexokinase gene was used for the present study. Because, other than being an abundant glycolytic enzyme, GAPDH has multiple unrelated functions. For instance, GAPDH has a potential role in apoptosis induced via various stress agents (Dastoor and Dreyer, 2001). It was also shown that level of cytosolic GAPDH had increased in response to the stress conditions like heat, anaerobiosis and high sucrose concentration (Yang *et al*., 1993). Moreover, expression of an isoform of GAPDH was shown to increase in response to Pb by Yıldırım *et al*. (2011).

3.2.2.1. Dose-dependent Pb response

For dose-dependent Pb exposure analysis, three different concentrations of Pb (25, 50, and 100 μM) were used to spike mid-log-grown cultures (40^{th} hour). The qRT-PCR experiments, which included both biological and technical replicates, were performed in triplicates. Hexokinase (reference gene) was also included in the same experiments along with the target genes.

3.2.2.1.1. ATP-dependent RNA helicase

In Real Time PCR experiments for ATP-dependent RNA helicase upon dose depent Pb exposure, the amplification curves together with the melting peaks obtained are presented in Figure 3.16. Amplification curves are given as fluorescence versus cycle number where LightCycler Software detected the Ct values automatically. The melting curve analysis showed that there was two different peaks corresponding to hexokinase and ATP-dependent RNA helicase with Tm values of 86.17 and 85.0, respectively. The presence of two peaks showed that only expected products were amplified away from dimers or non-specific amplifications.

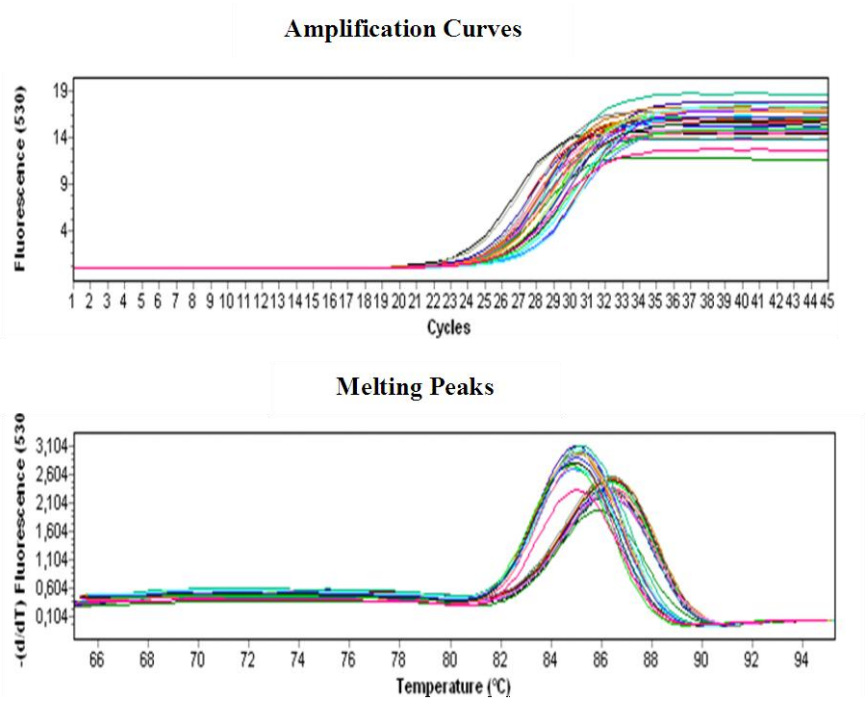

Figure 3.16. qRT-PCR analysis of ATP-dependent RNA helicase and hexokinase expression upon dose-dependent Pb exposure.

The qRT-PCR experiment results were further analyzed by using efficiency corrected mathematical model as described by Pfaffl (2002). In addition, the quantitation included normalization with the reference gene hexokinase. The results are presented in the Figure 3.17.

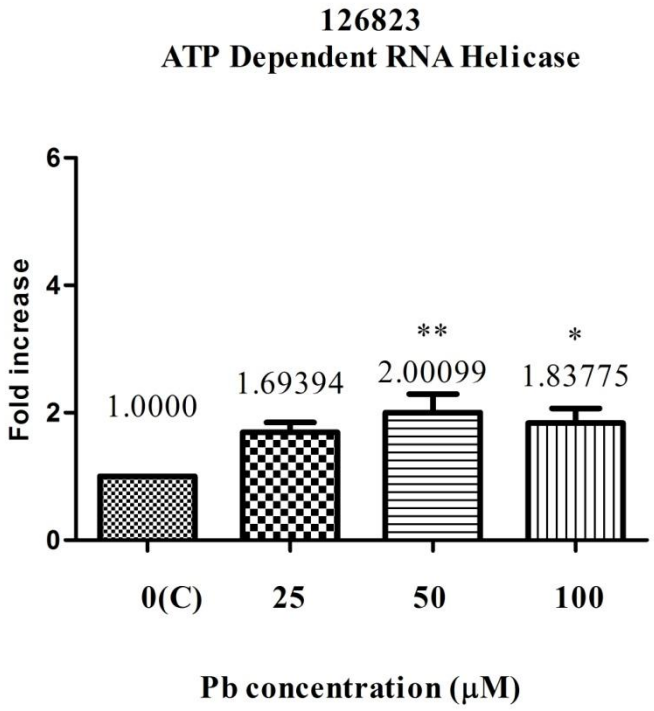

Figure 3.17. Changes in the expression level of ATP-dependent RNA helicase mRNA in response to dose-dependent Pb exposure.

As depicted from the Figure 3.17, only 50 and 100 μM Pb exposure caused a significant increase (2 and 1.84 fold, respectively) in ATP-dependent RNA helicase mRNA levels. 25 μM Pb exposure did not result in any significant change in the expression level as compared to the control.

The results obtained from Real Time PCR were generally consistent with the data obtained from the proteomic studies done by Yıldırım *et al*., 2011. No significant change in the mRNA level was observed in response to 25 µM Pb for ATP-dependent RNA helicase, as found by proteomics. They also showed that the level of this protein was 7.89-fold increased and almost doubled when exposed to 50 and 100 µM Pb, respectively. It was previously reported that many RNA helicases were involved in the adaptation of different stress conditions (Sanan-Mishra *et al*., 2004). For instance, a study was performed to reveal the regulation of CrhC, which belongs to a DEAD-box family of RNA helicases. Northern Blot and Western Blot analysis were performed with the *Anabaena* cells, having an optimum temperature of 30 °C, when exposed to cold stress (20 °C). Depending on their results, CrhC expression was not detectable at 30 °C, but observed in response to cold stress. The induction at the protein level corresponds to early transcript accumulation in cold shock, but not during prolonged exposure to low temperature (Chamot and Owttrim, 2000). In the study done by Briolat and Reysset (2002), ATP-dependent RNA helicase was found to be involved in the response to oxidative stress for the first time in *Clostridium perfringens* cells grown in the presence of oxygen and/or superoxide and hydroxyl radicals. In barley, the mRNA of *HVD1* gene (putative ATP-dependent RNA helicase) was found to be accumulated in response to salt stress. This change was also affected by the duration of salt exposure. Salt regulation of *HVD1* gene in barley was possibly composed of a rapid initial response and a long term response (Nakamura *et al*., 2004).

3.2.2.1.2. Polyadenylate binding protein

The amplification plots and melting curves obtained for polyadenylate binding protein and hexokinase are represented in Figure 3.18. The Tm values observed were 85.86 and 86.17 for polyadenylate binding protein and hexokinase cDNAs, respectively.

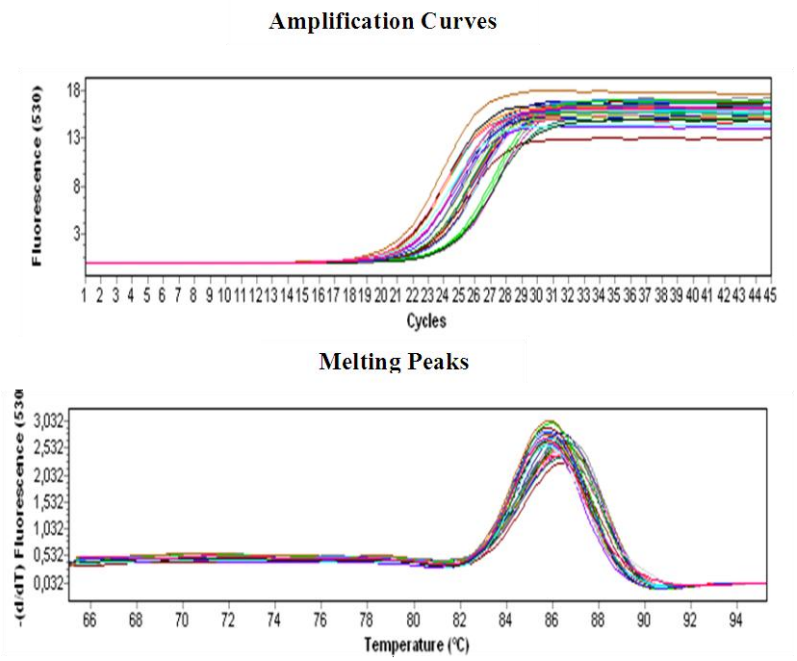

Figure 3.18. qRT-PCR analysis of polyadenylate binding protein and hexokinase expression upon dose-dependent Pb exposure.

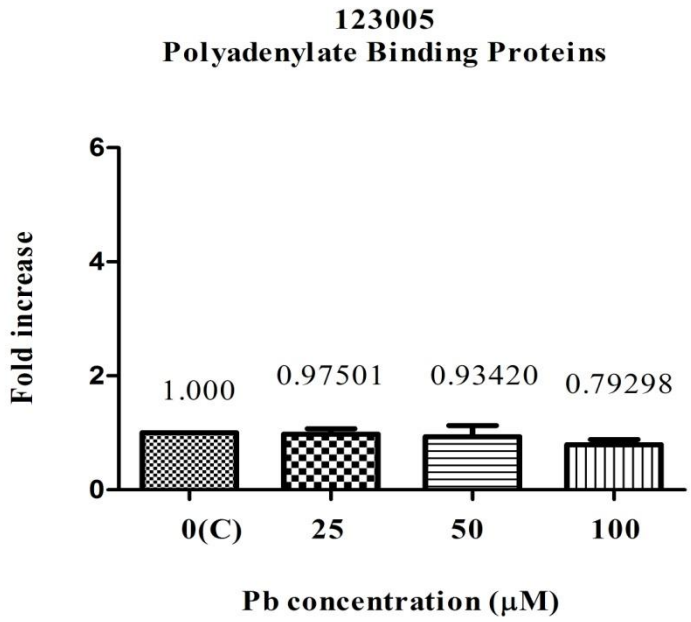

Figure 3.19. Changes in the expression level of polyadenylate binding protein mRNA in response to dose-dependent Pb exposure.

As seen from the Figure 3.19, we did not obtain any significant alteration in the mRNA level of polyadenylate binding protein when exposed to different concentration of Pb in spite of the fact that Yıldırım *et al*. (2011) showed polyadenylate binding protein as a new protein induced upon Pb exposure. This discrepancy between mRNA and protein level most likely suggests the regulation of its expression at post-transcriptional, translational, or post-translational level. In a study done by Tian *et al*. (2004) two hematopoietic cell lines with different stages of myeloid differentiation and livers of mice treated with different peroxisome proliferative activated receptor agonists were used to investigate correlation between the levels of mRNA and protein. For this purpose, DNA microarrays together with quantitative proteomic techniques such as ICAT, two-dimensional DIGE and MS was perfomed. As a result, only 29 genes showed significant change in mRNA and protein level in the same direction whereas 67 genes showed significant changes only

at mRNA level and 52 genes only at protein level as well as 2 genes showed opposite expression patterns of mRNA and protein. Among them, 5 out of 6 RNA-processing genes had a pattern of negative correlation. It was strongly suggested that post-transcriptional regulation is a conserved mechanism that controls the RNA processing genes (Tian *et al*., 2004). The changes in the protein abundance due to post-transcriptional control and modifications cannot be predicted from measurement of mRNA (Griffin *et al*., 2002; Washburn *et al*., 2003). Successive studies were performed in order to identify the regulation of the expression of proteins at either transcriptional or translational level. It was revealed that many complex biological processes are activated in cultured quiescent animal cells upon stimulation by serum or individual growth factors (Hersko *et al*., 1971; Rudland and Asua, 1979). In one study, transcriptional and translational control of cytoplasmic proteins after serum (fatal calf serum) stimulation was investigated. The synthesis of cytoplasmic proteins from quiescent and serum stimulated Swiss mouse 3T3 cells were compared by 2DE method. Based on the comparison, the polyadenylate binding protein was found to be present in both cells; however, its protein level was increased 4.2 fold in serum stimulated cells. In order to understand whether the expression of the proteins was controlled at transcriptional or translational level, the cells were exposed to a transcription inhibitor, namely actinomycin D. The data indicated that the synthesis of some proteins was inhibited partially or completely by the actinomycin D treatment. Among them, the expression of polyadenylate binding protein was found to be completely inhibited by actinomycin D in serum-stimulated cells, thus, the regulation seemed to occur at a transcriptional level (Thomas *et al*., 1981). In the following study, total mRNA from quiescent and serum stimulated cells was isolated and translated in the rabbit reticulocyte lysate system (Thomas and Thomas; 1986). As a result, the mRNA level of polyadenylate binding protein was not altered even its 4.2 fold increased expression by serum stimulation as previously reported by Thomas *et al*., (1981). Possibly, actinomycin D led to the activation of some control mechanisms that block the expression of polyadenylate binding protein (Thomas and Thomas, 1986). Therefore, the cellular level of polyadenylate binding protein is

regulated primarly at a translational level (Thomas and Thomas, 1986; Bag and Bhattacharjee, 2010).

3.2.2.1.3. Splicing factor RNPS1

The amplification plots and melting curves obtained for splicing factor RNPS1 and hexokinase are presented in Figure 3.20. The Tm values observed were 92.31 and 86.17 for splicing factor RNPS1 and hexokinase cDNAs, respectively.

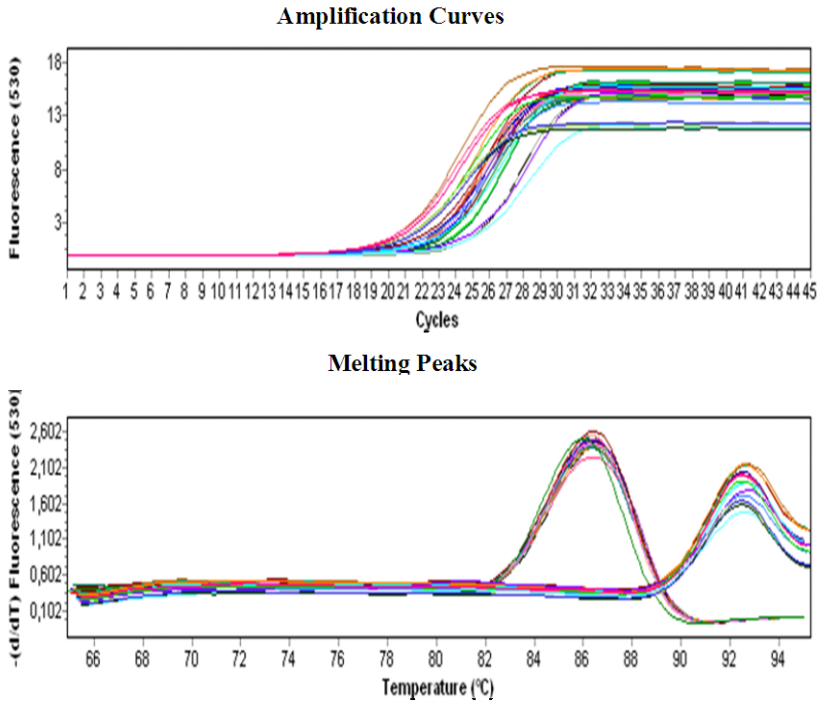

Figure 3.20. qRT-PCR analysis of splicing factor RNPS1 and hexokinase expression upon dose-dependent Pb exposure.

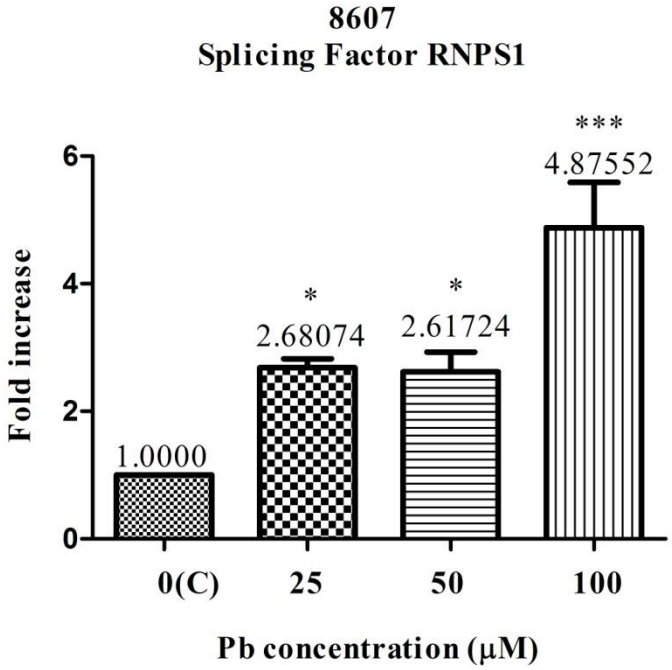

Figure 3.21. Changes in the expression level of splicing factor RNPS1 mRNA in response to dose-dependent Pb exposure.

The results showed that there was a significant change in the mRNA level of splicing factor RNPS1 as a function of increasing Pb concentrations (Figure 3.21). Although 25 and and 50 μM Pb exposures gave almost a similar increase (2.6 fold) in the mRNA level of splicing factor RNPS1, 100 μM Pb exposure increased this value by 4.9 fold. Our former proteomics study (Yıldırım *et al*., 2011) revealed no difference in the level of this protein in a dose-dependent manner. It is very likely that post-transcriptional regulation(s) plays a major role in determining final level of this protein during chronic exposure to Pb.

3.2.2.2. Time-dependent Pb response

For time-dependent Pb response analysis, three different concentrations of Pb (25, 50, and 100 µM) were used to spike mid-log-grown cultures of 40th h. The cultures were further incubated and harvested at 1, 2, 4 and 8 h, respectively.

3.2.2.2.1. ATP-dependent RNA helicase

The effect of time-dependent exposure to different concentrations of Pb on ATP-dependent RNA helicase was performed as described earlier. The results were summarized in Figure 3.22- 3.25, respectively.

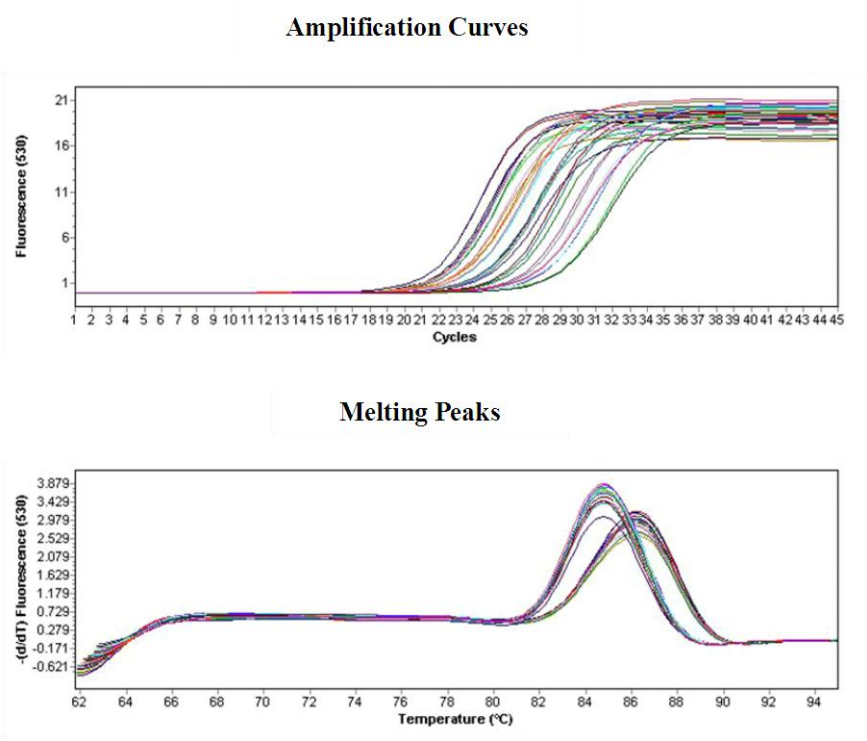

Figure 3.22. qRT-PCR analysis of ATP-dependent RNA helicase and hexokinase expression upon 1 h exposure to different doses (25, 50 and 100 µM) of Pb.

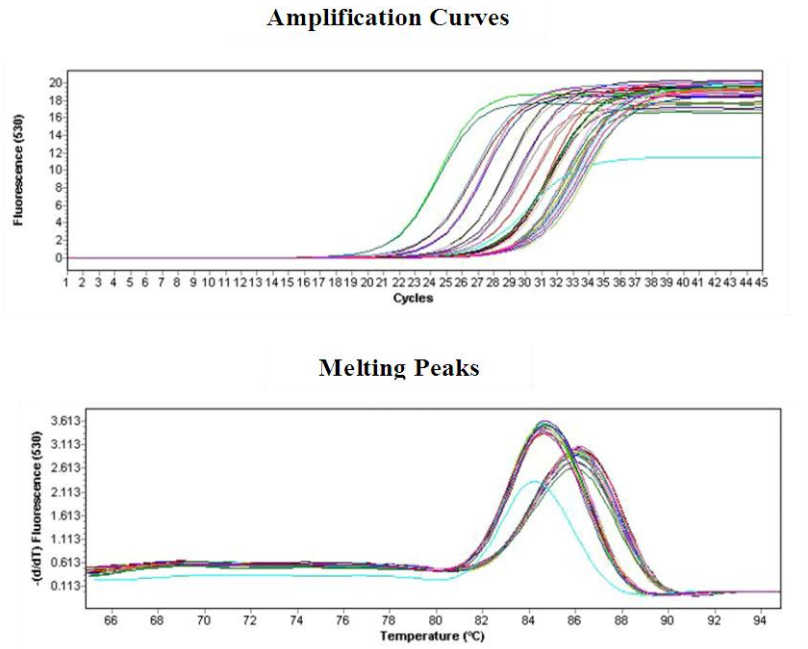

Figure 3.23. qRT-PCR analysis of ATP-dependent RNA helicase and hexokinase expression upon 2 h exposure to different doses (25, 50 and 100 μM) of Pb.

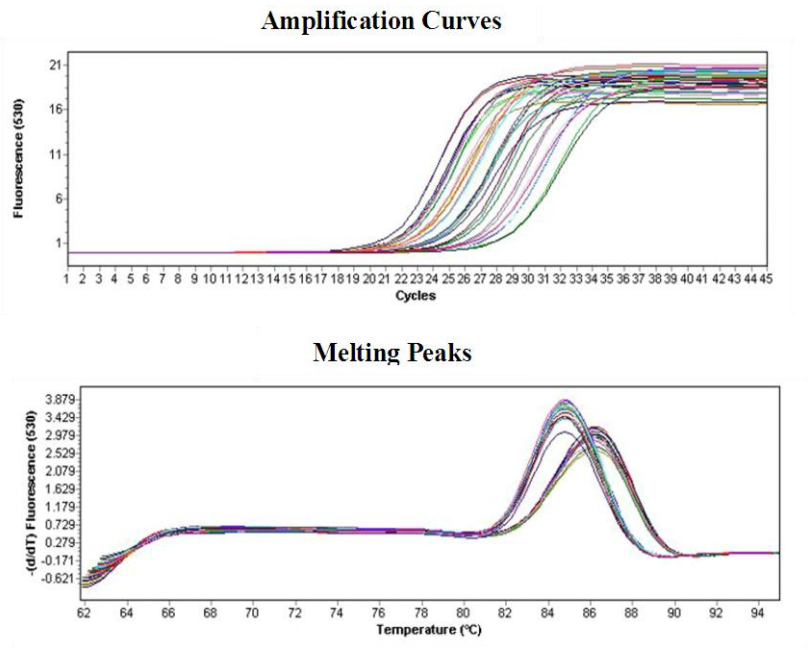

Figure 3.24. qRT-PCR analysis of ATP-dependent RNA helicase and hexokinase expression upon 4 h exposure to different doses (25, 50 and 100 μM) of Pb.

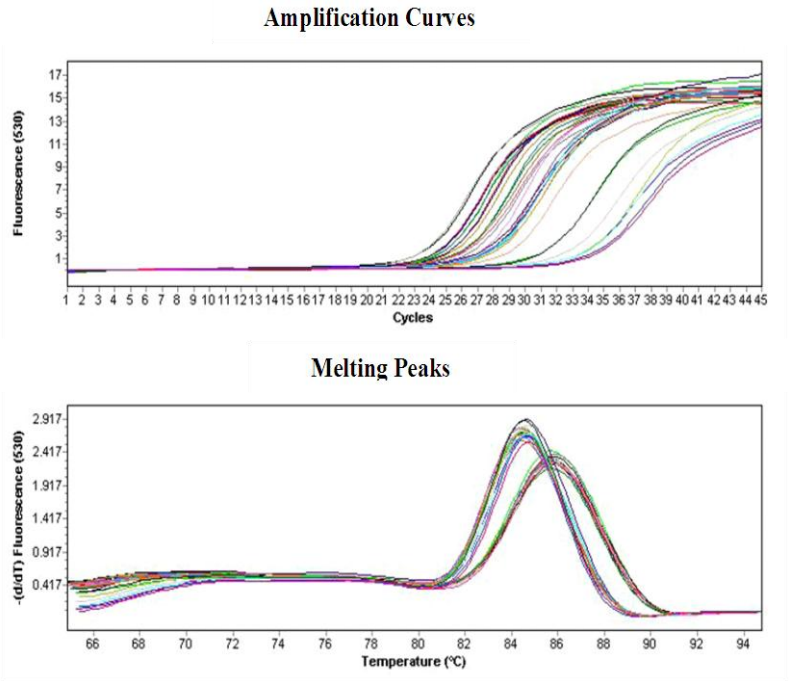

Figure 3.25. qRT-PCR analysis of ATP-dependent RNA helicase and hexokinase expression upon 8 h exposure to different doses (25, 50 and 100 μM) of Pb.

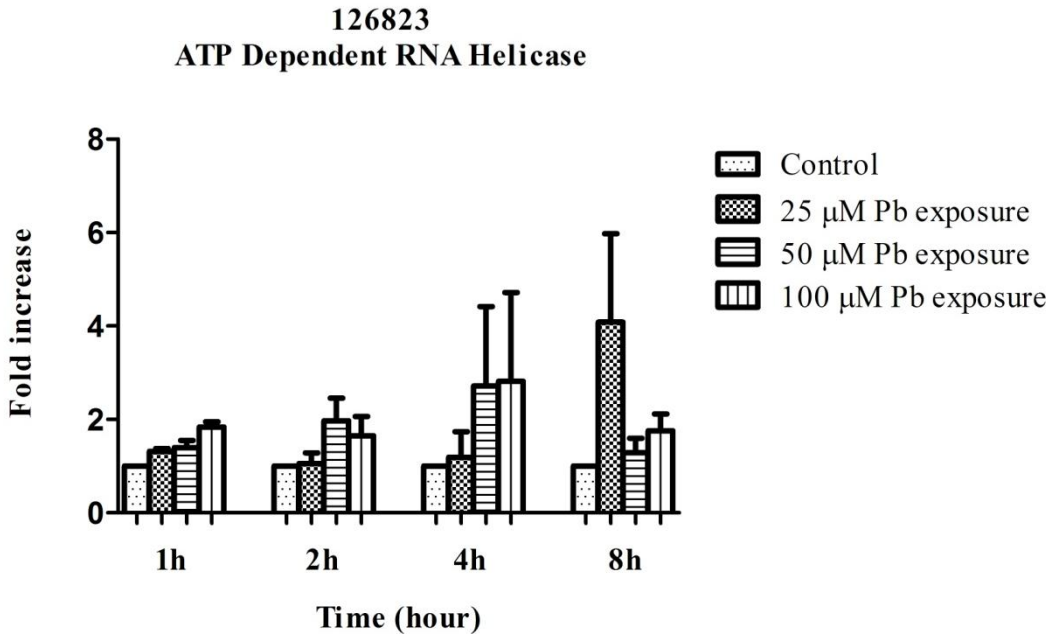

Figure 3.26. Changes in the expression level of ATP-dependent RNA helicase gene in response to time-dependent exposure to different doses of Pb.

Time-dependent Pb exposure data for ATP-dependent RNA helicase were analyzed as described earlier. The results were summarized in Figure 3.26. As depicted from this figure, there was no significant alteration in the mRNA level of this protein when exposed to Pb for varying durations.

3.2.2.2.2. Polyadenylate binding protein

The effect of time-dependent exposure to different concentrations of Pb on polyadenylate binding protein was performed as described earlier. The results were summarized in Figure 3.27-30.

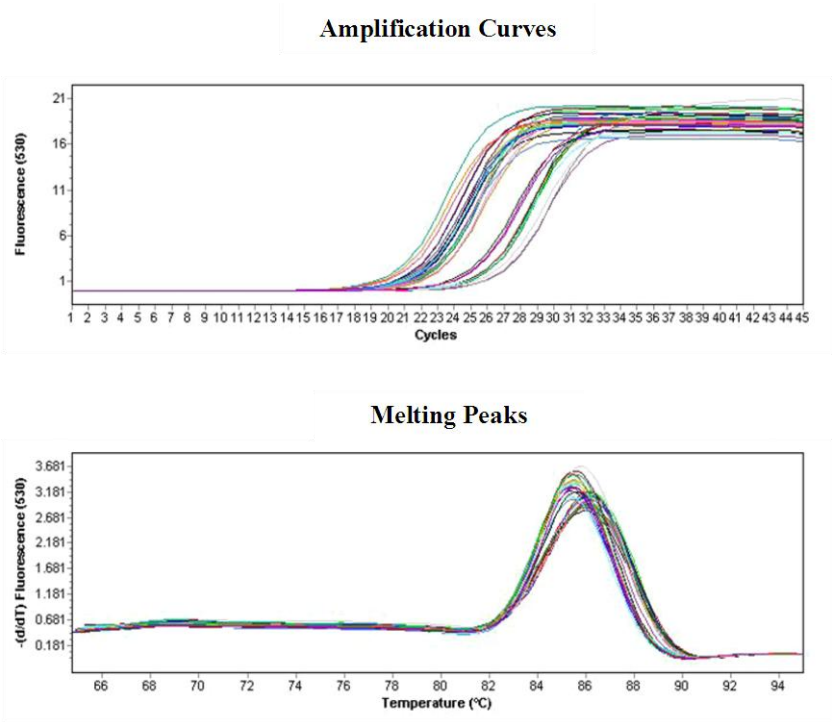

Figure 3.27. qRT-PCR analysis of polyadenylate binding protein and hexokinase expression upon 1 h exposure to different doses (25, 50 and 100 μM) of Pb.

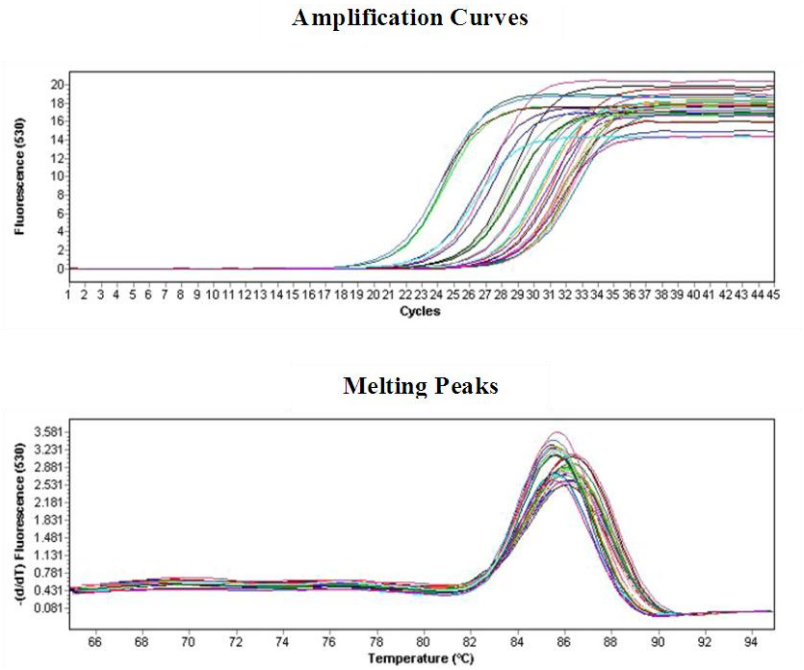

Figure 3.28. qRT-PCR analysis of polyadenylate binding protein and hexokinase expression upon 2 h exposure to different doses (25, 50 and 100 µM) of Pb.

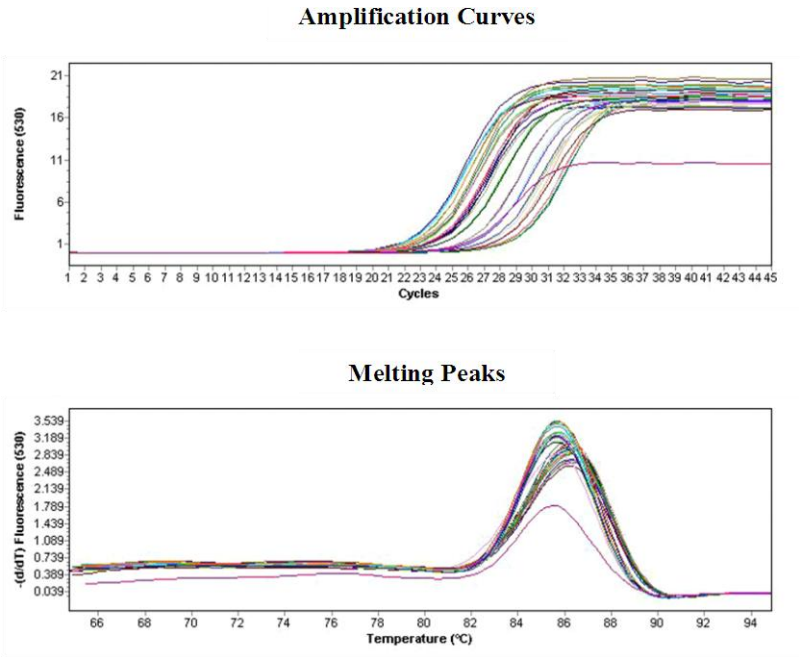

Figure 3.29. qRT-PCR analysis of polyadenylate binding protein and hexokinase expression upon 4 h exposure to different doses (25, 50 and 100 µM) of Pb.

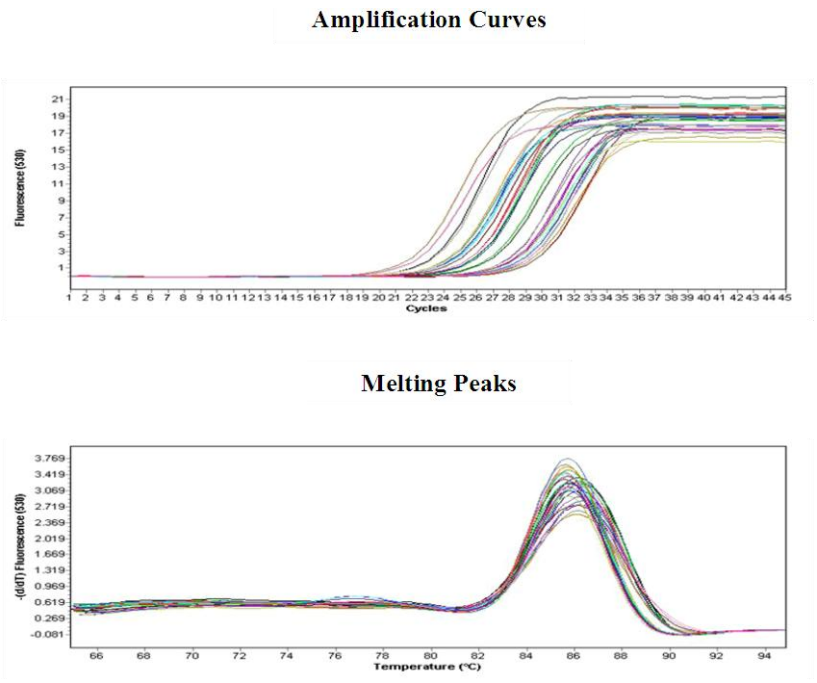

Figure 3.30. qRT-PCR analysis of polyadenylate binding protein and hexokinase expression upon 8 h exposure to different doses (25, 50 and 100 μM) of Pb.

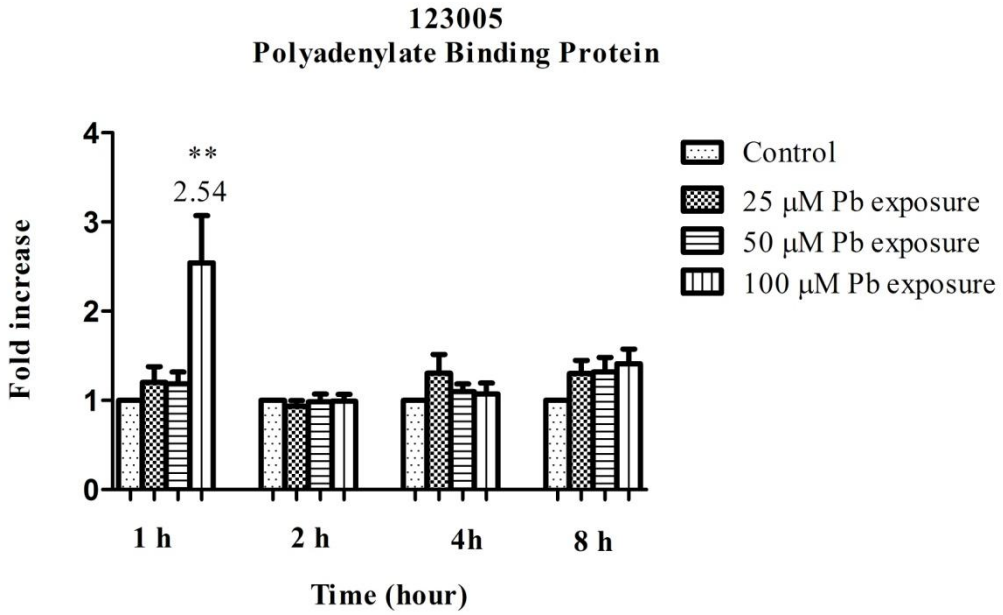

Figure 3.31. Changes in the expression level of polyadenylate binding protein gene in response to time-dependent exposure to different doses of Pb.

As seen in Figure 3.31, the only significant change in mRNA levels of polyadenylate binding protein was obtained upon 1 h exposure to 100 µM Pb where there was 2.5 fold increase in the expression level. However, this increase was not sustained during further exposure to this metal. In our former proteomics study (Yıldırım *et al*., 2011), this protein was not among the upregulated/induced proteins detected in a time-dependent manner. It follows that the above-mentioned 2.5 fold increment in mRNA level upon 1 h exposure was not reflected to the final level of the protein.

3.2.2.2.3. Splicing Factor RNPS1

The amplifications curves and melting peaks obtained for splicing factor RNPS1 were given in Figure 3.32-35.

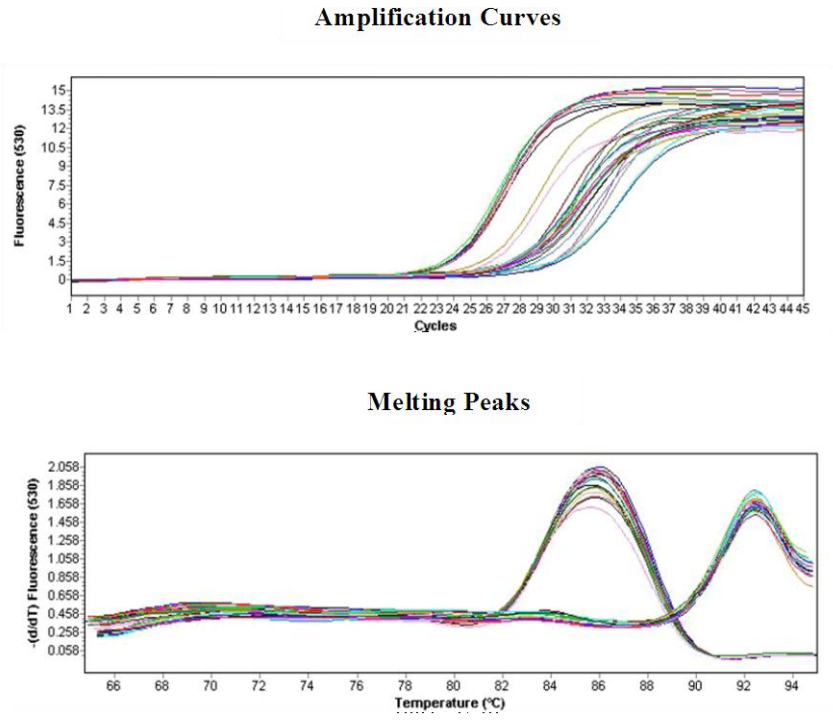

Figure 3.32. qRT-PCR analysis of splicing factor RNPS1 and hexokinase expression upon 1 h exposure to different doses (25, 50 and 100 µM) of Pb.

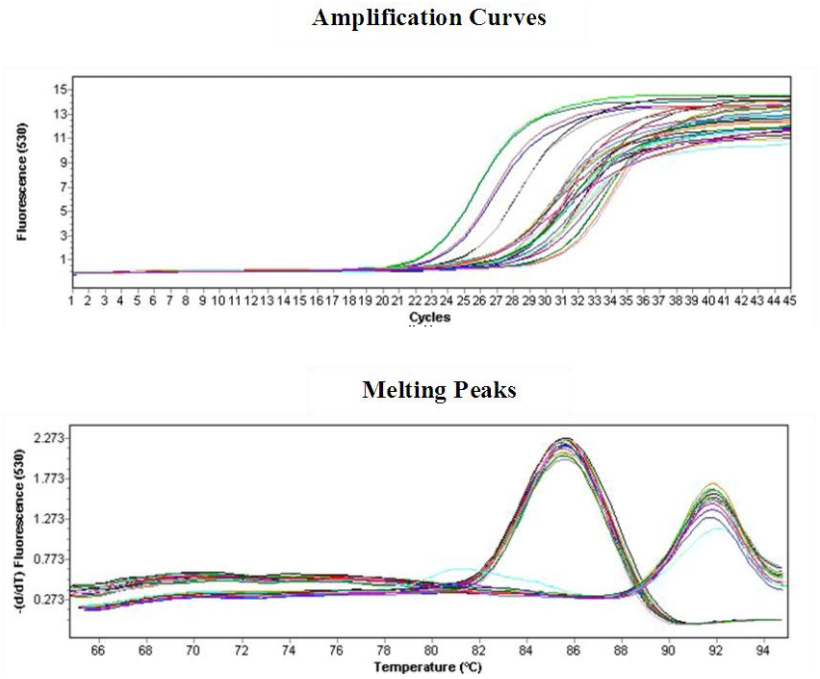

Figure 3.33. qRT-PCR results of splicing factor RNPS1 and hexokinase expression upon 2 h exposure to different doses (25, 50 and 100 μM) of Pb.

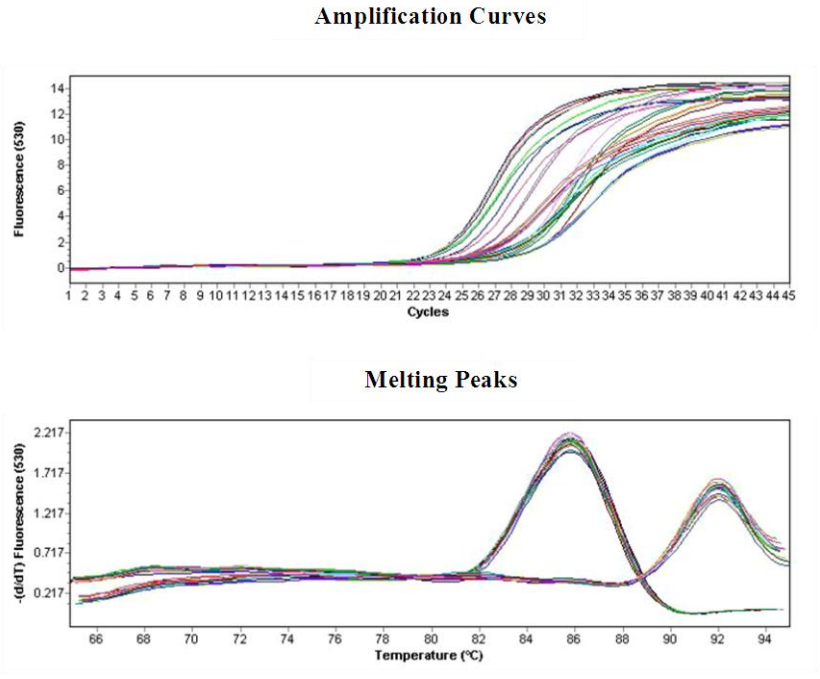

Figure 3.34. qRT-PCR analysis of polyadenylate binding protein and hexokinase expression upon 4 h exposure to different doses (25, 50 and 100 μM) of Pb.

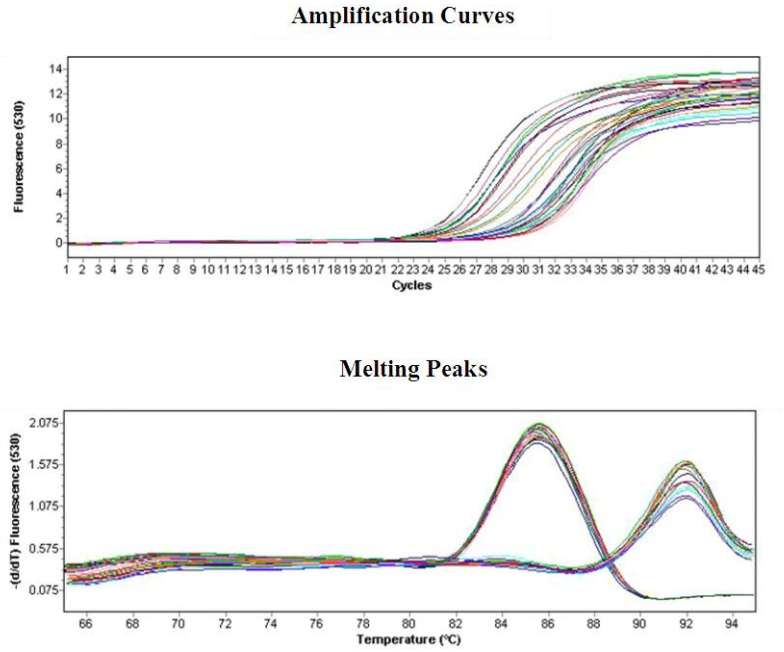

Figure 3.35. qRT-PCR analysis of polyadenylate binding protein and hexokinase expression upon 8 h exposure to different doses (25, 50 and 100 μM) of Pb.

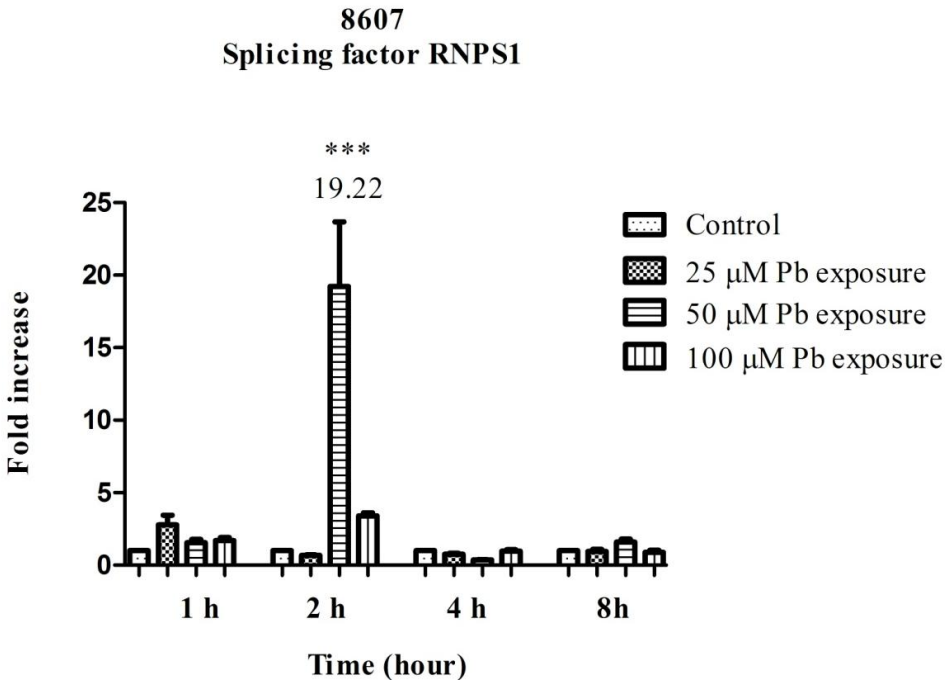

Figure 3.36. Changes in the expression level of splicing factor RNPS1 gene in response to time-dependent exposure to different doses of Pb.

As depicted from Figure 3.36, the only significant change was obtained upon 2 h exposure to 50 μM Pb with as much as 19.22-fold increase in the expression level of splicing factor RNPS1. Yıldırım *et al*. (2011) found that 3-fold increase in the level of this protein was maintained during 8 h exposure (except for the 4^{th} h) as induced by the same concentration of Pb. The expression level of plant SR family proteins is regulated under stress conditions by controlling phosphorylation status, subcellular distribution and even alternative splicing patterns (Duque, 2011). In Arabidopsis, the noncanonical SR protein SR45 is localized in enlarged nuclear speckles upon exposure to heat stress whereas a diffuse nucleoplasmic pattern of localization was observed under cold stress (Ali *et al*., 2003). Under different stress conditions such as heat, light and salt, the relative levels of SR30 splice variants were shown to increase by regulating its own splicing (Filichkin *et al*., 2011). Therefore, different mechanisms of regulation can take place for such proteins in response to variety of stress conditions.

As stated earlier, protein concentration is directly proportional to mRNA level, translation efficiency and protein degradation. However, changes in mRNA concentration can partially explain the variation in the level of protein concentration. In this study, upon dose-dependent exposue to Pb for 40 h representing chronic exposure, the increase in the mRNA levels of the ATP-dependent RNA helicase and splicing factor RNPS1 genes was evident. In this respect, the present findings supported our proteomic data (Yıldırım *et al*., 2011). Still, the fold increases were not the same at protein and mRNA levels. There are examples in which even similar mRNA expression levels are accompanied by a wide range of protein abundance with up to 20 fold difference or vice versa. For instance, *GAL2* showed a 500-fold increase in mRNA expression on galactose, whereas it showed only 10-fold increase when measured at protein level (Griffin *et al*., 2002). In our former study (Yıldırım *et al*., 2011), polyadenylate binding protein was found as two distinct spots in the 2DE gels and one of them was observed as a newly induced protein in response to all different doses of Pb. Based on the positions of these on the 2D gel, no significant change in the molecular mass of the proteins was observed whereas the isoelectric

point (pI) of the spots were different, suggesting possible post-translational modification. Although there was no significant change in the mRNA level of polyadenylate binding protein in response to different doses of Pb in the present study, the increase in the protein level might have been affected from the post-transcriptional regulations such as an increase in mRNA stability (Day and Tuite, 1998). On the other hand, upon time-dependent Pb exposure representing acute exposure, only polyadenylate binding protein mRNA showed 2.54-fold increase at 1st h of 100 μM Pb exposure and splicing RNPS1 mRNA showed 19.22-fold increase at 2nd h of 50 μM Pb exposure. The remaining treatments did not result in a significant increase in their mRNA level. Likewise, 3.3 fold increase in levels of splicing factor RNPS1 as an acute response to 1, 2 and 8 h exposure to 50 μM Pb (Yıldırım *et al*., 2011) was not detected when examined in the present study by qRT-PCR. A comparison of mRNA and protein data obtained from our present and former studies (Yıldırım *et al*., 2011) are documented in Table 3.5. To ensure a fast response to acute stress, mRNA levels might have been altered by post-transcriptional mechanisms involving mRNA stability, translation initiation, and protein stability (Paskitti *et al*., 2000; Tian *et al*., 2004 Kawaguchi *et al*., 2004). Indeed, only in a few studies, mRNA and protein levels were found to be correlated moderately or weakly. The differences in mRNA and protein levels can be explained by measurement noise, inability to detect the correct protein amounts due to post-translational modifications, post-transcriptional regulatory mechanisms that regulate gene expression specifically and differences in vivo half-lives of proteins (Gygi *et al*., 1999; Johnston and Carlson, 1991; Greenbaum *et al*., 2003; Fu *et al*., 2007; Abreu *et al*., 2009).

Table 3.5. A comparison of mRNA and protein data obtained from our present and former studies

Pb Dose/ Time of exposure		Fold increase					
		Polyadenylate binding protein		ATP-dependent RNA helicase		Splicing factor RNPS1	
		mRNA	protein	mRNA	protein	mRNA	protein
25 µM / 40 h (chronic)		nc	New	nc	nc	2,68	nc
25 µM (acute)	1 h	nc	nd	nc	nd	nc	nd
	2 h	nc	nd	nc	nd	nc	nd
	4 h	nc	nd	nc	nd	nc	nd
	8 h	nc	nd	nc	nd	nc	nd
50 µM / 40 h (chronic)		nc	New	2,00	7,89	2,62	nc
50 µM (acute)	1 h	nc	nc	nc	nc	nc	3,32
	2 h	nc	nc	nc	nc	19,22	3,12
	4 h	nc	nc	nc	nc	nc	nc
	8 h	nc	nc	nc	nc	nc	3,50
100 µM / 40 h (chronic)		nc	New	1,84	1,86	4,88	nc
100 µM (acute)	1 h	2,54	nd	nc	nd	nc	nd
	2 h	nc	nd	nc	nd	nc	nd
	4 h	nc	nd	nc	nd	nc	nd
	8 h	nc	nd	nc	nd	nc	nd

nc: no change, nd: not determined

CHAPTER 4

CONCLUSION

- The dynamics of expression of ATP-dependent RNA helicase, polyadenylate binding protein and splicing factor RNPS1 genes of *P. chrysosporium* in response to Pb exposure were studied by performing Real Time PCR experiments.

- *P. chrysosporium* cells were subjected to chronic exposure to 25, 50 and 100 μM Pb in order to observe dose-dependent response of the organism to this heavy metal. The highest Pb concentration used in this study was nearly 8 times higher than the upper level of Pb generally found in the industrial wastewaters. In these experiments, the cells were exposed to Pb till mid exponential phase (40 h) of growth. Under these conditions, the mRNA level of splicing factor RNPS1 showed 2.68, 2.62 and 4.86 fold increase, respectively, to the Pb doses employed. ATP-dependent RNA helicase mRNA displayed 2.00 and 1.84 fold increase only in response to 50 and 100 μM Pb exposure, respectively, which agreed well with the results of our former proteomics studies. On the other hand, polyadenylate binding protein mRNA did not show any significant change in response to the doses employed.

- In time-dependent Pb response experiments which involved spiking of the mid-log cells of *P. chrysosporium* for different time periods, polyadenylate binding protein mRNA showed 2.54 fold increase when exposed to 100 μM

Pb for 1 h. Splicing factor RNPS1 mRNA increased as much as 19.22-fold when exposed to 50 μM Pb for 2 h. Incubation of the mid-log cells with 25 μM, 50 μM or 100 μM Pb for 1 h, 2h, 4 h or 8 h did not lead to any alteration in the mRNA levels of ATP-dependent RNA helicase.

- The lack of exact correlation between mRNA levels of RNBPs studied with previously reported protein levels provided further clue about the necessity of conducting "-omics" and single gene transcription studies in parallel.

REFERENCES

Abbas A., Koc H., Liu F., Tien M., (2005), Fungal degradation of wood: initial proteomic analysis of extracellular proteins of *Phanerochaete chrysosporium* grown on oak substrate, *Curr Genet*, *47*, 49–56.

Abreu R. S., Penalva L. O., Marcotte E. M., Vogel C., (2009), Global signatures of protein and mRNA expression levels, *Mol*. *BioSyst*., *5*, 1512-1526.

Aerts J. L., Gonzales M. I., Topalian S. L., (2004), Selection of appropriate control genes to assess expression of tumor antigens using real-time RT-PCR, *BioTechniques, 36*, 84-91.

Aifa M. S., Sayadi S., Gargouri A., (1999), Heterologous expression of lignin peroxidase of *Phanerochaete chrysosporium* in *Aspergillus niger*, *Biotechnology Letters*, *21*, 849-853.

Albrecht D., Guthke R., Brakhage A. A., Kniemeyer O.,(2010), Integrative analysis of the heat shock response in *Aspergillus fumigatus*, *BMC Genomics*, *11* (32).

Ali G. S., Golovkin M., Reddy A. S. N., (2003), Nuclear localization and in vivo dynamics of a plant-specific serine/arginine-rich protein, *Plant Journal*, *36*, 883-893.

Asamuda N. U., Daba A.S., Ezeronye O. U., (2005), Bioremediation of textile effluent using *Phanerochaete chrysosporium*, *African Journal of Biotechnology*, *4* (13), 1548-1553.

Baldrian P., (2003), Interactions of heavy metals with white rot fungi, *Enzyme and Microbial Technology*, *32*, 78-91.

Bass B. L., (2002), RNA editing by adenosine deaminases that act on RNA, *Annu*. *Rev*. *Biochem*., 71, 817-846.

Bogan B. W., Lamar R. T., (1996), Polycyclic aromatic hydrocarbon-degrading capabilities of *Phanerochaete laevis* HHB-1625 and its extracellular ligninolytic enzymes, *Applied and Environmental Microbiology*, *64* (5), 1597-1603.

Bouws H., Wattenberg A., Zorn H., (2008), Fungal secretomes-nature's toolbox for white biotechnology, *Appl Microbiol Biotechnol*, *80*, 381–388.

Breen A., Singleton F. L., (1999), Fungi in lignocellulose breakdown and biopulping, *Current Opinion in Biotechnology*, *10*, 252-258.

Briolat V., Reysset G., (2002), Identification of the *Clostridium perfringens* genes involved in the adaptive response to oxidative stress, *Journal of Bacteriology*, 2333-2343.

Burdsall, H. H. Jr, (1985), A contribution to the taxonomy of the genus *Phanerochaete* (Corticiaceae, Aphyllophorales), *Mycological Memoir*, No. 10., J. Cramer, Braunschweig.

Bustin S. A., (2000), Absolute quantification of mRNA using real-time reverse transcription polymerase chain reaction assays, *Journal of Molecular Endocrinology*, *25*, 169-193.

Bustin S. A., Benes V., Nolan T., Pfaffl M.W., (2005), Quantitative real time RT-PCR – a perspective, *Journal of Molecular Endocrinology*, *34*, 597-601.

Bustin S. A., Benes V., Garson J. A., Hellemans J., Huggett J., Kubista M., Mueller R., Nolan T., Pfaffl M. W., Shipley G. L., Vandesompele J., Wittwer C. T., (2009), The MIQE guidelines: minimum information for publication of quantitative Real Time PCR experiments, *Clinical Chemistry*, 55, 611-622.

Carthew R. W., Sontheimer E. J., (2009), Origins and Mechanisms of miRNAs and siRNAs, *Cell*, *136*, 642-655.

Chamot D., Owttrim G. W., (2000), Regulation of Cold Shock-Induced RNA Helicase Gene Expression in the Cyanobacterium *Anabaena* sp. Strain PCC 7120, *Journal of Bacteriology*, *182* (5), 1251-1256.

Chang S., Chen W., Yang J., (2009), Another formula for calculating the gene change rate in real-time RT-PCR, *Mol Biol Rep*, *36*, 2165–2168.

Chen G. Q., Zhang W.J, Zeng G. M., Huang J. H., Wang L., Shen G. L., (2011), Surface-modified *Phanerochaete chrysosporium* as a biosorbent for Cr (VI)-contaminated wastewater, *Journal of Hazardous Materials*, *186*, 2138-2143.

Chen Y., Varani G., (2005), Protein families and RNA recognition, *FEBS Journal*, *272*, 2088–2097.

Chini V., Foka A., Dimitracopoulos G., Spiliopoulou I., (2007), Absolute and relative Real Time PCR in the quantification of tst gene expression among methicillin-resistant *Staphylococcus aureus*: evaluation by two mathematical models, *Letters in Applied Microbiology*, *45*, 479–484.

Cikos S., Bukovska A., Koppel J., (2007), Relative quantification of mRNA: comparison of methods currently used for Real Time PCR data analysis, *BMC Molecular Biology*, *8*,113.

Çeribaşı I. H., Yetiş Ü., (2001), Biosorption of Ni(ii) and Pb(ii) by *Phanerochaete chrysosporium* from a binary metal system-Kinetics, *Water SA*, *27*.

Dastoor Z., Dreyer J. L., (2000), Nuclear trasnlocation and aggregate formation of heat shock cognate protein 70 (Hsc70) in oxidative stress and apoptosis, *J. Cell Sci*. *113*, 2845-2854.

Day D. A., Tuite M. F., (1998), Post-transcriptional gene regulatory mechanisms in eukaryotes: an overview, *Journal of Endocrinology*, *157*, 361-371.

Dervaux S., Vandesompele J., Hellemans J., (2010), How to do successful gene expression analysis using Real Time PCR, *Methods*, *50*, 227-230.

Duque P., (2011), A role for SR proteins in plant stress responses, *Plant Signaling & Behavior*, *6*(1), 49-54.

Dussault A. A., Pouliot M., (2006), Rapid and simple comparison of messenger RNA levels using real- time PCR, *Biol. Proced. Online* , *8*(1),1-10.

Edwards K. J., (2008), Performing Real Time PCR, Edwards K., Logan J., Saunders N., Chapter 4, Horizon Bioscience.

Fan J., Yang X., Wang W., Wood W. H., Becker K. G., Gorospe M., (2002), Global analysis of stress-regulated mRNA turnover by using cDNA arrays. *Proc. Natl. Acad. Sci*., *99*, 10611–10616.

Filichkin S. A., Priest H. D., Givan S., (2010), Genome-wide mapping of alternative splicing in *Arabidopsis thaliana*, *Genome Res*., *20*, 45-58.

Fleige S., Pfaffl M.W., (2006), RNA integrity and the effect on the real-time qRT-PCR performance, *Molecular Aspects of Medicine*, *27*, 126–139.

Fu N., Drinnenberg I., Kelso J., Wu J. R., Paabo S., *et al* (2007), Comparison of protein and mRNA expression evolution in humans and chimpanzees. *PLoS ONE, 2* (2).

Fujii H., Chiou T. J., Lin S. I., Aung K., Zhu J. K., (2005), A miRNA involved in phosphate starvation response in *Arabidopsis*, *Curr*. *Biol*., *15*, 2038-2043.

Fujii H., Chiou,T. J., Lin S. I., Aung K., Zhu, J. K. (2005). A miRNA involved in phosphate-starvation response in *Arabidopsis*, *Curr*. *Biol*., 15, 2038-2043.

Fulda S., Huang F., Nilsson F., Hagemann M., Norling B., (2000), Proteomics of Synechocystis sp. strain PCC 6803 identification of periplasmic proteins in cells grown at low and high salt concentrations, *Eur. J. Biochem*., *267*, 5900-5907.

Garcia-Martinez J., Aranda A., Perez-Ortin J., (2004), Genomic run-on evaluates transcription rates for all yeast genes and identifies gene regulatory mechanisms. *Mol*. *Cell*, *15*, 303-313.

Gatton M. L., Peters J. M., Gresty K., Fowler E. V., Chen N., Cheng Q., (2006), Detection sensitivity and quantitation of *Plasmodium falciparum var* gene transcripts by real-time RT-PCR in comparison with conventional RT-PCR, *Am J Trop Med Hyg*., *75* (2), 212–218.

Giglio S., Monis P. T., Saint C. P.,(2003), Demonstration of preferential binding of SYBR Green I to specific DNA fragments in real-time multiplex PCR, *Nucleic Acids Research, 31*.

Ginzinger D. G., (2002), Gene quantification using real-time quantitative PCR: An emerging technology hits the mainstream, *Experimental Hematology*, *30*, 203-512.

Gott J. M., Emeson R. B., (2000), Functions and mechanisms of RNA editing, *Annu*. *Rev*. *Genet*., 34, 499-531.

Gou Y., Xiao P., Lei S., Deng F., Xiao G. G., Liu Y., Chen X., Li L., Wu S., Chen Y., Jiang H., Tan L., Xie J., Zhu X., Liang S., Deng H.,(2008), How is mRNA expression predictive for protein expression? A correlation study on human circulating monocytes, *ABBS*, *40* (5), 426-436.

Gray N. K., Coller J. M., Dickson K. S., Wickens M., (2000), Multiple portions of poly(A)-binding protein stimulate translation in vivo, *The EMBO Journal*, *19* (17), 4723-4733.

Greenbaum D., Colangelo C., Williams K., Gerstein M., (2003), Comparing protein abundance and mRNA expression levels on a genomic scale, *Genome Biology*, *4* (9).

Griffin T. J., Ideker T., Rist B., Eng J., Hood L., Aebersold R., (2002), Complementary Profiling of Gene Expression at the Transcriptome and Proteome Levels in *Saccharomyces cerevisiae*, *Molecular & Cellular Proteomics*, *1.4*, 323-333.

Guarro J., Gene J., Stchigel A. M., (1999), Developments in fungal taxonomy, *Clinical microbiology reviews*, *12* (3), 454-500.

Gygi S. P., Rochon Y., Franza B. R., Aebersold R., (1999), Correlation between protein and mRNA abundance in yeast, *Molecular and Cellular Biology*, *19*, 1720-1730.

Hellemans J., Mortier G., Paepe A., Speleman F., Vandesompele J., (2007), qBase relative quantification framework and software for management and automated analysis of real-time quantitative PCR data, *Genome Biology*, *8*, R19.

Hofstätter H., Tschernutter M., Kunert R.,(2010),Comparison of hybridization methods and Real Time PCR: their value in animal cell line characterization, *Appl Microbiol Biotechnol*, *87*, 419-425.

Howard R.L., Abotsi E., Jansen van Rensburg E.L., Howard S., (2003), Lignocellulose biotechnology: issues of bioconversion and enzyme production, *African Journal of Biotechnology*, *2* (12), 602-619.

Huang D. L., Zeng G. M., Feng C. L., Hu S., Jıang X. Y., Tang L., Su F. F., Zhang Y., Zeng W., Lıu H. L., (2008), Degradation of lead contaminated lignocellulosic waste by *Phanerochaete chrysosporium* and the reduction of leadtoxicity, *Environ. Sci., Technol*., *42*, 4946-4951.

Huang D. L., Zeng G. M., Jiang X. Y., Feng C. L., Yu H. Y., Huang G. H., Liu H.L., (2006), Bioremediation of Pb-contaminated soil by incubating with *Phanerochaete chrysosporium* and straw, *Journal of Hazardous Materials* , *134*, 268–276.

Igwe J. C., Ogunewe D. N., Abia A.A., (2005), Competitive adsorption of Zn (II), Cd (II) and Pb (II) ions from aqueous and non- aqueous solution by maize cob and husk, *African Journal of Biotechnology*, *4* (10), 1113-1116.

Janse B. J. H., Cullen G. D., Zapanta L., Dougherty M.J., Tien, (1997), Are Bacteria omnipresent on *Phanerochaete chrysosporium* Burdsall?, *Applied and Environmental Microbiology*, *63* (7), 2913-2914.

Jarmoskaite I., Russell R., (2010), DEAD-box proteins as RNA helicases and chaperones, *WIREs RNA, 2*, 135-152.

Johnston M., Carlson M., (1991), The molecular and cellular biology of the yeast *Saccharomyces*: Gene Expression, Broach J. R., Pringle J. R., Jones E. W. (eds), Cold Spring Harbor Laboratory Press, Cold SpringHarbor, NY, 2, 193-281.

Jones-Rhoades M.J., Bartel D.P., (2004), Computational identification of plant microRNAs and their targets, including a stress induced miRNA, *Mol. Cell*, *14*, 787-799.

Kawaguchi R., Girke T., Bray A. B., Bailey-Serres J., (2004), Differential mRNA translation contributes to gene regulation under non-stress and dehydration stress conditions in *Arabidopsis thaliana*, *The Plant Journal*, *38*, 823-839.

Kempken F., Kück U., (1996), *restless*, an Active *Ac*-like transposon from the fungus *Tolypocladium inflatum*: structure, expression, and alternative RNA splicing, *Molecular and Cellular Biology*, *16*, 6563-6572.

Kielkopf C. L., Lücke S., Green M. R., (2004), U2AF homology motifs: protein recognition in the RRM world *Genes Dev.*, *18*, 1513-1526.

Köhler A., Hurt E., (2007), Exporting RNA from the nucleus to the cytoplasm, *Nature Rev. Mol. Cell Biol.*, *8* (10), 761-73.

Koker T. H., Nakasone K. K., Haarhof J., Burdsall H. H., Janse B. J. H., (2003), Phylogenetic relationships of the genus *Phanerochaete* inferred from the internal transcribed spacer region, *Mycol. Res*., 107 (9), 1032–1040.

Kurihara H., Wariishi H., Tanaka H., (2002), Chemical stress responsive genes from lignin degrading fungus *Phanerochaete chrysosporium* exposed to dibenzo-p-dioxin, *FEMS Microbiology Letters*, *212*, 217-220.

Lamar R. T., Schoenike B., Wymelenberg A. V., Stewart P., Dietrich D. M., Cullen D., (1995), Quantitation of fungal mRNAs in complex substrates by reverse

transcription PCR and its application to *Phanerochaete chrysosporium*- colonized soil, *Applied and Environmental Microbiology*, *61*, 2122-2126.

Latchman, D.S. (2005), Gene regulation: a eukaryotic perspective, Fifth edition, Taylor and Francis, Oxford and New York.

Lattenmayer C., Trummer E., Schriebl K., Vorauer-Uhl K., Mueller D., Katinger H., Kunert R., (2007), Characterisation of recombinant CHO cell lines by investigation of protein productivities and genetic parameters. *J. Biotechnol*., *128*, 716-725.

Lawrence L., Kuei I., (1992), Assay validation using the concordance correlation coefficient, *Biometrics*, *48*, 599-604.

Lida K., Seki M., Sakurai T., Satou M., Akiyama K., Toyoda T., Konagaya A., Shinozaki K., (2004), Genome-wide analysis of alternative pre-mRNA splicing in *Arabidopsis thaliana* based on full-length cDNA sequences, *Nucleic acid research, 32* (17).

Lim Y. W., Keun S. B., Jongsık C., Kang H. L., Won J. J., Kyung S. B., (2007) Accurate Delimitation of *Phanerochaete chrysosporium* and *Phanerochaete sordida* by specific PCR primers and cultural approach, *J. Microbiol. Biotechnol*., 17(3), 468–473.

Linder P., (2006), Dead-box proteins: a family affair active and passive players in RNP-remodeling, *Nucleic Acids Research*, *34* (15), 4168-4180.

Liu H. H., Liu J., Fan S. L., Song M. Z., Han X. L., Liu F., Shen F. F., Molecular cloning and characterization of a salinity stress-induced gene encoding DEAD-box helicase from the halophyte *Apocynum venetum*, *Journal of Experimental Botany*, *59* (3), 633–644.

Livak K. J., Schmittgen T. D., (2001), Analysis of relative gene expression data using real-time quantitaive PCR and the $2^{-\Delta\Delta Ct}$ method, *Methods*, *25*, 402-408.

Lopez-Garcıa M. T., Santamarta I., Liras P., (2010), Morphological differentiation and clavulanic acid formation are affected in a *Streptomyces clavuligerus* adpA-deleted mutant, *Microbiology*, *156*, 2354–2365.

Lunde B. M., Moore C., Varani G., (2007), RNA-binding proteins: modular design for efficient function, *Molecular Cell Biology*, 8.

Ma S., Bhattacharjee R. B., Bag J., (2009), Expression of poly(A) protein is upregulated during recovery from heat shock in HeLa cells, *FEBS Journal*, *276*, 552-570.

Magnus D. A, Evans M. C., Jacobson A., (2003), Poly(A)-binding proteins: multifunctional scaffolds for the post-transcriptional control of gene expression, *Genome Biology, 4* (7), Article 223.

Martinez. D., Larrondo. L.F., Putnam. N., Gelpke. M.D., Huang. K., Chapman. J., Helfenbein. K.G., Ramaiya. P., Detter. J.C., Larimer. F., Coutinho P. M., Henrissat. B., Berka. R., Cullen. D., Rokhsar. D., (2004), Genome sequence of the lignocellulose degrading fungus *Phanerochaete chrysosporium* strain RP78. *Nat Biotechnol. , 22*, 695-700.

Mata J., Matguerat S., Bahler J., (2005), Post-transcriptional control of gene expression: a genome-wide perspective, *Trends in Biochemical Sciences*, *30*, (9).

Michel F. C., Dass S. B., Grulke E. A., Reddy C. A., (1981), Role of manganese peroxidases and lignin peroxidases of *Phanerochaete chrysosporium* in the decolorization of kraft bleach plant effluent, *Applied and Environmental Microbiology*, *57*(8), 2368-2375.

Mukhtar M., Parveen Z., Logan D.A.,(1998), Isolation of RNA from the filamentous fungus *Mucor circinelloides*, *Journal of Microbiological Methods*, *33*, 115-118.

Nagano-Ito M., Banba A., Ichikawa S., (2009), Functional cloning of genes that suppress oxidative stress-induced cell death: TCTP prevents hydrogen peroxide-induced cell death, *FEBS Letters*, *583*, 1363-1367.

Nakamura T., Muramoto Y., Yokota S., Uedab A., Takabe T., (2004), Structural and transcriptional characterization of a salt-responsive gene encoding putative ATP-dependent RNA helicase in barley, *Plant Science*, *167*, 63–70.

Nilsen T. W., Graveley B. R., (2010), Expansion of the eukaryotic proteome by alternative splicing, *Nature*, *463* (28).

Oliveira L. S., Santana A. L. B. D., Maranhao C. A., Miranda R. C. M., Galvao de Lima V. L., Silva S. I., Nasciento M. S., Bieber L., (2010), Natural resistance of five woods to *Phanerochaete chrysosporium* degradation, *International Biodeterioration and Biodegradation*, *64*, 711-715.

Özcan S., (2003), Proteome analysis of Pb (II), Ni (II) and Cr (III) response in *Phanerochaete chrysosporium*, PhD thesis, METU.

Özcan S, Yıldırım V, Kaya L, Dirk Albrecht D., Becher D., Hecker M., Ozcengiz G., (2007), *Phanerochaete chrysosporium* soluble proteome as a prelude for the analysis of heavy metal stress response, *Proteomics*, *7*, 1249–1260.

Paskitti M. E., McCreary B. J., Herman J. P., (2000), Stress regulation of adrenocorticosteroid receptor gene transcription and mRNA expression in rat hippocampus: time-course analysis, *Molecular Brain Research*, 80 (2), 142-152.

Pfaffl M. W., (2001), A new mathematical model for relative quantification in real-time RT-PCR, *Nucleic Acid Research*, *29*, 2002-2007.

Pfaffl M. W., Horgan G. W., Demplfle L., (2002), Relative expression software tool (REST) for group-wise comparison and statistical analysis of relative expression results in Real Time PCR, *Nucleic Acids Research*, *30*.

Pfaffl M. V., (2004), Quantification strategies in Real Time PCR, Bustin S. A., A-Z of quantitative PCR, pp. 87-112, International University Line (IUL).

Platts A. E., Johnson G. D., Linnemann A. K., Kraetz S.A.,(2008), Real Time PCR quantification using a variable reaction efficiency model, *Analytical Biochemistry*, *380*, 315–322.

Prouty, A. L., (1990), Bench-scale development and evaluation of a fungal bioreactor for color removal from bleach effluence. *Appl*. *Microbiol*. *Biotechnol*. *32*: 490-493.

Reader U., Thompson W., Broda P., (1987) Establishing molecular genetics for *Phanerochaete chrysosporium*, *Phil. Trans. Soc. Lond*., 321, 475-483.

Reddy M. K., Maruthi Y. A., Lakshmi K.A., (2010), *Aspergillus flavus* and *Phanerochaete chrysosporium* as potentıal delignifying mycoflora of dump yard: a case study, *Rasayan J. Chem*., *3* (3), 438-444.

Ruggeri B., Sassi G., (2003), Experimental sensitivity analysis of a trickle bed bioreactor for lignin peroxidases production by *P. chrysosporium*, *Process Biochemistry*, *38*, 1669-1676.

Sachs M. S., (1998), Post-transcriptional control of gene expression in filamentous fungi, *Fungal Genetics and Biology*, *23*, 117-125.

Sagliocco F., Laloo B., Cosson B., (2006), The ARE-associated factor AUF1 binds poly (A) in vitro in competition with PABP1, *Biochem J*., *400*, 337-347.

Sakashita E., Tatsumi S., Werner D., Endo H., Mayeda A., (2004), Human RNPS1 and its associated factors: a versatile alternative pre-mRNA splicing regulator *in vivo*, *Molecular and Cellular Biology*, *24* (3), 1174–1187.

Saliciani A. M., Xi M., Vanderveer L. A., Balsara B., Testa J. R., Dunbrack R. L., Godwin A. K., (2000), Identification and structural analysis of human RBM8A and RBM8B: two highly conserved RNA-binding motif proteins that interact with OVCA1, a Candidate Tumor Suppressor, *Genomics*, *69*, 54-62.

Say R., Denizli A., Arıca M. Y., (2001), Biosorption of cadmium (II), lead (II) and copper (II) with the filamentous fungus *Phanerochaete chrysosporium*, *Bioresource Technology*, *76*, 67-70.

Shary S., Kapich A. N., Panisko E. A., Magnuson J. K., Cullen D., Hammel K. E., (2008), Diffrerential expression in *Phanerochaete chrysosporium* of membrane associated proteins relevant to lignin degradation, *Applied and Environmental Microbiology*, *74*,7252-7257.

Siomi H., Dreyfusst G., (1997), RNA-binding proteins as regulators of gene expression, *Current Opinion in Genetics and Development*, *7* (3), 345-353.

Smith C. W. J., Valcarcel J., (2000), Alternative pre-mRNA splicing: the logic of combinatorial control, *Trends in Biochemical Sciences*, *25* (8), 381-388.

Srinivasan C., D'souza T. M., Boomınathan K., Reddy C. A., (1995), Demonstration of laccase in the white rot basidiomycete *Phanerochaete chrysosporium* BKM-F1767, *Applied and Environmental Microbiology*, 61 (12), 4274-4277 .

Stewart P., Kersten P., Wymelenberg A. V., Gaskell J., Cullen D., (1996), Lignin peroxidase gene family of *Phanerochaete chrysosporium* : Complex regulation by carbon and nitrogen limitation and identification of a second dimorphic chromosome, *Journal of Bacteriology*, *174*, 5036-5042.

Sunkar R., Kapoor A., Zhu J. K., (2006), Post-transcriptional induction of two Cu/Zn superoxide dismutase genes in *Arabidopsis* is mediated by downregulation of mir398 and important for oxidative stress tolerance, *The Plant Cell*, *18*, 2051–2065.

Sunkar R., Zhu J. K., (2004), Novel and stress-regulated microRNAs and other small RNAs from *Arabidopsis*, *The Plant Cell*, 16, 2001-2019.

Teeri T. T., (2004), Genome sequence of an omnipotent fungus, *Nature Biotechnology*, *22*.

Thakur I.S., (2005), Microbial bioremediation of persistent chlorinated aromatic compounds in the environment, (Ed.) Varma A., Podila G., Biotechnological Applications of Microbes (pp. 239-262), I. K. International Pvt. Ltd.

Tian Q., Stepaniants S. B., Mao M., Weng L., Feetham M. C., Doyle M. J., Yi E. C., Dai H., Thorsson V., Eng J., Goodlett D., Berger J. B., Gunter B., Linseley P. S., Stoughton R. B., Aebersold R., Collins S. J., Hanlon W. A., Hood L. E., (2004), Integrated genomic and proteomic analyses of gene expression in mammalian cells, *Molecular and Cellular Proteomics*, *3*, 960-969.

Tomari Y., Zamore P.D., (2005), Perspective: machines for RNAi, *Genes Dev*., *19*, 517–529.

Trembley J. H., Tatsumi S., Sakashita E., Loyer P., Slaughter C. A., Suzuki H., Endo H., Kidd V. J., Mayeda A., (2005), Activation of pre-mRNA splicing by human RNPS1 is regulated by CK2 phosphorylation, *Molecular and Cellular Biology*, *25* (4), 1446-1457.

Wang T., Brown M. J., (1999), mRNA Quantification by Real time TaqMan polymerase chain reaction: validation and comparison with RNase protection, *Analytical Biochemistry*, *269*, 198–201.

Wang Y., Liu C. L., Storey J. D., Tibshirani R. J., Herschlag D., Brown P. O., (2002), Precision and functional specificity in mRNA decay, *PNAS*, *99* (9), 5860-5865.

Wong M. L., Medrano J. F.,(2005), Real Time PCR for mRNA quantitation, *BioTechniques* , *39*, 75-85.

Wymelenberg A. V., Minges P., Sabat G., Martinez D., Aerts A., Salamov A., Grigoriev I., Shapiro H., Putnam n., Belinky P., Dosoretz C., Gaskell J., Kersten P. J., Cullen D., (2006), Computational analysis of the *Phanerochaete chrysosporium* v2.0 genome database and mass spectrometry identiWcation of peptides in

ligninolytic cultures reveal complex mixtures of secreted proteins, *Fungal Genetics and Biology*, *43*, 343–356.

Wymelenberg A. V., Sabat G., Martinez D., Rajangam A. S., Teeri T. T., Gaskell J., Kersten P. J., Cullen D., (2005), The *Phanerochaete chrysosporium* secretome: database predictions and initial mass spectrometry peptide identifications in cellulose-grown medium, *Journal of Biotechnology*, *118*, 17-34.

Yang C., Carrier F., (2001), The UV-inducible RNA-binding protein A18 (A18 hnRNP) plays a protective role in the genotoxic stress response, *The Journal of Biological Chemistry*, 276 (50), 47277- 47284.

Yang Y., Kwon H. B., Peng H. P., Shih M. C., (1993), Stress responses and metabolic regulation of glyceraldehyde-3-phosphate dehydrogenase genes in Arabidopsis, *Plant Physiol*., *101*, 209-216.

Yetiş Ü., Dolek M. A., 1, Dilek F. B., Özcengiz G., (2000), The removal of Pb(II) by *Phanerochaete chrysosporium*, *Wat. Res*., *34*, 4090-4100.

Yıldırım V., Özcan S., Becher D., Hecker M., Özcengiz G., (2011), Characterization of proteome alterations in *Phanerochaete chrysosporium* in response to lead exposure, *Proteome Science, 9*, 1-12.

Yu E., Owttrim G. W., (2000), Characterization of the cold stress-induced cyanobacterial DEAD-box protein CrhC as an RNA helicase, *Nucleic Acids Research, 28* (20), 3926-3934.

Yuan J. S., Reed A., Chen F., Steward Jr C. N., (2006), Statistical analysis of Real Time PCR data, *BMC Bioinformatics*, *7*.

Yuan J. S., Wang D., Stewart C. N. Jr., (2008), Statistical methods for efficiency adjusted Real Time PCR quantification, *Biotechnol. J*., *3*, 112-123.

Zapanta L. S., Hattori T., Rzetskaya M., Tien M., (1998), Cloning of *Phanerochaete chrysosporium leu2* by complementation of bacterial auxotrophs and transformation of fungal auxotrophs, *Applied and Environmental Microbiology*, *64* (7), 2624-2629.

APPENDIX A

COMPOSITION AND PREPARATION OF CULTURE MEDIA

A.1. Liquid Media

Growth Medium (Prouty, 2000)	g/L
$KH_2 PO_4$	2
$MgSO_4$	0.5
$CaCl_2$	0.1
NH_4Cl	0.12
Glucose	10.0
Thiamine	0.001
pH	4.5
Temperature (^oC)	35
Shaking rate (rpm)	200

A.2. Solid Media

Sabaroud Dextrose Agar Slant	g/L
Sabaroud Dextrose Agar	65

Dispense 7.5 ml of agar medium to each tube and Sterilized at 121 ^oC for 15 min

Solidify in slanted position

APPENDIX B

BUFFERS AND SOLUTIONS

B.1. Boiling Extraction Buffer

Boric acid	0.2 M
EDTA	30 mM
Sodium dodecyl sulfate	1%;

pH 9.0, adjusted with NaOH

B.2. Solution D

Guanidium thiocyanate	4 M
Sodium citrate (pH:7)	25 mM
Sarcosyl	0.5 %
2-mercaptoethanol	0.1 M

B.3. TE buffer

Tris-HCl	10mM
Sodium EDTA	1mM

B.4. Tris-Acetate-EDTA Buffer (TAE) (50 X)

Tris Base	242 g
Glacial Acetic Acid	57.1 mL
EDTA (0.4 M, pH 8.0)	125 mL
Distilled water added to	1000 mL

APPENDIX C

CHEMICALS AND THEIR SUPPLIERS

C.1. Chemicals

Agarose	Sigma
Boric Acid	Merck
CaCl2 H2O	Merck
Chloroform	Merck
EDTA	AppliChem
Ethanol	Botafarma
Ethidium bromide	Sigma
Glucose	Merck
Isopropanol	Merck
KH_2PO_4	Merck
MgSO4 7H2O	Merck
NH4Cl	Merck
Phenol	Sigma
Phenol-choloroform- isoamylalcohol	Applichem
SDS	Sigma
Sabaroud 4% Glucose Agar	Merck
Thiamine	Sigma

C.2. Enzymes

ProteinaseK	Sigma-Aldrich
RNase	Fermentas
Taq DNA polymerase	Fermentas

C.3. Size Markers

O'GeneRuler 100 bp DNA ladder	MBI Fermentas
Lambda DNA/EcoRI+HindIII marker	Fermentas

C.4. Kits

RNeasy Mini Kit	Qiagen
DNA-free Kit	Ambion
RNAase Free DNAase set	Qiagen
LC FastStart DNA Master SYBR Green I	Roche
Transcriptor First Strand cDNA Synthesis Kit	Roche